University of South Carolina
Scholar Commons

Theses and Dissertations

2018

Climate Metric Coherence: Stationarity of the Relationships Between North Pacific Climate Indices and Ecological Processes in the Gulf of Alaska

Michael Opiekun
University of South Carolina

Follow this and additional works at: https://scholarcommons.sc.edu/etd

 Part of the Marine Biology Commons

Recommended Citation

Opiekun, M.(2018). *Climate Metric Coherence: Stationarity of the Relationships Between North Pacific Climate Indices and Ecological Processes in the Gulf of Alaska.* (Master's thesis). Retrieved from https://scholarcommons.sc.edu/etd/4761

This Open Access Thesis is brought to you by Scholar Commons. It has been accepted for inclusion in Theses and Dissertations by an authorized administrator of Scholar Commons. For more information, please contact dillarda@mailbox.sc.edu.

Climate metric coherence: Stationarity of the relationships between North Pacific climate indices and ecological processes in the Gulf of Alaska

by

Michael Opiekun

Bachelor of Science
University of Miami, 2016

Submitted in Partial Fulfillment of the Requirements

For the Degree of Master of Science in

Marine Science

College of Arts and Sciences

University of South Carolina

2018

Accepted by:

Ryan Rykaczewski, Director of Thesis

Tammi Richardson, Reader

George Voulgaris, Reader

David Wethey, Reader

Cheryl L. Addy, Vice Provost and Dean of the Graduate School

© Copyright by Michael Opiekun, 2018
All Rights Reserved.

Dedication

To my parents, Debbie and Jeff. Thank you for your constant love and support.

Acknowledgements

I would like to thank Dr. Ryan R. Rykaczewski for his support throughout this endeavor. I would also like to thank my lab mate Brendan Turley for the morale boosts and our unique and deep talks when maybe we should have been working on fish stuff. I would also like to thank the undergraduate support, Lev Looney, for his unique interruptions and continued laughs. I would also like to thank two professors for their advice and support throughout my time at the University of South Carolina: Dr. Claudia Benitez-Nelson and Dr. Lori Ziolkowski.

Abstract

The Pacific Decadal Oscillation (PDO) has been used to characterize the dominant basin-scale climate variability, in the North Pacific. The PDO index has been correlated to Pacific salmon (*Oncorhynchus spp.*) population dynamics in the Gulf of Alaska (GOA) during the late 1900s, but the stationarity of the statistical relationships between salmon production and the basin-scale index (and between the regional physical processes and the basin-scale index) has not been quantified. A change in the relationship between the PDO and salmon catches has been noted during the late 1980s, motivating further investigation of variability in climate and ecosystem properties during this period.

To test relationships between North Pacific basin-scale and GOA regional scale oceanographic variability, an empirical orthogonal function (EOF) analysis was used to explore changing temporal and spatial patterns in oceanographic properties during the mid 1900s to early 2000s. Physical properties and climate indices were compared across the winter of 1988/89 to characterize the variability in relationships between properties in different periods. EOF loading patterns were compared using rolling 15-year windows to estimate variability and consistency of patterns throughout the 1900s and 2000s. An EOF analysis was also used to compare temporal metrics of oceanic and atmospheric variability along the GOA continental shelf with residuals from Pacific salmon spawner-recruitment curves.

In this thesis, I show that many physical properties in the GOA exhibit non-stationary relationships across the 1988/89 boundary. Relationships between physical

properties and salmon productivities also exhibit non-stationarities during the late 1980s. Only SSHa showed a shift in the dominant EOF spatial pattern in the late 1980s that was consistent with the proposed shift in salmon-climate relationships. SST did not show a sustained temporal or spatial change in the GOA, but rather a short-lived spatial change in the 1980s, that reverted back to the pre-1980s pattern. No other property showed a change in patterns of variability during the late 1980s, nor did any properties maintain a stationary relationship with salmon indices. Local and regional SSHa indices may better represent variability in the GOA and the properties that impact salmon survival than basin-scale indices.

Table of Contents

List of Figures

List of Abbreviations

AL ..... Aleutian Low

EOF ..... Empirical Orthogonal Function

GOA ..... Gulf of Alaska

MLD ..... Mixed Layer Depth

NPGO ..... North Pacific Gyre Oscillation

PC ..... Principal Component

PDO ..... Pacific Decadal Oscillation

SR ..... spawner-recruitment curve

SSHa ..... Sea Surface Height Anomalies

SSS ..... Sea Surface Salinity

SST ..... Sea Surface Temperature

Chapter 1

Introduction

1.1 Background

The North Pacific basin is the home of many large, economically important fisheries. These fisheries generate tens of billions of dollars in revenue each year (FAO Yearbook 2015), supporting local and national economies. The fisheries in the northeastern North Pacific, specifically the Gulf of Alaska (GOA), support multi-hundred-million-dollar industries in the state of Alaska and the western provinces of Canada (National Marine Fisheries Service 2014; Stopha 2017). Few fisheries in the GOA basin are more important than the Pacific salmon (*Oncorhynchus spp.*) fisheries. The Pacific salmon fisheries are culturally significant, having been used for thousands of years by native peoples in northwestern North America for sustenance and survival (Halffman et al. 2015). Understanding the association between salmon population dynamics and ecosystem variability is necessary for their continued sustainability and exploitation.

For decades, oceanographers have attempted to relate climate and ocean variability with population dynamics to better understand the driving mechanisms behind population and recruitment variability. It is well recognized by fisheries oceanographers that fishing pressure is not the only factor driving population fluctuations, but thoroughly grasping the relationships between populations and shifting physical processes is

extremely challenging, if not nearly impossible, especially if those processes were not easily observed. As a method to summarize large-scale climate processes, oceanographers commonly use climate and ocean variability summaries as indices (Hurrell 1995; Mantua et al. 1997; Di Lorenzo et al. 2008; Linkin and Nigam 2008). If these indices effectively characterize variability, they can simplify the analyses of the interactions between biological and oceanic or atmospheric properties (Mantua et al. 1997, Mantua and Hare 2002; Di Lorenzo et al. 2008).

Sea surface temperature (SST) has persistently been used as a metric to explain variability in marine ecological time series (Pauly 1980; Clark et al. 2003). Increased seasonal temperatures are known to have varied impacts on fishes including individual impacts (Lee et al. 2003) and ecological impacts (Nurdin et al. 2013). Due to its ecological importance and relative ease of observation, SST has been used to define many basin-wide climate indices around the globe (Hurrell 1995; Mantua et al. 1997; Linkin and Nigam 2008).

In the North Pacific, the first mode of anomalous SST is the Pacific Decadal Oscillation (PDO; Figure 1.1 a, b; Mantua and Hare 2002). The PDO is often called a long-lived El Niño-like pattern, with distinct phases of North Pacific SST and sea surface height anomalies (SSHa) lasting between 15-25 years (Mantua and Hare 2002). The warm phase of the PDO is characterized by anomalously cool SST in the central North Pacific and anomalously warm SST along the eastern North Pacific. The SST anomalies associated with cool phase of the PDO are reversed from those of the warm phase. The PDO is partially driven by the position of the Aleutian Low (AL), the main source of North Pacific pressure variability (Mantua and Hare 1997). A strong, southward AL is

associated with the warm phase of the PDO, and a weak, northward AL is associated with the cool phase of the PDO. The most variability expressed by the PDO occurs in winter and springtime, and this has been related to forcings from the El Niño Southern Oscillation (Newman et al. 2003). The inception of the PDO was partly due to the interest in understanding Pacific salmon population dynamics in the Gulf of Alaska due to population shifts in the late 1970s (Mantua and Hare 1997).

The second mode of climate variability in the North Pacific is the North Pacific Gyre Oscillation (NPGO; Figure 1.1 a, c), expressed as the second mode of variability in SSHa and SST anomalies (Di Lorenzo 2008). The NPGO has been correlated to sea surface salinity (SSS), chlorophyll, nitrate, phosphate, silicate, and oxygen concentrations in the western North Pacific. These properties have each been shown to affect primary producers (Di Lorenzo et al. 2008) allowing a better understanding of the base of the food web and upper trophic levels. The positive phase of the NPGO is associated with low SSHa in the GOA and high SSHa in the central North Pacific. The negative phase of the NPGO is associated with high SSHa in the GOA and low SSHa in the central North Pacific.

The mid-1970s were documented as a period of change as the PDO changed from the negative phase to the positive phase (Hare and Mantua 2000; Litzow 2006; Overland et al. 2008; Yeh et al. 2011). Biological and physical patterns changed throughout the North Pacific. The late 1980s have also been considered a change in North Pacific climate (Hare and Mantua 2000; Overland et al. 2008; Yeh et al. 2011) but less is understood about this time period due to a lack of clear changes in physical indices (Hare

and Mantua 2000). A change in the dominant mode of variability could have substantial consequences for biological and physical processes.

The PDO and NPGO are both important in the climate dynamics of the North Pacific, especially the GOA. The GOA is a large marine ecosystem due to the synchronous variability among properties in the GOA (Sherman 2015). One example of this synchrony is evident in the phases of the PDO, where anomalous warming occurs throughout the GOA during the warm phase, and anomalous cooling occurs during the cool phase. The Alaska Gyre, making up the main circulation in the GOA, is part of the North Pacific subpolar gyre (Stabeno et al. 2004; Figure 1.2). It is formed from the bifurcation of the North Pacific Current as it nears North America and splits into the California Current, flowing south, and the Alaska Current, flowing north. The Alaska Current flows north and splits to form the Alaska Coastal Current (ACC), that flows along the most northern coastal region of the GOA, and a smaller section of the Alaska Current that flows off the coastal shelf. The ACC and the Alaska Current rejoin to form the Alaskan Stream, flowing southwest out of the GOA along the Aleutian Islands. The Alaska Gyre is cyclonic, creating upwelling in the central GOA and downwelling along the coast. Despite the downwelling along the coast, the GOA is a highly productive region as exemplified by the multiple highly exploitative fisheries. Seasonal fluctuations of light and iron are two of the main processes that affect primary production in the GOA (Fietchter et al. 2009). When ample light is present, high primary production along the coast is due to riverine input of iron from glacier and snowpack melt and limited mixing from deeper waters.

Both the PDO and NPGO have been associated with variability in biological processes in the GOA basin (Mantua et al. 1997; Di Lorenzo 2008; Litzow et al. 2013). The salmon fisheries in the GOA have been correlated to the PDO index (Mantua et al. 1997; Hare et al. 2011). Fisheries have exploited Pacific salmon since the late 19th century, with a substantial increase in catches beginning in the late 1970s (Stopha 2018). The addition of hatchery raised salmon as a supplement to the native populations and increased use of new fishing technology in the late 20th century has led to the salmon fishery consistently catching the most fish in recorded history. With such high fishing pressure and important economic weight, managing salmon populations is necessary to maintain exploitable populations. Current management is based on biological studies completed by Alaska Department of Fish and Game biologists and previous catches (Stopha 2018). Therefore, it is important to understand how salmon interacts with their environment to determine the best management practices to maintain this important fishery.

Such management influencing studies include comparing salmon population and recruitment variability to climate indices and properties. Indices unfortunately do not provide a robust understanding of the drivers behind biological variability due to their nature. The PDO index is the first empirical orthogonal function (EOF) of anthropogenically-detrended SST anomalies poleward of 20º N in the North Pacific (Zhang et al. 1997) and the NPGO index is the second principal component (PC) of SSHa poleward of 20º N in the North Pacific (Di Lorenzo et al. 2008). SST expresses the connectivity between the ocean and atmospheric processes and is slow to change creating an artifact of past anomalous events (Namias and Born 1970; Checkley and Lindegren

2014). Since SST is integrative on a temporal scale, it is highly autocorrelated in space and time which can create the facade of strong correlation statistics (Valcu and Kempenaers 2010). SSHa is an integral of water-column dynamics, expressing the impacts that multiple properties have on the water column. When an EOF analysis is applied to each of these properties over a large area, the direct impact that an individual property might have on an organism is removed since spatial variability is included from regions that the fish never interact with. Therefore, using \ regional indices instead of basin-scale indices to use in ecological studies, can provide a more mechanistic understanding of biological relationships with changing climate dynamics.

Instead of using basin-scale climate indices, oceanic and atmospheric models are capable of providing effective assimilations of data and algorithms to estimate properties around the world. Data assimilation models use mathematical approximations of ocean and atmospheric physics, using specific variables constrained by assimilated data in specific layers of the model at regular intervals to estimate properties in different regions (Moore et al. 2004; Carton and Giese 2008). Models provide properties that are calculated on a grid, allowing spatial dynamics to be resolved on scales smaller than basin scales. Regional indices can provide a mechanistic understanding when used in ecological analyses since they can be tailored to the location of ecological importance unlike basin-scale indices which include variability that the organisms may never interact. Understanding how organisms react to changing climate is the ultimate goal, so the most mechanistic understanding of these relationships should be pursued.

1.2 Outline of the Thesis

The North Pacific climate is ever-changing. The location of the bifurcation of the North Pacific Current shifts meridionally as does the AL, creating different climate patterns along coastal Alaska and Canada affecting marine populations (Malik et al. 2016). Understanding the relationships between climate properties and organisms, and among climate properties, is important to develop the best management solutions for exploited species.

Throughout my thesis, I use monthly property averages from the Simple Ocean Data Assimilation (SODA) model, version 2.2.4, to calculate regional indices using EOF analyses. I focus my efforts on six physical properties in the GOA that have been shown to impact or act as proxies for biological processes: SST, SSHa, sea surface salinity (SSS), vertical velocity, mixed layer depth (MLD), and wind stress. SST is used as a direct comparison to the PDO index since the method of calculation of the regional SST index is very similar to the method that is used to calculate the PDO index (Zhang et al. 1997). SST is also a proxy for survival of fish and availability of food sources for smolt (Cole 2000). SSHa is an influenced by water column processes (Calman 1987) and may summarize processes that affect salmon dynamics better than an index of ocean surface dynamics alone. SSS is a proxy for water density and freshwater input, an important process in the GOA for iron input (Crusius et al. 2017) that may relate to abundance of food sources for smolt. Vertical velocity and wind stress are proxies for upwelling, and along the downwelling dominated coast of the GOA, anomalous upwelling may be important for nutrient availability for primary producers (Fiechter et al. 2009; Crusius et al. 2017) acting as a proxy for food availability and survival of smolt. MLD is a proxy for

mixing and may relate to nutrient availability in the euphotic zone corresponding to food availability and therefore survival of smolt (Ferland et al. 2011). Wind stress, SSS as a proxy for freshwater input, and MLD may affect water column stability that, in conjunction with solar irradiance intensity, may influence the timing of the spring bloom and the length of the growing season for salmon in the GOA (Henson 2007). Similarly, an optimal amount of stratification following winter mixing may influence salmon survival due to the amount of primary production in the spring (Gargett 1997).

In Chapter 2, I explore the climate change in the late 1980s and the relationships between GOA shelf indices and Pacific salmon recruitment indices in the GOA. Salmon recruitment indices were calculated by taking the residuals from a Ricker spawner-recruitment curve (Ricker 1954). I focus on the year of ocean entry for salmon smolt with the assumption that this period has the largest impact on salmon survival (Irvine et al. 2013), making it the most important period to understand salmon recruitment and production variability. I use the a priori split of 1988/89 to explore the relationships between salmon indices and GOA shelf indices before and after the period of change in the North Pacific.

In Chapter 3, the late 1980s climate shift is characterized using temporal and spatial EOF analyses of multiple properties to evaluate the relationships among regional indices and basin-scale indices. Due to the extreme economic importance of the salmon fisheries in the GOA, I focus my study efforts to characterize the change based on properties solely in the GOA that have been shown to affect ecological processes. I test the stationarity of the relationships among regional indices and relationships between regional and basin-scale indices across the late 1980s using several EOF-based analyses.

Using an a priori break of 1988/89, I compare property PCs and EOF spatial patterns before and after the split to full period PCs to gauge stationarity within a single regional index. The PCs and EOF spatial patterns of indices are also compared among time periods to describe stationarity among regional indices. I also test whether the change in the late 1980s is specific to that period by comparing the EOF spatial patterns and PCs between adjacent rolling 15-year windows throughout the period of 1969-2008.

Broad scale dynamics such as those indexed by the PDO and NPGO have important effects on the GOA, but they may not specifically capture the variability within the GOA basin. By focusing on the GOA region, this study helps to increase the understandings of regional-scale dynamics that can vary from the overall variability in the North Pacific. The 1980s climate change enables the comparison of before and after change dynamics in the GOA to increase our knowledge of relationships among physical properties.

In this thesis, I attempt to expand the understanding of climate and ocean dynamics and their impacts on regional -scale dynamics and biological variability. Using multiple physical properties and their relationships among each other and their relationships to salmon recruitment indices, I document a change in climate variability in the North Pacific to show that previously used climate indices may not be the best summaries that can be used to understand biological variability. Concluding remarks are presented in Chapter 4.

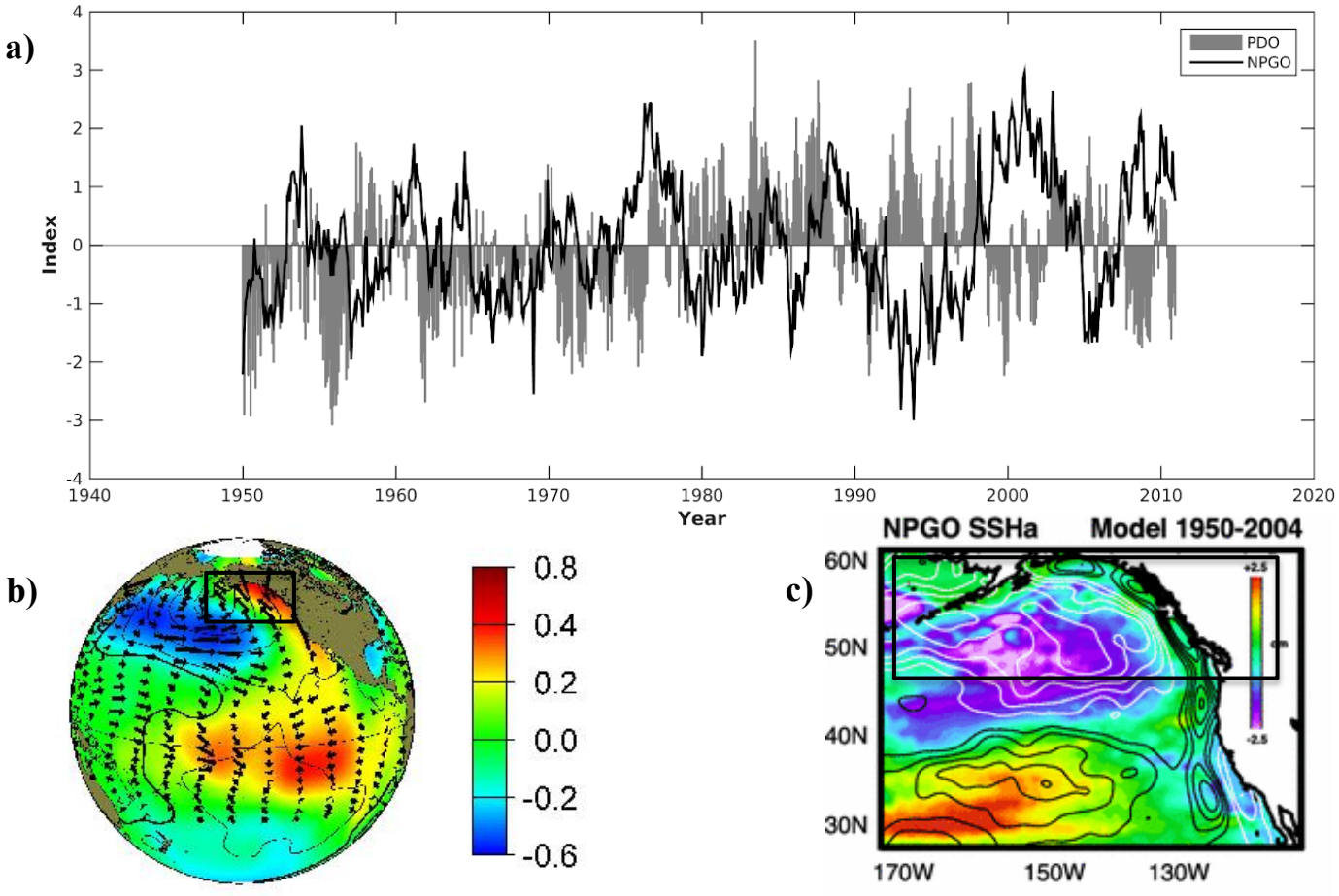

Figure 1.1. The Pacific Decadal Oscillation and North Pacific Gyre Oscillation indices with spatial loadings. a) The PDO (gray bars) and NPGO (black line) indices. b) SST spatial loadings of the PDO index warm phase (modified from Mantua et al. 1997). c) SSHa spatial loadings of the NPGO index (modified from Han et al. 2017).

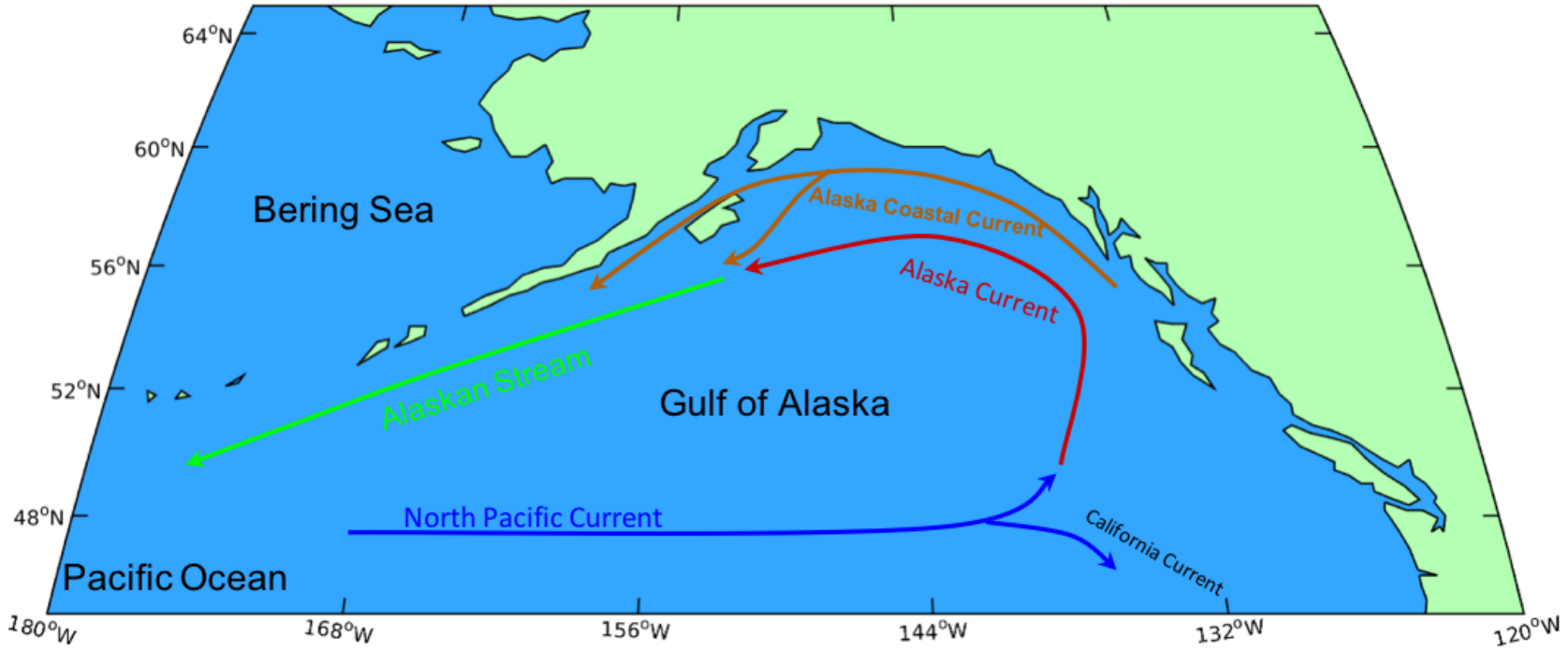

Figure 1.2 Circulation in the Gulf of Alaska.

1.3 References

Calman J (1987) Introduction to sea-surface topography from satellite altimetry. Johns Hopkins APL Technical Digest 8(2):206–211.

Carton JA, Giese BS (2008) A reanalysis of ocean climate using simple ocean data assimilation (SODA). Mon Weather Rev 136:2999–3017. doi: 10.1175/2007MWR1978.1

Checkley Jr DM, Lindegren M (2014) Sea Surface Temperature Variability at the Scripps Institution of Oceanography Pier*. J Phys Oceanogr 44:2877–2892. doi: 10.1175/JPO-D-13-0237.1

Clark RA, Fox CJ, Viner D, Livermore M (2003) North Sea cod and climate change – modelling the effects of temperature on population dynamics. Glob Chang Biol 9:1669–1680. doi: 10.1046/j.1529-8817.2003.00685.x

Crusius J, Schroth AW, Resing JA, Cullen J, Campbell RW (2017) Seasonal and spatial variabilities in northern Gulf of Alaska surface water iron concentrations driven by shelf sediment resuspension, glacial meltwater, a Yakutat eddy, and dust. Glob Biogeochem Cycl 31:942–960. doi: 10.1002/2016GB005493

Cole J (2000) Coastal sea surface temperature and coho salmon production off the north-west United States. Fish Oceanogr 9:1–16.

Di Lorenzo E, Schneider N, Cobb KM, Chhak K, Franks PJS, Miller AJ, McWilliams JC, Bograd SJ, Arango H, Curchister E, Powell TM, Rivere P (2008) North Pacific Gyre Oscillation links ocean climate and ecosystem change. Geophys Res Lett 35:1–6. doi: 10.1029/2007GL032838

FAO yearbook (2015) Fishery and Aquaculture Statistics. 2015. Rome, Italy.

Ferland J, Gosselin M, Starr M (2011) Environmental control of summer primary production in the Hudson Bay system: The role of stratification. J Mar Syst 88:385–400.

Fiechter J, Moore AM, Edwards CA, Bruland KW, Di Lorenzo E, Lewis CVW, Powell TM, Curchister EN, Hedstrom, K (2009) Modeling iron limitation of primary production in the coastal Gulf of Alaska. Deep Res Part II Top Stud Oceanogr 56:2503–2519. doi: 10.1016/j.dsr2.2009.02.010

Gargett AE (1997) The optimal stability 'window': a mechanism underlying decadal fluctuations in North Pacific salmon stocks? Fish Oceanogr 6:109-117. doi: 10.1046/j.1365-2419.1997.00033.x

Halffman CM, Potter BA, McKinney HJ, Finney BP, Rodrigues AT, Yang DY, Kemp BM (2015) Early human use of anadromous salmon in North America at 11,500 y ago. Proc Natl Acad Sci 112:12344–12348. doi: 10.1073/pnas.1509747112

Han W, Meehl GA, Stammer D, Hu A, Hamlington B, Kenigson J, Palanisamy H, Thompson P (2017) Spatial patterns of sea level variability associate with natural internal climate modes. Sur Geophys 38(1): 217–250.

Hare SR, Mantua NJ, Francis RC (2011) Inverse Production Regimes: Alaska and West Coast Pacific Salmon, Fisheries 24:6–14.

Hare SR, Mantua NJ (2000) Empirical evidence for North Pacific regime shifts in 1977 and 1989. Prog Oceanogr 47:103–145. doi: 10.1016/S0079-6611(00)00033-1

Henson, SA (2007) Water column stability and spring bloom dynamics in the Gulf of Alaska. J Mar Res 65(6):715–732. doi: 10.1357/002224007784219002

Hurrell JW (1995) Decadal Trends in the North Atlantic Oscillation: Regional Temperatures and Precipitation. Science 269:676–679. doi: 10.1126/science.269.5224.676

Irvine JR, O'Neill M, Godbout L, Schnute J (2013) Effects of smolt release timing and size on the survival of hatchery-origin coho salmon in the strait of Georgia. Prog Oceanogr 115:111–118. doi: 10.1016/j.pocean.2013.05.014

Lee CG, Farrell AP, Lotto A, MacNutt MJ, Hinch SG, Healey MC (2003) The effect of temperature on swimming performance and oxygen consumption in adult sockeye (Oncorhynchus nerka) and coho (O. kisutch) salmon stocks. J Exp Biol 206:3239–3251. doi: 10.1242/jeb.00547

Linkin ME, Nigam S (2008) The North Pacific Oscillation-West Pacific teleconnection pattern: Mature-phase structure and winter impacts. J Clim 21:1979–1997. doi: 10.1175/2007JCLI2048.1

Litzow MA (2006) Climate regime shifts and community reorganization in the Gulf of Alaska: how do recent shifts compare with 1976/1977? ICES J Mar Sci 63:1386–1396. doi: 10.1016/j.icesjms.2006.06.003

Litzow MA, Mueter FJ, Hobday AJ (2014) Reassessing regime shifts in the North Pacific: Incremental climate change and commercial fishing are necessary for explaining decadal-scale biological variability. Glob Chang Biol 20:38–50. doi: 10.1111/gcb.12373

Mantua NJ, Hare SR (2002) The Pacific Decadal Oscillation. J. Oceanogr. 58:35–44.

Mantua NJ, Hare SR, Zhang Y, Wallace JM, Francis RC (1997) Pacific interdecadal climate oscillation with impacts on salmon production. Am Meteorol Soc 78:1069–1079. doi: 10.1175/1520-0477

Moore AM, Arango HG, Di Lorenzo E, Cornuelle BD, Miller JM, Neilson DJ (2004) A comprehensive ocean prediction and analysis system based on the tangent linear and adjoint of a regional ocean model. 7:227–258. doi: 10.1016/j.ocemod.2003.11.001

Newman M, Alexander MA, Ault TR, Cobb KM, Deser C, Di Lorenzo E, Mantua NJ, Miller AJ, Minobe S, Nakamura H, Schneider N, Vimont DJ, Phillips AS, Scott JD, Smith CA (2016) The Pacific decadal oscillation, revisited. J Clim 29:4399–4427. doi: 10.1175/JCLI-D-15-0508.1

Namias J, Born RM (1970) Temporal coherence in the North Pacific sea-surface temperature patterns. J Geophys Res 75:5952–5955. doi:10.1029/JC075i030p05952

National Marine Fisheries Service (2014) Fisheries Economics of the United States, 2012. U.S. Dept. Commerce, NOAA Tech. Memo. NMFS-F/SPO-137, 175p.

Nurdin S, Mustapha MA, Lihan T (2013) The relationship between sea surface temperature and chlorophyll-a concentration in fisheries aggregation area in the archipelagic waters of spermonde using satellite images. AIP Conf Proc 1571:466–472. doi: 10.1063/1.4858699

Overland JE, Alheit J, Bakun A, Hurrell JW, Mackas DL, Miller AJ (2010) Climate controls on marine ecosystems and fish populations. J Mar Syst 79:305–315. doi: 10.1016/j.jmarsys.2008.12.009

Overland JE, Rodionov S, Minobe S, Bond N (2008) North Pacific regime shifts: Definitions, issues and recent transitions. Prog Oceanogr 77:92–102. doi: 10.1016/j.pocean.2008.03.016

Pauly D (1980) On the interrelationships between natural mortality, growth parameters, and mean environmental temperature in 175 fish stocks. ICES J Mar Sci 39:175–192. doi: 10.1093/icesjms/39.2.175

Ricker WE (1954) Stock and recruitment. J Fish Res Board Can 11:559–623.

Sherman K (2015) Sustaining the world's large marine ecosystems. ICES J Mar Sci 72(9) 2521–2531. doi: 10.1093/icesjms/fsv136

Stopha M (2018) Alaska salmon fisheries enhancement annual report 2017. Alaska Department of Fish and Game, Division of Commercial Fisheries, Regional Information Report 5J18-02, Juneau.

Yeh SW, Kang YJ, Noh Y, Miller AJ (2011) The North Pacific climate transitions of the winters of 1976/77 and 1988/89. J Clim 24:1170–1183. doi: 10.1175/2010JCLI3325.1

Zhang Y, Wallace JM, Battisti DS (1997) ENSO-like interdecadal variability: 1900-93. J Clim 10:1004–1020. doi: 10.1175/1520-0442

Chapter 2

Climate and population dynamics: exploring the decay of statistical relationships between sea surface temperature and salmon productivity in the Gulf of Alaska

2.1 Introduction

Biological processes are often related with temperature to help explain variability in recruitment and production (Pauly 1980; Clark et al. 2003). Fisheries oceanographers utilize temperature time-series to explain adult and juvenile survival, relating life-stage based mortality to direct and indirect effects of temperature change (Lee et al. 2003; Nurdin et al. 2013). Large-scale climate indices such as the Pacific Decadal Oscillation (PDO; Mantua et al. 1997) in the North Pacific summarize basin-scale SST variability into a single metric that has been used in biological studies (Mantua et al. 1997). Considered a low-frequency, El Niño-like oscillation (Mantua and Hare 2002), the PDO itself was originally defined to help explain the variability in the production of Pacific salmon species (*Oncorhynchus spp.*) in the Gulf of Alaska (GOA; Mantua et al. 1997). While the PDO has been used extensively, like other large-scale indices, specific species-ecosystem relationships are not well understood. The PDO incorporates variability in North Pacific SST anomalies poleward of 20º (Zhang et al. 1997), therefore including variability in regions that certain organisms never enter.

The GOA is home to multiple economically and culturally important fisheries; none as important as the Pacific salmon (*Oncorhynchus spp.*) fisheries (Stopha 2018). Chum salmon, (*Oncorhynchus keta*), pink salmon (*Oncorhynchus gorbuscha*), and

sockeye salmon (*Oncorhynchus nerka*) account for a large portion of the economic importance of GOA salmon species (Stopha 2018). Culturally, salmon are harvested in subsistence fisheries, where communities rely on the fish for their survival and well-being (Pacific Fishery Management Council 2016). Management practices for salmon populations have been in place since the 1970s and are more consistently based on single-species fisheries management with less weight put on their interactions with climate properties. Improved understanding of how salmon interact with their environment is necessary to manage their populations in the best manner.

Recruitment indices have been used in fisheries management as a proxy for the survival of offspring and to estimate approximate spawner populations, but recruit and spawner populations can be difficult to measure. Population estimates are less challenging for salmon due to their high stream fidelity, constituting stream fidelity rates of over 97% in certain species (Quinn 1993). Salmon are counted individually and acoustically when they return to the streams where they hatched. Due to variable life history traits, certain species do not return to their natal streams with their original cohort, so aging is used to identify the year of spawning (Peterman et al. 1998). Pink salmon are unique in their life histories since they smolt in their first few months and return to their natal streams after approximately only 18 months in the ocean, creating a two-year lifecycle. Distinct even-odd year populations are present, and these adults almost never mix between the populations (Beacham et al. 2012). Sockeye and chum salmon both have different residence times in the freshwater and ocean realms and therefore must be traced to the year of their origin.

Spawner-recruitment (SR) curves have been used to model populations and estimate physical and biological impacts on recruit survival (Ricker, 1954; Jensen et al. 1996). One of the initial spawner-recruitment curves, the Ricker spawner-recruitment curve model (hereafter "Ricker curve"; Ricker, 1954), estimates recruits per spawner each year by assuming a theoretical relationship between the number of spawners and the number of recruits. Deviations from the curve are assumed to be natural variations in the survival of the offspring before recruitment. To explore the influence of environmental processes on recruitment, deviations from the spawner-recruit curve are correlated to different processes (Cushing 1971; Mueter et al. 2002; Schirripa et al. 2009). The Ricker curve is used for salmon because of the assumed density related mortality in freshwater and upon ocean entry (Huntsman et al. 2017). Freshwater mortality is not believed to be the most important in salmon population dynamics (Irvine et al. 2013), but it is necessary to account for it in the spawner-recruitment curve.

Historically, SST has been linked with biological and other physical properties as covariates. The PDO is considered to be the first mode of variability of both SST and sea surface height anomalies (SSHa; Mantua and Hare 2002), since SST and SSHa are considered to maintain a steady relationship through time. Similarly, the North Pacific Gyre Oscillation (NPGO) is considered the second mode of climate variability in the North Pacific, described by the second mode of SSHa and SST variability (Di Lorenzo et al. 2008). During the late 1980s, a shift occurred in the climate drivers in the North Pacific (Hare and Mantua 2000; Overland et al. 2008; Yeh et al. 2011), but the biological and physical implications are not well understood in the GOA.

In this study, I test the stationarity of the relationships between GOA salmon populations and GOA shelf indices. To focus the study, I ask: does a specific index maintain a stationary relationship with salmon-community-wide or individual species indices across the 1980s shift? In this study, GOA shelf physical properties were summarized into principal component (PC) indices using an empirical orthogonal function (EOF) analysis. The indices were then correlated to salmon Ricker curve residuals before and after 1988/89 using Pearson correlation coefficients, to describe the relationships between individual salmon populations and the environment with which they interact. Overall species and community relationships with each index were compared using a z-test of mean Fisher z-transformed, Pearson correlation coefficients. A reduced correlation between properties and salmon recruitment indices may be linked to a change in the covariance among regional properties, possibly identifying spurious relationships between salmon recruitment indices and physical properties that were previously believed to be consistent and important.

Six properties along the GOA shelf are used in this study that have been shown to act as proxies for either salmon production and survival, or biological processes: SST, SSHa, sea surface salinity (SSS), vertical velocity, mixed layer depth (MLD), and wind stress. SST has been correlated with salmon survival (Downton and Miller 1998; Cole 2000; Mueter et al. 2002, Chittenden et al. 2009). Di Lorenzo et al. (2008) showed a correlation between primary productivity and SSHa indices in the North Pacific. SSHa has been shown to be correlated to chlorophyll concentrations in the North Pacific (Wilson and Adamec 2001; Di Lorenzo et al. 2008). Mueter et al. (2002) showed salmon are weakly correlated with SSS. SSS is also a proxy for freshwater runoff which has been

shown to correlate to nutrient availability (Crusius et al. 2017). Wind stress has been shown to affect vertical velocity and MLD (Pacanowski and Philander 1981; Lincoln et al. 2016), each affecting nutrient availability for phytoplankton (Fiechter et al. 2009; Crusius et al. 2017). Wind stress, MLD, and SSS may act as a proxy for or directly impact the timing of stratification influencing the timing of the spring bloom and overall water column stability following the winter. The amount of stratification and the timing and duration of the spring bloom may affect salmon survival by influencing the amount of food available for smolt (Gargett 1997; Henson 2007).

The winter of 1988/89 is used to separate the two periods, 1961-1988 (first period) and 1989-2010 (second period), to simplify comparisons across the late 1980s. The summer of 1988 was attributed with anomalously high temperatures across North America coupled with shifting Pacific jet streams and anomalous tropical SST, creating a convection feedback loop (Ting and Wang 1997). The year was also a La Niña year, contributing to cooler water in the North Pacific and increased winds (Overland et al. 2010). Winter is also the period of greatest variability (Yeh et al. 2011) and associated with the greatest influence in the PDO and El Nino Southern Oscillation (Newman et al. 2003), making it the ideal period to split 1988 and 1989.

2.2 Methods

2.2.1 Spawner-Recruitment Curves and Residuals

Spawner and recruitment (catch plus returns) abundance time-series data were provided by Randall M. Peterman's group at Simon Fraser University in Burnaby, British Columbia. 41 GOA based salmon stocks were used in this analysis, including 11 chum salmon stocks, 22 pink salmon stocks, and 8 sockeye salmon stocks (Figure 2.1a-c).

Collection methodology for chum (Pyper et al. 2002), pink (Pyper et al. 2001), and sockeye (Peterman et al. 1998) salmon data can be found elsewhere. Recruits were lagged to their cohort year.

Recruits-per-spawner was calculated by dividing the number of recruits by the number of counted fish that migrate upstream. A Ricker curve model

(1) $\log(R_{nt}/S_{nt}) = \log(\alpha_n) - \beta_n S_{nt}$

was fit to each stock's recruits-per-spawner time-series to estimate the ideal relationship between the number of spawners and the returning recruits using. R_{nt} represents recruits of year class t and stock n. S_{nt} represents spawners of year class t and stock n. α_n and β_n are constants of stock n. A Ricker curve assumes density related mortality, which is important in the freshwater and ocean entry stages of salmon (Huntsman et al. 2017), which is the main driving factor for its use over a Beverton-Holt curve (Jensen et al. 1996) or a Generalized Additive Model. Also, using the Ricker curve follows the procedures from Mueter et al. (2002). SR residuals were calculated by subtracting Ricker curve values from the corresponding recruits-per-spawner values. The residuals, returned to time-series form, were then correlated with physical properties.

2.2.2 Climate and Oceanographic Properties

The Simple Ocean Data Assimilation (SODA) model version 2.2.4 with monthly averages on a temporal resolution on a 0.5º x 0.5º grid was used for all physical properties. The shelf of the GOA, shallower than 3000 meters and within the area bounded by 44º-62º N and 180º -120º W (Figure 2.1 a), was used to estimate the region where salmon smolts most likely are affected by physical processes during the period of ocean entry.

Two periods were used in this study: 1961-1988 and 1989-2010. The monthly mean was calculated over the shelf at each grid point over each period, and then subtracted from the original data to remove the seasonality, creating anomalies. An EOF analysis was applied to each property to capture the variability over the shelf. The first EOF (EOF1) of the region represents the leading mode of variability over the shelf forming a single, monthly time series that was correlated to salmon spawner-recruitment residuals. Each time series was then averaged over the entire year (January-December) to generate mean yearly anomalies.

Six properties were used in this analysis: SST, SSHa, sea surface salinity (SSS), water column vertical velocity, mixed layer depth (MLD), and wind stress (Figure 2.2-2.7). The EOF analysis distilled the variability of each property over the GOA shelf into a single time-series to be correlated with spawner-recruitment residuals. The EOF of wind stress was calculated by combining the meridional and zonal wind stress components into one analysis to include the variability present in both directions, since meridional and zonal wind components are not independent.

2.2.3 Statistical Analysis

Using a Pearson correlation, the time-series of EOF1 for each property was correlated to each salmon stock Ricker curve residual time-series. Salmon indices were lagged to their year of ocean entry year according to each species' average residence time in freshwater; sockeye salmon were lagged two years, and chum and pink salmon were lagged one year. The correlation coefficients were transformed using a Fisher z-transformation (Mudholkar 1983) into a normal distribution by weighting each correlation coefficient for sample size and correlation coefficient value. The correlations

were aggregated into four groups, three based on the species, and a fourth group that includes all species. All correlations between stocks and a single property were transformed into a normal distribution, and a z-test was used to test if the mean of the pre- and post- 1988/89 z-scores were significantly different than zero. A z-test was also used to determine if the pre- and post 1988/89 z-value means were different. The analyses were broken into all species and individual species comparisons. A stationary relationship between salmon and a property would be characterized by a mean z-score that is significantly different than zero in both time periods and the mean z-score between the two time periods are not significantly different.

To classify a stationary relationship between the salmon community or species and an index, the mean z-value of each period must remain significantly different than zero and the means of the two periods must not be significantly different. If the mean z-value was not significantly different than zero, it is believed that the relationship was not meaningful even if the two periods' mean z-values were not significantly different.

2.3 Results

For the correlations that were estimated between salmon SR residuals and each index, z-scores were compared across 1988/89 to explore whether if each relationship remained consistent across the 1988/89 winter. SST, SSHa, and wind stress each had dynamic relationships with salmon across the 1988/89 winter. SST had a mean positive relationship with all species' Ricker curve residuals before 1989, but the relationship reduced to near zero after 1989 (Figure 2.8 a). Chum salmon had a positive mean relationship with SST that was significantly different than zero before 1989, but the relationship after 1988, while not significantly different than the relationship before 1989,

was not significantly different than zero. Sockeye salmon before 1989 had a positive mean correlation with SST, but a negative mean correlation after 1988 (Figure 2.8 e). Pink salmon had a positive mean correlation with SST before and after 1988/89, but the two-mean z-values were significantly different from one another (Figure 2.8 f). Salmon had the same relationships to SSHa as they did with SST, except that both mean z-values after 1988 for sockeye and pink salmon were not significantly different than zero (Figure 2.9 e-f). Wind stress had mean relationships with all species and pink salmon before 1989 that were significantly different than zero (Figure 2.10 a-b). All species, pink, and sockeye salmon all had significantly different relationships with wind stress across the 1988/89 winter (Figure 2.10 e-f).

SSS, vertical velocity, and MLD each had less dynamic relationships with salmon during each period. Relationships between salmon and SSS both before and after 1988/89 were never significantly different, but the pre-1989 mean correlation was significantly different than zero for all species, chum, and sockeye salmon, that then was not significantly different than zero after 1988 (Figure 2.11 a-f). Vertical velocity never had a mean relationship with salmon that was significantly different than zero. Sockeye salmon did have a change in their relationship with vertical velocity across 1988/89 (Figure 2.12 e). MLD had a consistent near zero mean correlation with each salmon group except post-1988 sockeye salmon (Figure 2.13 e). Relationships were never significantly different from one another across 1988/89.

The correlation between SST EOF1 and the PDO index in the period before 1989 was high and significant ($r = 0.74$, $p << 0.01$). The correlation between SST EOF1 and the PDO index in the period after 1988 was also high and significant ($r = 0.85$, $p << 0.01$).

2.4 Discussion

SST and SSHa had significant relationships with the, chum, pink, sockeye, and all species as described by several studies (Downton and Miller 1998; Cole 2000; Mueter et al. 2002; Di Lorenzo et al. 2008; Chittenden et al. 2009). But in this study, those relationships are dynamic and not stationary across 1988/89. Similarly, wind stress had a significant relationship with pink salmon and all species before 1989, but the relationship fell apart after 1988. No property maintained a significant relationship with any salmon group's mean z-value across 1988/89 where both period mean z-values were significantly different than zero. This means that no properties maintained a stationary relationship with GOA salmon.

The original correlation between the PDO and Pacific salmon indices in the GOA (Mantua et al. 1997) suggested a stationary relationship for all species with SST and by extension of the PDO definition, SSHa. SST and SSHa maintained similar relationships with salmon both before and after 1988/89, but neither property maintained a stationary relationship with salmon indices across 1988/89. The mean relationship with SST and pink salmon did remain positive after 1988, but the relationship changed and became significantly different than the mean relationship before 1989. Similarly, SST had a mean relationship that was significantly different than zero with sockeye salmon after 1988, but the relationship changed from positive to negative, which is not considered stationary.

Since SST and SSHa do not maintain stationary relationships with salmon, the assumption that the PDO maintains a meaningful relationship with salmon, is not robust. Kilduff et al. (2015) showed that the NPGO index has become a better predictor of salmon survival rates over the PDO index. SST maintains a strong relationship across

1988/89 with the PDO index, further reducing the possibility of a meaningful relationship between the PDO salmon species found by Mantua et al. (1997). The PDO summarizes variability across the North Pacific (Zhang et al. 1997), but much of this variability is area that is not part of GOA salmon's ecosystem.

In this study, I have assumed that the most important period in a salmon's life cycle is the period of ocean entry. By focusing on the physical variability of the GOA shelf throughout the year, the potential to identify regional impacts of oceanographic variability on salmon production is limited to only the period when the smolt enter the ocean and reside on the shelf and when adults return to their natal streams. If salmon are not responding to the variability along their locations of ocean entry, then the period of ocean entry may not be the source of population driving mortality, but just a small piece of the puzzle. This study focuses on a single region where salmon populations have been shown to vary synchronously (Mueter et al. 2002; Pyper et al. 2005; Malick et al. 2015). Salmon in similar locations should have similar relationships to the indices from this study if they are actually being affected by the properties.

This study does not focus on the specific month of ocean entry, which may have an effect on salmon smolt survival (Beamish and Mahnken 2001) but focuses on the period of ocean entry and residence. It has been shown that juvenile salmon remain in the shelf region for several months (Boldt and Haldorson 2011), and this residence time may have a greater impact on salmon survival then just the period of ocean entry alone (Malick et al. 2011). Sustained food sources and limited predation allows the juvenile salmon to grow and survive, and juvenile densities may dictate the ability to feed or the likelihood of predation (Duffy and Beauchamp 2011).

If the period of ocean entry and shelf residence is not as important as previously believed, other periods with many more mechanistic challenges need to be tested. Age of ocean entry, size at ocean entry (Malick et al. 2011), age of return from the oceanic realm, and the period of time spent in the ocean are all candidates to explore the impacts of climate processes on specific salmon dynamics. Beamish and Mahnken (2001) related size of ocean entry and period of ocean entry to survival and concluded that the availability of nutrients to support adequate food sources for smolt may be the most important for survival. Results of my analysis comparing SSHa and wind stress with salmon production support this idea. However, MLD and vertical velocity might also be associated with nutrient supply, and my results did not indicate that these properties had a relationship with salmon production.

Since SST, and by definition the PDO index, does not exhibit stationary correlations with deviations from the SR curve. It has been shown that the NPGO is a good predictor of salmon survival after the late 1980s (Kilduff et al. 2015), and PC1 of SSHa had similar predictive capabilities as PC1 of SST before 1989. The 1980s climate shift (Hare and Mantua 2000; Litzow 2006; Overland et al. 2008; Yeh et al. 2011) may have resulted in a change in the modes of variability for SSHa where the PC1 of SSHa became the PC2 of SSHa. The PC2 of SSHa in the North Pacific is the defining index for the NPGO (Di Lorenzo et al. 2008), supporting the findings from Kilduff et al. (2015).

Overall, salmon did not maintain a stationary relationship with any shelf index across the 1988/89 North Pacific climate shift. The loss of established relationships with salmon allude to a shift in salmon relationships with GOA indices or a shift in an unknown driver of salmon populations.

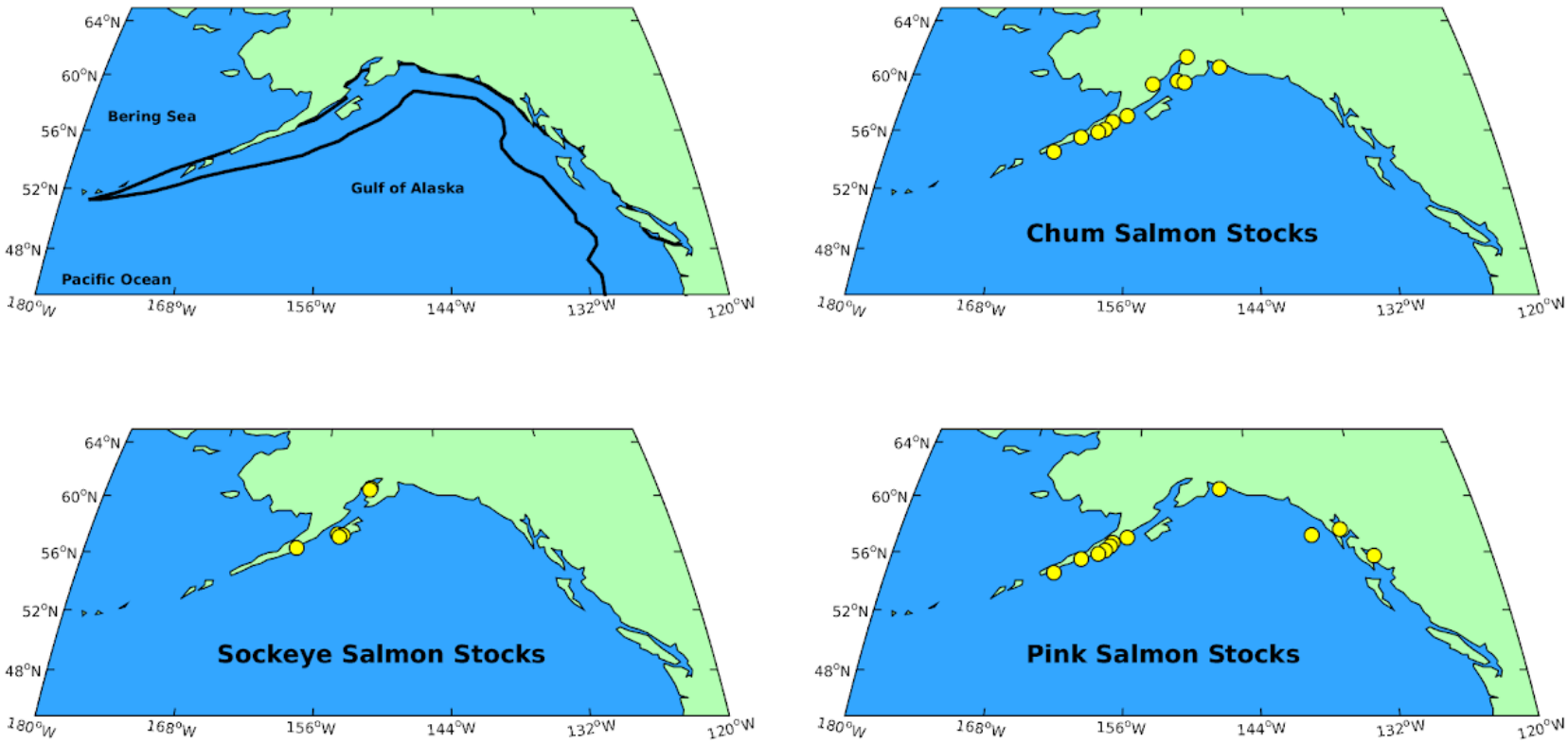

Figure 2.1. Gulf of Alaska shelf study area (a) and salmon stock locations for b) chum salmon, c) pink salmon, and d) sockeye salmon.

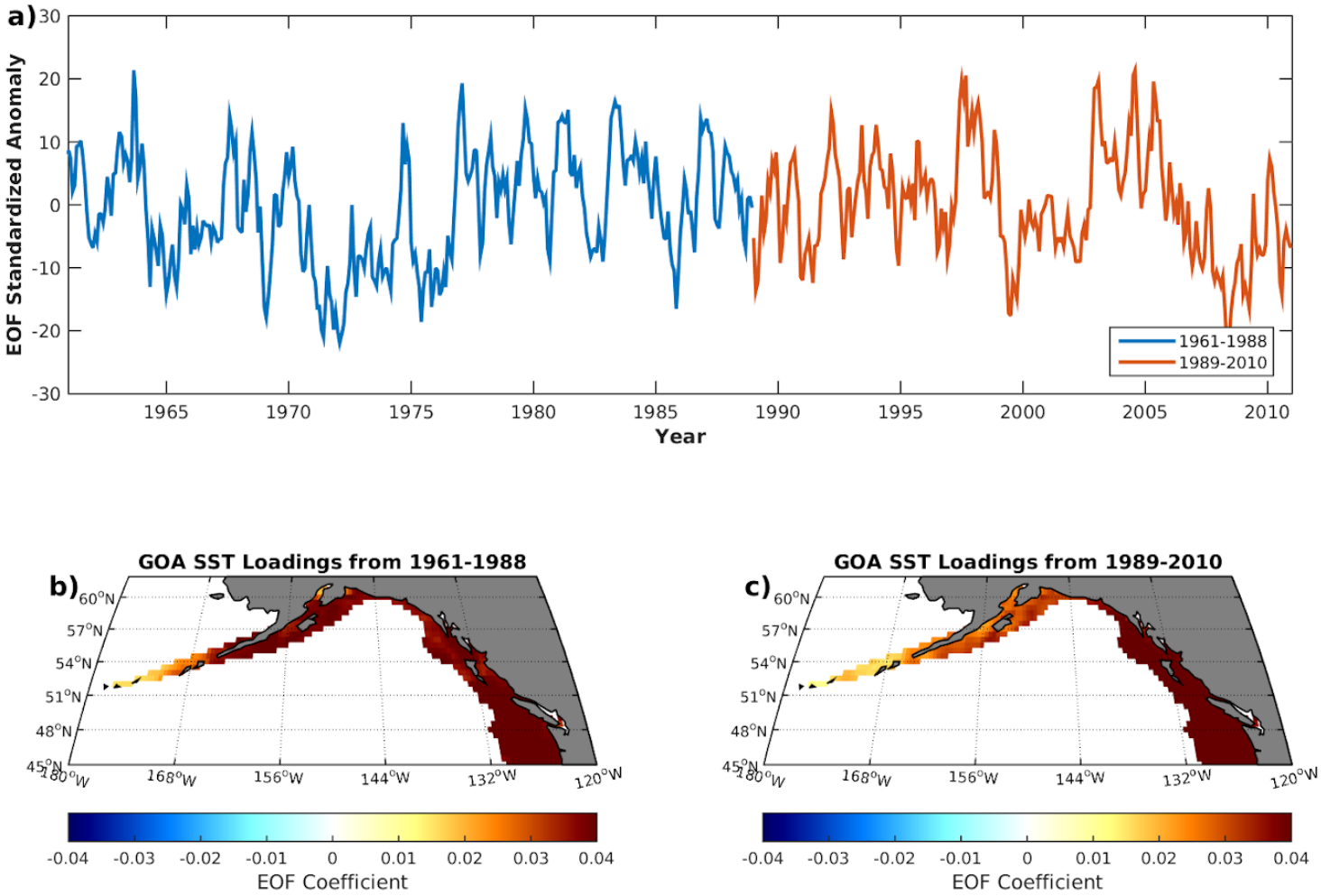

Figure 2.2. a) Sea surface temperature PC1 time series for the first period (blue line) and second period (red line) and the spatial loadings for b) first period and c) second period.

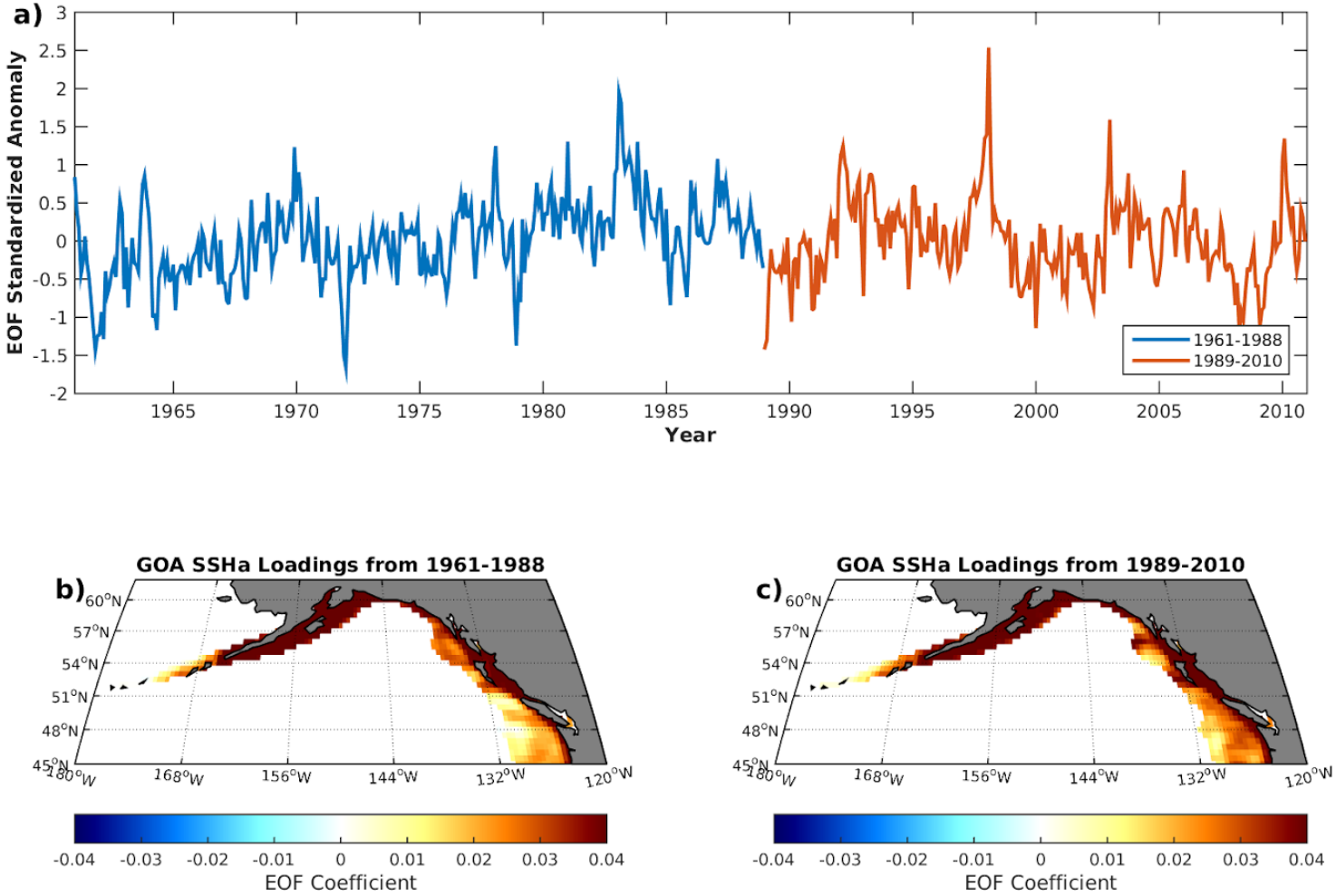

Figure 2.3. a) Sea surface height anomaly PC1 time series for the first period (blue line) and second period (red line) and the spatial loadings for b) first period and c) second period.

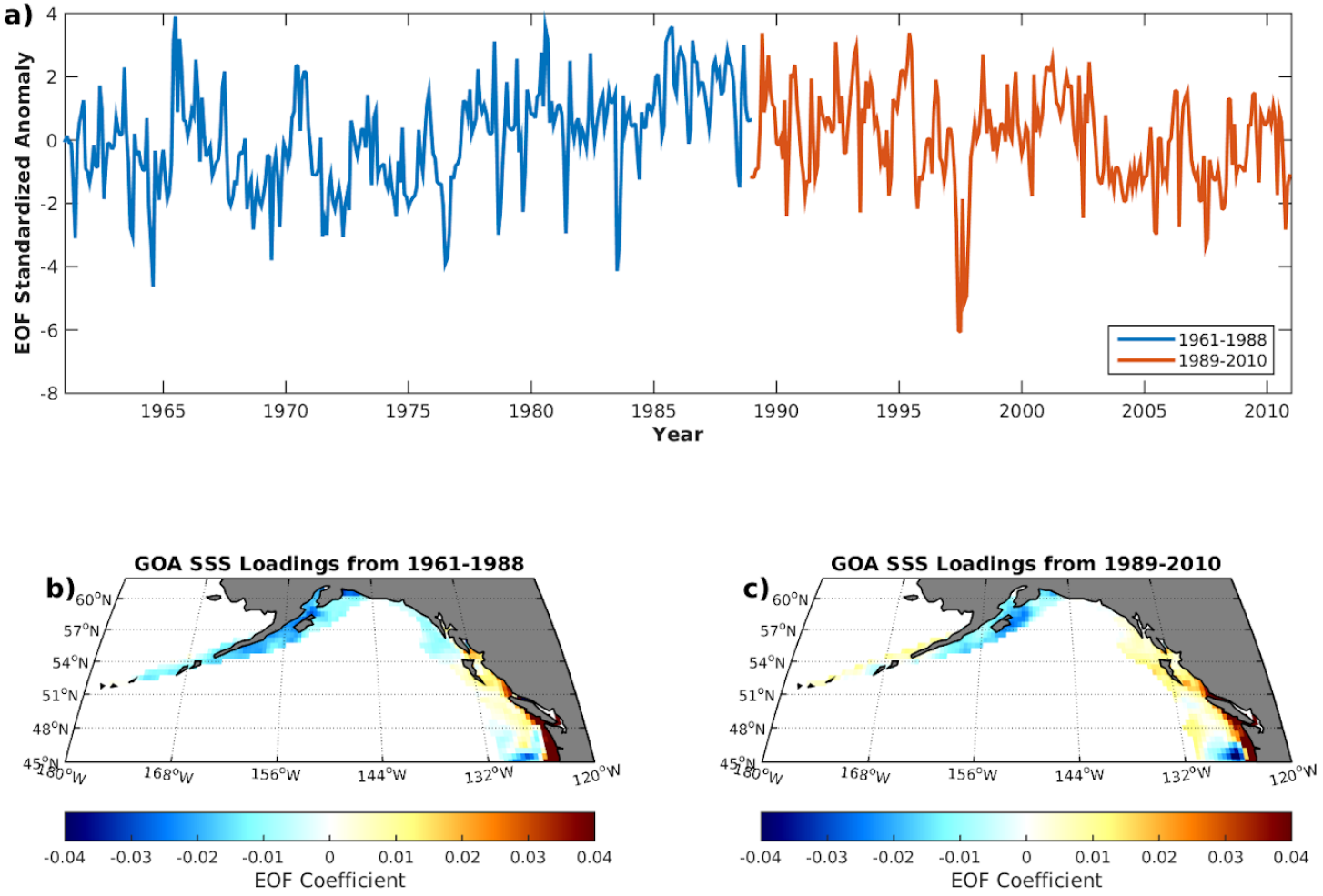

Figure 2.4. a) Sea surface salinity PC1 time series for the first period (blue line) and second period (red line) and the spatial loadings for b) first period and c) second period.

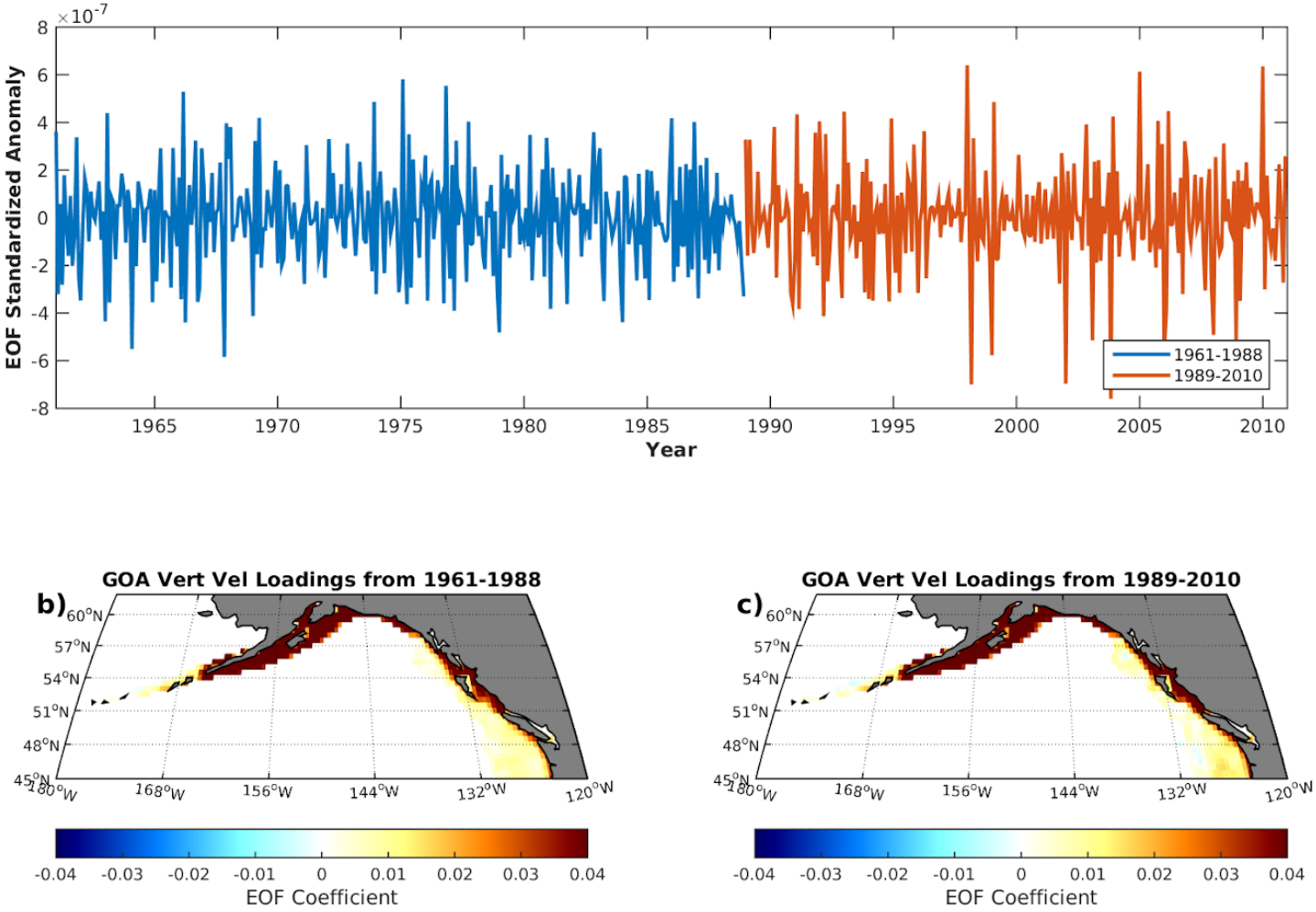

Figure 2.5. a) Vertical velocity PC1 time series for the first period (blue line) and second period (red line) and the spatial loadings for b) first period and c) second period.

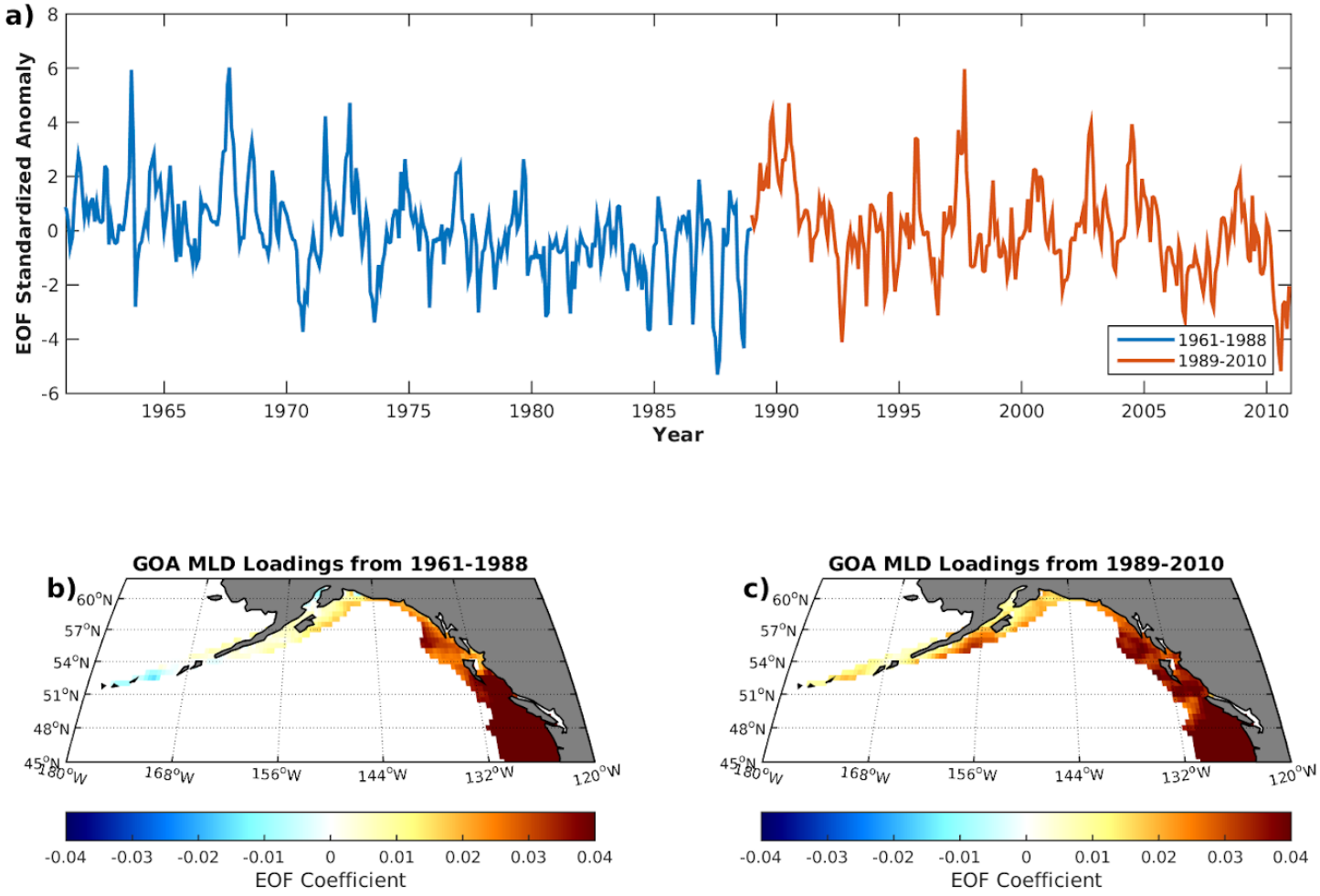

Figure 2.6. a) Mixed layer depth PC1 time series for the first period (blue line) and second period (red line) and the spatial loadings for b) first period and c) second period.

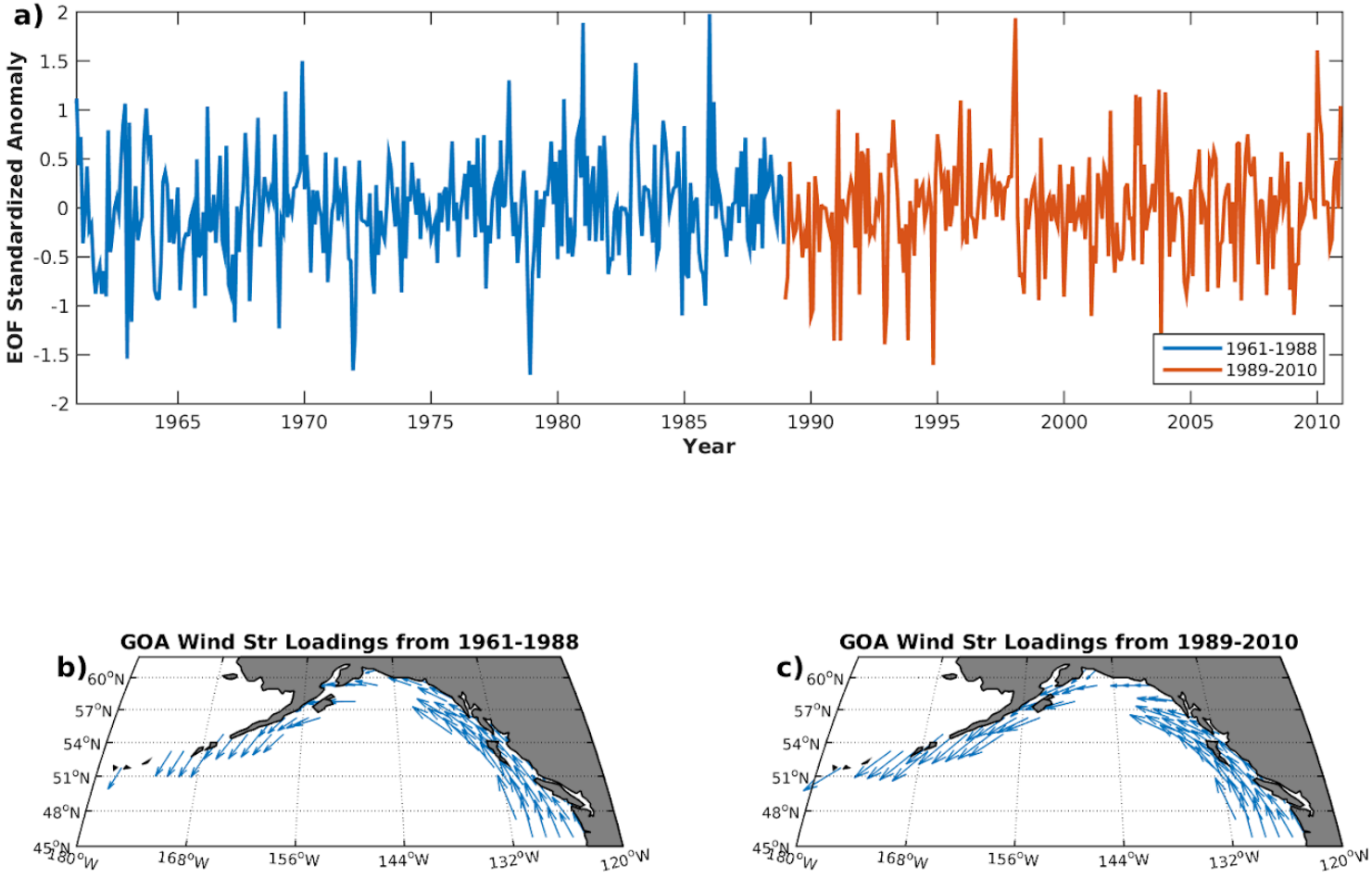

Figure 2.7. a) Wind stress PC1 time series for the first period (blue line) and second period (red line) and the spatial loadings for b) first period and c) second period.

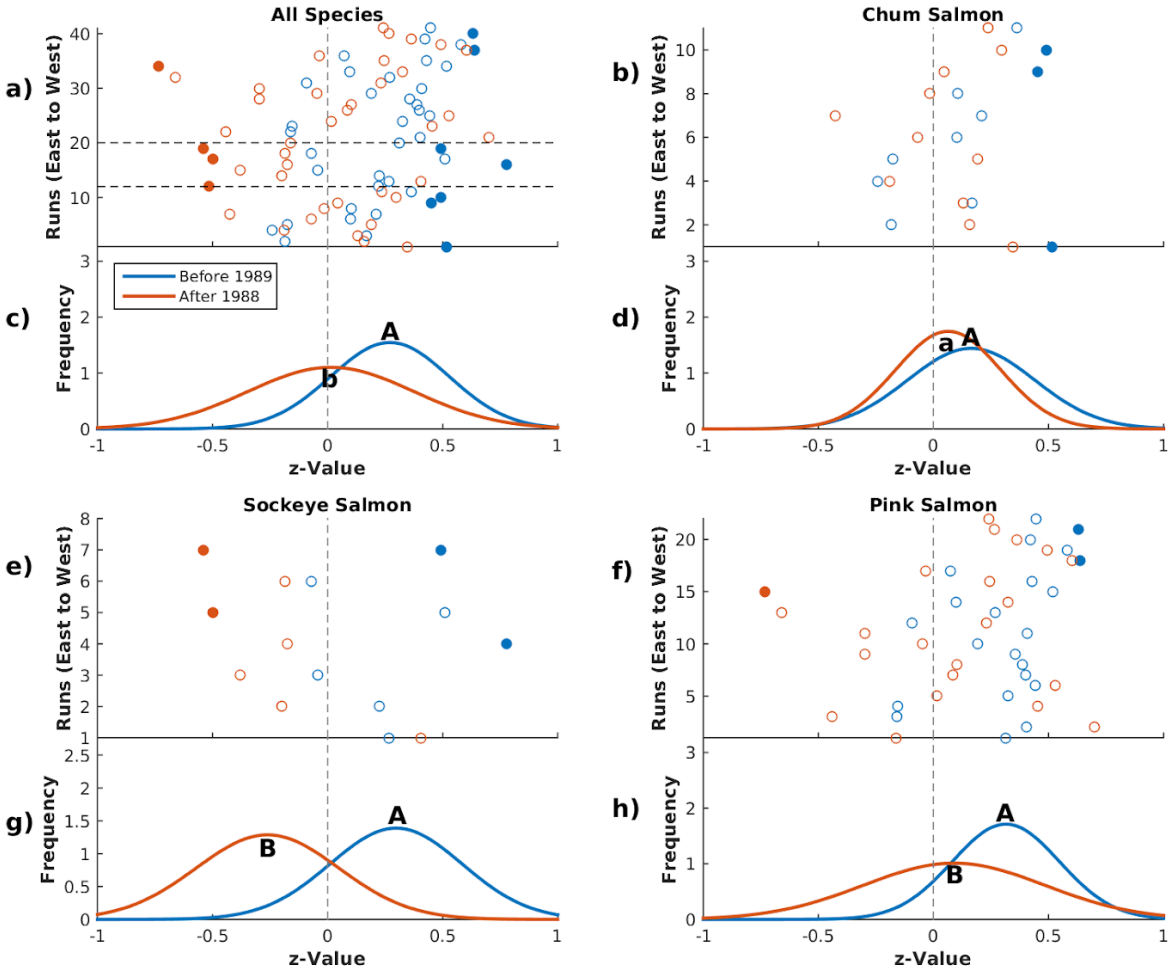

Figure 2.8 Fisher's z-value transformations of Pearson correlation coefficients with sea surface temperature EOF1 for a) all salmon stocks, b) chum salmon stocks, e) sockeye salmon stocks, and f) pink salmon stocks. Blue circles represent the correlation in the period before 1989 and the orange circles represent the correlation in the period after 1988. Closed circles are significant at 0.05. Frequency of correlation values for c) all salmon stocks, d) chum salmon stocks, g) sockeye salmon stocks, and h) pink salmon stocks. Blue lines represent the correlation in the period before 1989 and the orange lines represent the correlation in the period after 1988. Letters represent how the mean z-value correlate between periods, same letters are not significantly different at 0.05 significance level. Capital letters represent a mean z-value significantly different than zero at a 0.05 significance level.

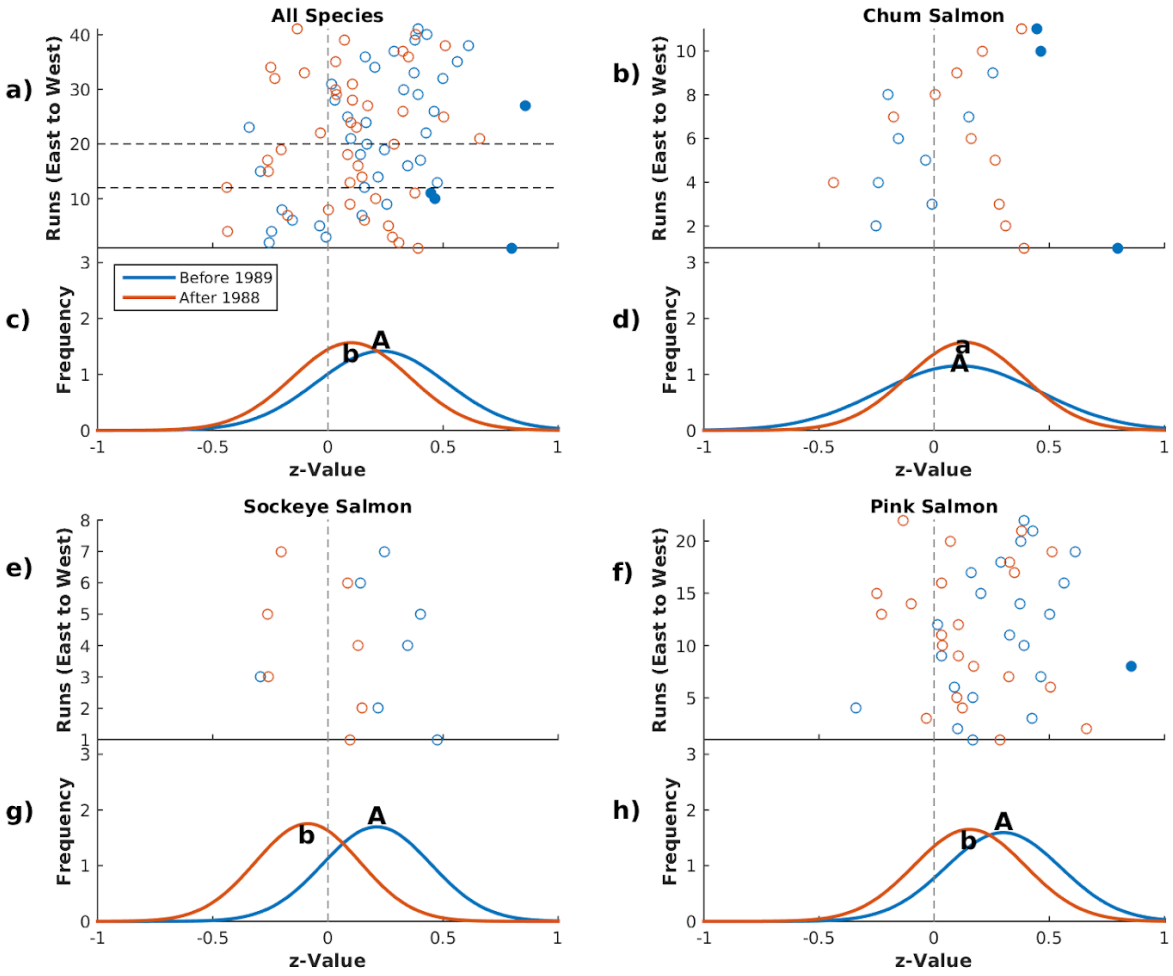

Figure 2.9 Fisher's z-value transformations of Pearson correlation coefficients with sea surface height anomalies EOF1 for a) all salmon stocks, b) chum salmon stocks, e) sockeye salmon stocks, and f) pink salmon stocks. Blue circles represent the correlation in the period before 1989 and the orange circles represent the correlation in the period after 1988. Closed circles are significant at 0.05. Frequency of correlation values for c) all salmon stocks, d) chum salmon stocks, g) sockeye salmon stocks, and h) pink salmon stocks. Blue lines represent the correlation in the period before 1989 and the orange lines represent the correlation in the period after 1988. Letters represent how the mean z-value correlate between periods, same letters are not significantly different at 0.05 significance level. Capital letters represent a mean z-value significantly different than zero at a 0.05 significance level.

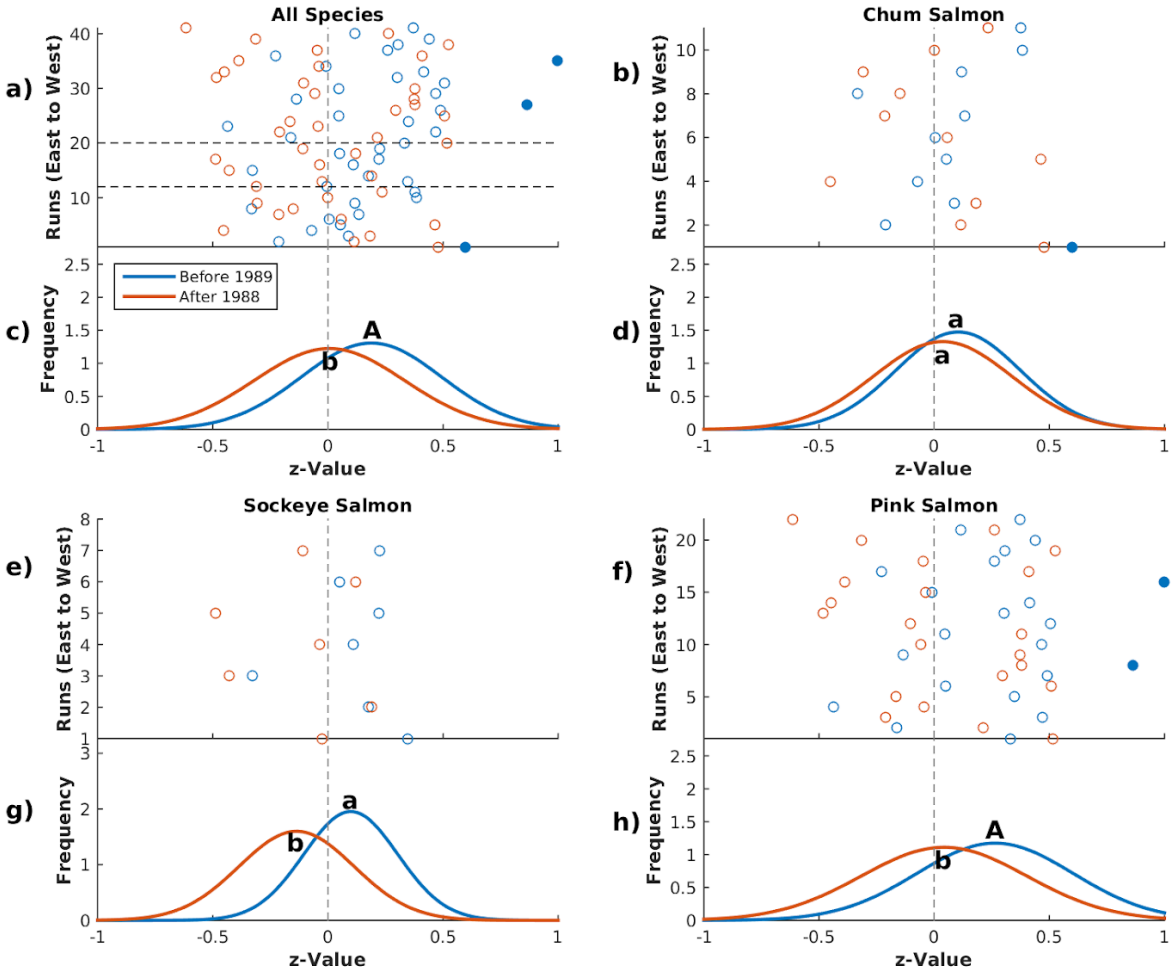

Figure 2.10 Fisher's z-value transformations of Pearson correlation coefficients with wind stress EOF1 for a) all salmon stocks, b) chum salmon stocks, e) sockeye salmon stocks, and f) pink salmon stocks. Blue circles represent the correlation in the period before 1989 and the orange circles represent the correlation in the period after 1988. Closed circles are significant at 0.05. Frequency of correlation values for c) all salmon stocks, d) chum salmon stocks, g) sockeye salmon stocks, and h) pink salmon stocks. Blue lines represent the correlation in the period before 1989 and the orange lines represent the correlation in the period after 1988. Letters represent how the mean z-value correlate between periods, same letters are not significantly different at 0.05 significance level. Capital letters represent a mean z-value significantly different than zero at a 0.05 significance level.

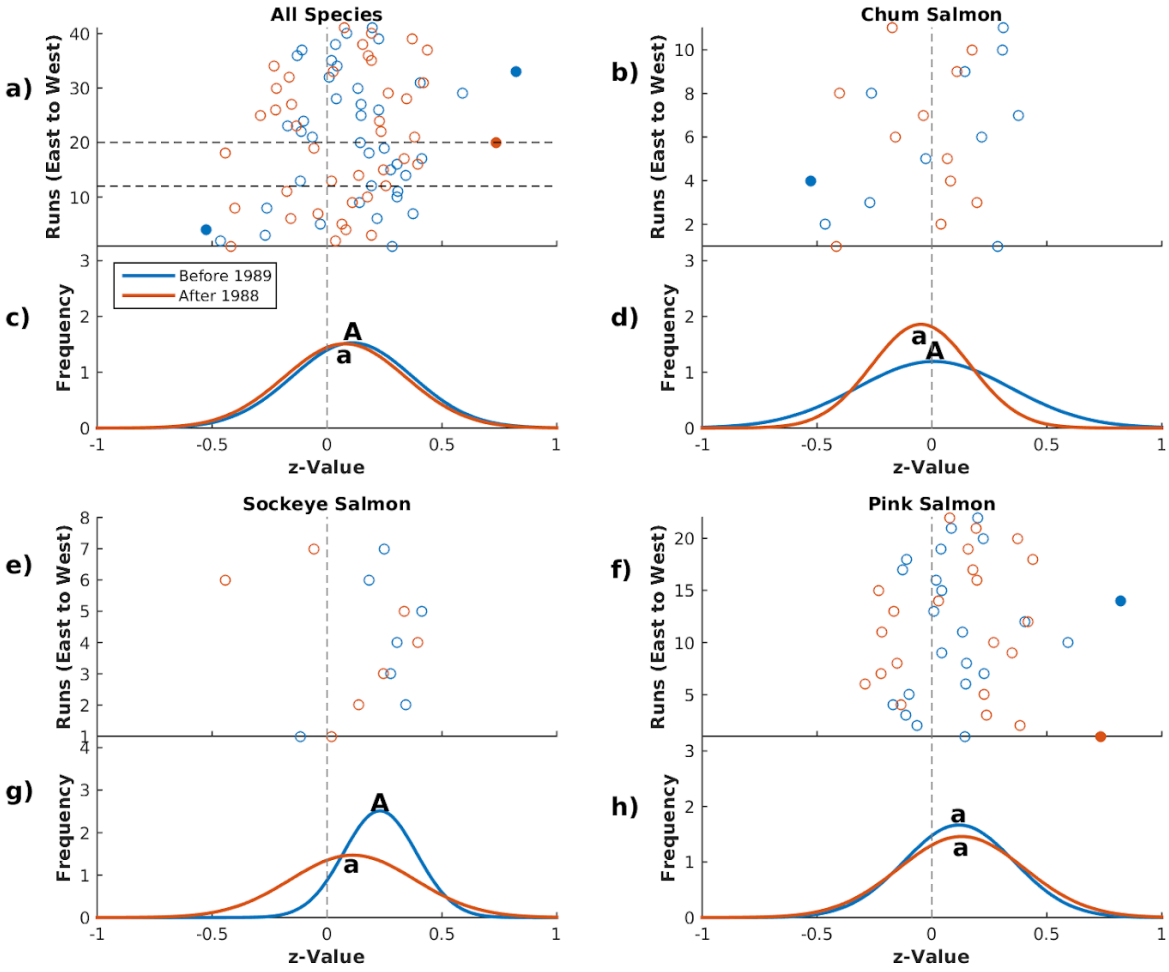

Figure 2.11 Fisher's z-value transformations of Pearson correlation coefficients with vertical velocity EOF1 for a) all salmon stocks, b) chum salmon stocks, e) sockeye salmon stocks, and f) pink salmon stocks. Blue circles represent the correlation in the period before 1989 and the orange circles represent the correlation in the period after 1988. Closed circles are significant at 0.05. Frequency of correlation values for c) all salmon stocks, d) chum salmon stocks, g) sockeye salmon stocks, and h) pink salmon stocks. Blue lines represent the correlation in the period before 1989 and the orange lines represent the correlation in the period after 1988. Letters represent how the mean z-value correlate between periods, same letters are not significantly different at 0.05 significance level. Capital letters represent a mean z-value significantly different than zero at a 0.05 significance level.

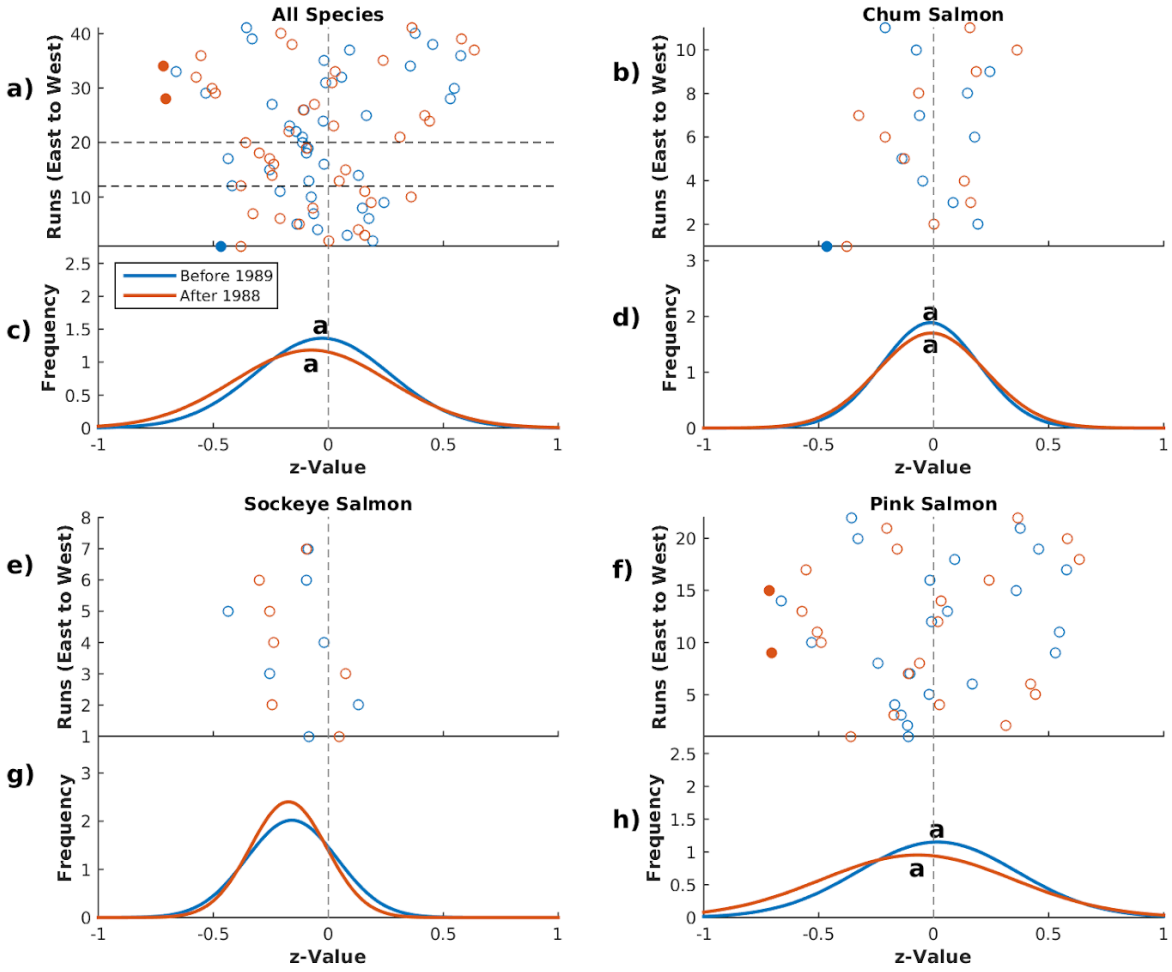

Figure 2.12 Fisher's z-value transformations of Pearson correlation coefficients with mixed layer depth EOF1 for a) all salmon stocks, b) chum salmon stocks, e) sockeye salmon stocks, and f) pink salmon stocks. Blue circles represent the correlation in the period before 1989 and the orange circles represent the correlation in the period after 1988. Closed circles are significant at 0.05. Frequency of correlation values for c) all salmon stocks, d) chum salmon stocks, g) sockeye salmon stocks, and h) pink salmon stocks. Blue lines represent the correlation in the period before 1989 and the orange lines represent the correlation in the period after 1988. Letters represent how the mean z-value correlate between periods, same letters are not significantly different at 0.05 significance level. Capital letters represent a mean z-value significantly different than zero at a 0.05 significance level.

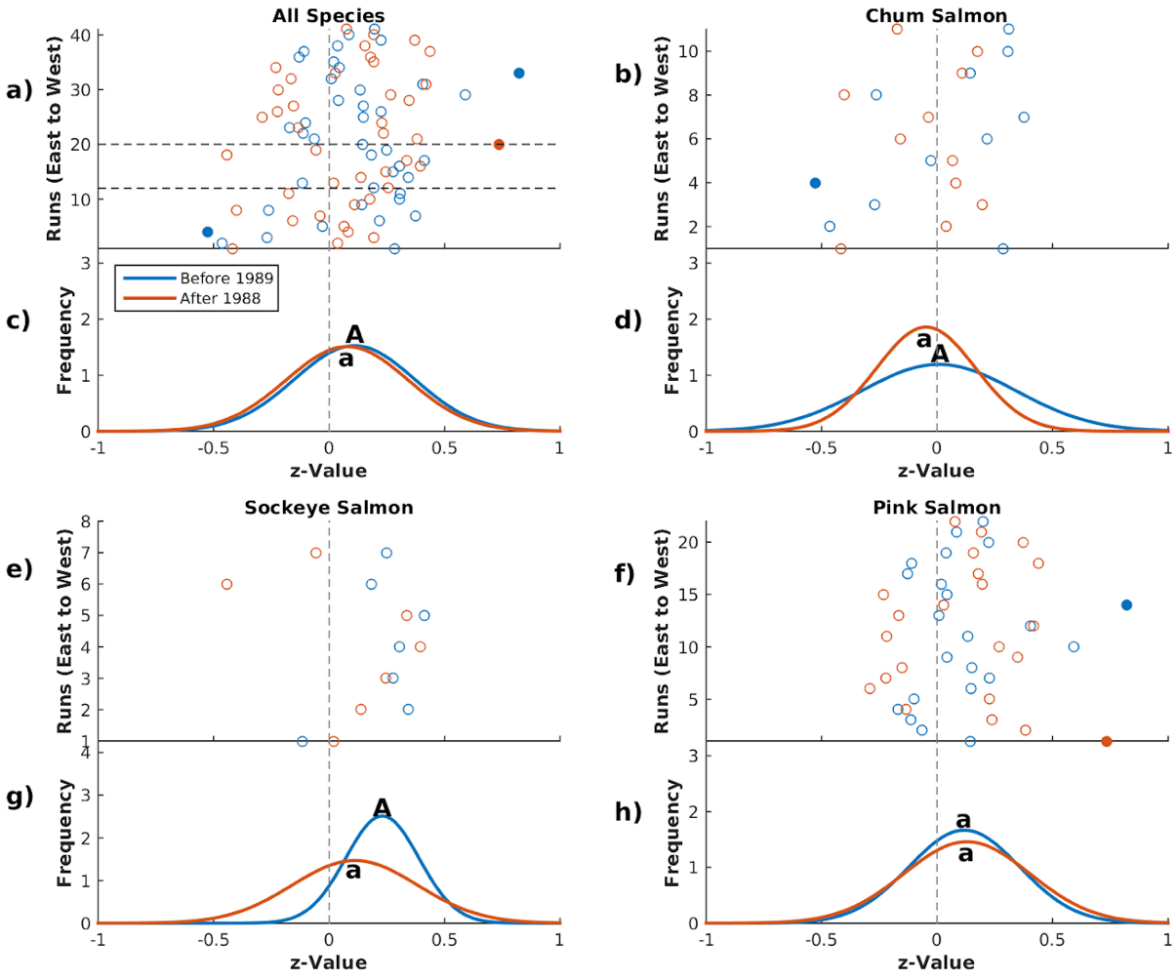

Figure 2.13 Fisher's z-value transformations of Pearson correlation coefficients with sea surface salinity EOF1 for a) all salmon stocks, b) chum salmon stocks, e) sockeye salmon stocks, and f) pink salmon stocks. Blue circles represent the correlation in the period before 1989 and the orange circles represent the correlation in the period after 1988. Closed circles are significant at 0.05. Frequency of correlation values for c) all salmon stocks, d) chum salmon stocks, g) sockeye salmon stocks, and h) pink salmon stocks. Blue lines represent the correlation in the period before 1989 and the orange lines represent the correlation in the period after 1988. Letters represent how the mean z-value correlate between periods, same letters are not significantly different at 0.05 significance level. Capital letters represent a mean z-value significantly different than zero at a 0.05 significance level.

2.5 References

Alexander AM, Scott DJ, Deser C (2000) Processes that influence sea surface temperature and ocean mixed layer depth variability in a coupled model. J Geophys Res 5:16,823–16,842. doi: 10.1029/2000JC900074

Beacham TD, McIntosh B, MacConnachie C, Spilsted B, White BA (2012) Population structure of pink salmon (*Oncorhynchus gorbuscha*) in British Columbia and Washington, determined with microsatellites. Fish Bull 110(2):242–256.

Beamish RJ, Mahnken C (2001) A critical size and period hypothesis to explain natural regulation of salmon abundance and the linkage to climate and climate change. Prog Oceanogr 49:423–437. doi: 10.1016/S0079-6611(01)00034-9

Boldt JL Haldorson LJ (2011) Seasonal and geographic variation in juvenile pink salmon diets in the northern Gulf of Alaska and Prince William Sound. Trans Am Fish Soc 132(6):1035–1052. doi: 10.1577/T02-091

Chittenden CM, Butterworth KG, Cubitt KF, Jacobs MC, Ladouceur A, Welch DW, McKinley RS, (2009) Maximum tag to body size ratios for an endangered coho salmon (*O. kisutch*) stock based on physiology and performance. Envrion Biol Fish 84:129–140. doi: 10.1007/s10641-008-9396-9

Clark RA, Fox CJ, Viner D, Livermore M (2003) North Sea cod and climate change – modelling the effects of temperature on population dynamics. Glob Chang Biol 9:1669–1680. doi: 10.1046/j.1529-8817.2003.00685.x

Cole J (2000) Coastal sea surface temperature and coho salmon production off the north-west United States. Fish Oceanogr 9:1–16.

Crusius J, Schroth AW, Resing JA, Cullen J, Campbell RW (2017) Seasonal and spatial variabilities in northern Gulf of Alaska surface water iron concentrations driven by shelf sediment resuspension, glacial meltwater, a Yakutat eddy, and dust. Glob Biogeochem Cycl 31:942–960. doi: 10.1002/2016GB005493

Cushing DH (1971) The dependence of recruitment on parent stock in different groups of fishes. J Mar Sci 33(3):340–362. doi: 10.1093/icesjms/33.3.340

Di Lorenzo E, Schneider N, Cobb KM, Chhak K, Franks PJS, Miller AJ, McWilliams JC, Bograd SJ, Arango H, Curchister E, Powell TM, Rivere P (2008) North Pacific Gyre Oscillation links ocean climate and ecosystem change. Geophys Res Lett 35:1–6. doi: 10.1029/2007GL032838

Downton MW, Miller KA (1998) Relationships between Alaskan salmon catch and North Pacific climate on interannual and interdecadal time scales. Can J Fish Aquat Sci 55(10):2255–2265.

Duffy EJ, Beauchamp DA (2011) Seasonal patterns of predation on juvenile Pacific salmon by anadromous cutthroat trout in Puget Sound. Trans Am Fish Soc 137(1):165–181. doi: 10.1577/T07-049.1

Hare SR, Mantua NJ (2000) Empirical evidence for North Pacific regime shifts in 1977 and 1989. Prog Oceanogr 47:103–145. doi: 10.1016/S0079-6611(00)00033-1

Huntsman BM, Falke JA, Savereide JW, Bennett KE (2017) The role of density-dependent and -independent processes in spawning habitat selection by salmon in an Arctic riverscape. PLoS One 12:1–21. doi: 10.1371/journal.pone.0177467

Irvine JR, O'Neill M, Godbout L, Schnute J (2013) Effects of smolt release timing and size on the survival of hatchery-origin coho salmon in the strait of Georgia. Prog Oceanogr 115:111–118. doi: 10.1016/j.pocean.2013.05.014

Jensen AL (1996) Beverton and Holt life history invariants result from optimal trade-off of reproduction and survival. Can J Fish Aqua Sci 53(4):820–822. doi: 10.1139/cjfas-53-4-820

Kilduff DP, Di Lorenzo E, Botsford LW, Teo SLH (2015) Changing central Pacific El Ninos reduce stability of North American salmon survival rates. Proc Nat Acad Sci 112(35):10962–10966. doi: 10.1073/pnas.1503190112

Lee CG, Farrell AP, Lotto A, MacNutt MJ, Hinch SG, Healey MC (2003) The effect of temperature on swimming performance and oxygen consumption in adult sockeye (Oncorhynchus nerka) and coho (O. kisutch) salmon stocks. J Exp Biol 206:3239–3251. doi: 10.1242/jeb.00547

Malick MJ, Haldorson LJ, Piccolo JJ, Boldt JL (2011) Growth and survival in relation to body size of juvenile oink salmon in the northern Gulf of Alaska. Mar Coast Fish 3(1):261–270. doi: 10.1080/19425120.2011.593467

Malick MJ, Cox SP, Mueter FJ, Peterman RM (2015) Linking phytoplankton phenology to salmon productivity along a north-south gradient in the Northeast Pacific Ocean. Can J Fish Aquat Sci 72:697–708. doi: 10.1139/cjfas-2014-0298

Mantua NJ, Hare SR, Zhang Y, Wallace JM, Francis RC (1997). A Pacific interdecadal climate oscillation with impacts on salmon production. Bull Amer Meteor Soc, 78, 1069–1079.

Mantua, NJ, Hare SR (2002) The Pacific Decadal Oscillation. J Ocean 58:35–44.

Mudholkar GS (1983) Fisher's z-transformation. Encyclopedia of Statistical Sciences, 3:130–135.

Mueter FJ, Peterman RM, Pyper BJ (2002) Opposite effects of ocean temperature on survival rates of 120 stocks of Pacific salmon (Oncorhynchus spp.) in northern and southern areas. Can J Fish Aquat Sci 59:456–463. doi: 10.1139/F02-020

Newman M, Compo GP, Alexander MA (2003) ENSO-forced variability of the Pacific decadal oscillation. J Clim 16:3853–3857. doi: 10.1175/1520-0442

Nurdin S, Mustapha MA, Lihan T (2013) The relationship between sea surface temperature and chlorophyll-a concentration in fisheries aggregation area in the archipelagic waters of spermonde using satellite images. AIP Conf Proc 1571:466–472. doi: 10.1063/1.4858699

Overland JE, Rodionov S, Minobe S, Bond N (2008) North Pacific regime shifts: Definitions, issues and recent transitions. Prog Oceanogr 77:92–102. doi: 10.1016/j.pocean.2008.03.016

Overland JE, Alheit J, Bakun A, Hurell JW, Mackas DL, Miller AJ (2010) Climate controls on marine ecosystems and fish populations. J Mar Syst 79:305–315. doi: 10.1016/j.jmarsys.2008.12.009

Pacanowski RC, Philander SGH (1981) Parameterization of vertical mixing in numerical models of tropical oceans. J Phys Ocenogr 1:1443–1451.

Pacific Fishery Management Council (2016) Review of 2015 Ocean Salmon Fisheries: Stock Assessment and Fishery Evaluation Document for the Pacific Coast Salmon Fishery Management Plan. (Document prepared for the Council and its advisory entities.) Pacific Fishery Management Council, 7700 NE Ambassador Place, Suite 101, Portland, Oregon 97220-1384.

Pauly D (1980) On the interrelationships between natural mortality, growth parameters, and mean environmental temperature in 175 fish stocks. ICES J Mar Sci 39:175–192. doi: 10.1093/icesjms/39.2.175

Peterman RM, Pyper BJ, Lapointe MF, Adkison MD, Walters CJ (1998) Patterns of covariation in survival rates of British Columbian and Alaskan sockeye salmon (Oncorhynchus nerka) stocks. Can J Fish Aquat Sci 55(11):2503–2517. doi:10.1139/f98-179.

Pyper BJ, Mueter FJ, Peterman RM, Blackbourn DJ, Wood CC (2001) Spatial covariation in survival rates of Northeast Pacific pink salmon (Oncorhynchus gorbuscha). Can J Fish Aquat Sci 58:1501–1515. doi: 10.1139/f01-096

Pyper BJ, Mueter FJ, Peterman RM, Blackbourn DJ, Wood CC (2002) Spatial covariation in survival rates of Northeast Pacific chum salmon. Trans Am Fish Soc 131:343–363. doi: 10.1577/1548-8659(2002)131

Pyper BJ, Mueter FJ, Peterman RM (2011) Across-species comparisons of spatial scales of environmental effects on survival rates of northeast Pacific salmon. Trans Am Fish Soc 134(1):86–104. doi: 10.1577/T04-034.1

Ricker WE (1954) Stock and recruitment. J Fish Res Board Can. 11:559–623.

Schirripa MJ, Goodyear CP, Methot RM (2009) Testing different methods of incorporating climate data into the assessment of the US West Coast sablefish. J Mar Sci 66:1605–1613.

Stopha M (2018) Alaska salmon fisheries enhancement annual report 2017. Alaska Department of Fish and Game, Division of Commercial Fisheries, Regional Information Report 5J18-02, Juneau.

Ting MF, Wang H (1997) Summertime US precipitation variability and its relation to Pacific sea surface temperature. J Clim 10:1853–1873. doi: 10.1175/1520-0442

Quinn TP (1993) A review of homing and straying of wild and hatchery-produced salmon. Fish Res 18:29–44. doi: 10.1016/0165-7836(93)90038-9

Yeh SW, Kang YJ, Noh Y, Miller AJ (2011) The North Pacific climate transitions of the winters of 1976/77 and 1988/89. J Clim 24:1170–1183. doi: 10.1175/2010JCLI3325.1

Zhang Y, Wallace JM, Battisti DS (1997) ENSO-like interdecadal variability: 1900-93. J Clim 10:1004–1020. doi: 10.1175/1520-0442

Chapter 3

Climate metric coherence: Does the Pacific Decadal Oscillation act as a stationary index of climate variability in the Gulf of Alaska?

3.1 Introduction

North Pacific climate variability has been summarized by multiple indices (Hurrell, 1995; Mantua et al. 1997; Di Lorenzo et al. 2008) throughout the late 20th century. These indices provide a simple metric to compare against ecological processes. These climate indices are routinely associated with biological processes (Mantua et al. 1997; Post et al. 1999; Buchheister et al. 2017), sometimes without a strong understanding of the underlying mechanistic relationships.

The Pacific Decadal Oscillation (PDO) is a basin-scale climate index, described as the first mode of sea surface temperature (SST) and sea surface height anomaly (SSHa) variability in the North Pacific (Mantua et al. 1997). The PDO is a long-frequency—15-25 years (Mantua and Hare 2002)—El Nino-like pattern in the North Pacific. During the warm (cool) phase of the PDO, anomalous warming (cooling) occurs in the northeast Pacific and anomalous cooling in the central and western North Pacific. The PDO was originally defined as a metric to explain salmon catch variability prior to the 1990s (Mantua et al. 1997).

The North Pacific Gyre Oscillation (NPGO) is described as the second mode of SSHa or SST variability in the North Pacific (Di Lorenzo et al. 2008). The NPGO is correlated with the first mode of GOA and California Current nutrient and salinity

variability, which have been correlated to biological processes in both regions (Di Lorenzo et al. 2008).

The PDO and NPGO have been used in ecological studies as metrics for drivers of biological processes, but the mechanistic relationships between physical properties and ecological indices are not well understood. SST and SSHa are often interchangeable as ocean climate conditions (Casey and Ademeck 2002; Mantua and Hare 2002; Di Lorenzo et al. 2008), but SSHa is an integrative metric for the entire water column that may provide a better index of the drivers of ecological variability. SST is influenced by processes affecting the ocean-atmosphere boundary integrating climatological and oceanic processes (Alexander and Scott 2000). The processes that affect the water column and the surface may be considerably similar, but do not necessarily maintain a stationary relationship spatially and temporally. Therefore, using individual, localized forcing variables to understand ecological relationships may provide better insight to biological variability than the use of basin-scale climate indices.

The Gulf of Alaska (GOA) basin in the North Pacific is part of the subpolar gyre and is home to many fisheries. The GOA is a large marine ecosystem dominated by downwelling along the coast and a cyclonic central gyre with a coastal current fed by the bifurcation of the North Pacific Current (Freeland 2006). The GOA is a highly productive region, supporting several economically important fisheries. The PDO has been used as a proxy for SST anomalies in the GOA and used to explain Pacific salmon (*Oncorhynchus Sp.*) variability in the region (Hare et al. 2011).

Basin-scale indices were initially used due to limitations of data collection and overall availability of data. With the increase in computational algorithms and computing

power, climate and ocean models are readily available, providing a greater suite of properties that can be considered in analyses of ocean conditions. Data assimilation models combine in-situ and satellite measurements with numerical simulations of ocean circulation to provide estimates of physical properties in a regular grid across the global oceans (Carton and Giese 2008; Barnier et al. 1997). The Simple Ocean Data Assimilation (SODA) model is a reanalysis model that assimilates data from multiple sources to provide full ocean coverage, at multiple depths, for many properties. The properties from the SODA model can be used in studies, in the place of climate indices, to provide a more specific set of properties that impact organisms and their environments.

During the late 1980s, a change in the spatial and temporal characteristics of North Pacific climate variability was believed to have occurred (Hare and Mantua 2000; Litzow 2006; Overland et al. 2008; Yeh et al. 2011), but the physical and biological changes associated with this change are not well understood. A shift in the main pattern of variability in the North Pacific in 1988/89 was expressed in biological indices but not expressed clearly in physical processes (Hare and Mantua 2000). This shift may have been related to a variety of changes in the variability of properties and biological processes, leading to decoupling of previously described relationships. The PDO was well correlated with salmon indices in the GOA before the 1980s (Mantua et al. 1997) and, from the definition of the PDO and NPGO, SST and SSHa were considered to be interchangeable (Zhang et al. 1997; Mantua et al. 1997; Di Lorenzo et al. 2008). Since the changes in the 1980s were not well documented in physical indices, but were documented in the biology, previously noted physical relationships with biological processes may not have remained consistent across 1988/89. A loss of coherence in

variability of physical properties might reduce the likelihood that previously identified relationships with biological processes remained stationary and useful in management policies.

Of the physical properties that have been shown to be proxies for biological productivity, six are used in this study: SST, SSHa, sea surface salinity (SSS), vertical velocity, mixed layer depth (MLD), and wind stress. SST can influence organismal growth, respiration, and, indirectly, the availability of prey (Downton and Miller 1998; Cole 2000). SSHa is sensitive to many atmospheric and oceanic processes including SST, wind stress, advection and ocean currents, and upwelling. SSHa has been shown to be a good summary for those processes (Calman 1987), and it can be a proxy for biological processes (Wilson and Adamec 2001). SSS is a measure of evaporation and freshwater input into the system (Donguy and Henin 1976) and can influence MLD due to salinity-driven density gradients (Lukas and Lindstrom 1991). More precipitation occurs on coastal Alaska during the warm phase of the PDO, while less precipitation occurs during the cold phase of the PDO (Wendler et al. 2017) affecting regional SSS. Freshwater can create steep SSS gradients as well as influence the locations and densities of different organisms (Cloern et al. 2017). Wind stress is a proxy for mixing in the surface layer which can impact the nutrient availability for primary producers and influence light availability in the mixed layer. Wind stress also is a driver of mixing in the upper layer of the water column. Wind stress anomalies are correlated to the PDO; the warm phase of the PDO exhibits anomalous, cyclonic winds in the GOA, and the cold phase of the PDO exhibits anomalous anticyclonic winds in the GOA (Mantua and Hare 2002). MLD is sensitive to atmospheric and oceanic processes that are associated with variability in

upper water column stability. Wind stress, water density, freshwater input, and vertical velocity all contribute to variability of the MLD. MLD is a proxy for the amount of stratification, influencing primary production as a result of the amount of nutrients that are available. Stronger stratification can result in lower nutrient availability for primary producers and therefore, less primary production if nutrients are limiting (Ferland et al. 2011). Vertical velocity is a measure of upwelling and downwelling and is influenced by wind stress. Nutrient availability in the GOA is typically iron limited (Martin et al. 1991). Iron is mixed into the mixed layer due to upwelling, making vertical velocity another proxy for nutrient availability in the mixed layer.

In this study, I compared properties in the GOA and basin-scale indices across 1988/89 from the mid-1900s to the early 2000s, to describe temporal and spatial climate dynamics and relationships among properties and climate indices. To focus the study, I asked three questions: 1) Do GOA indices maintain stationary patterns both temporally and spatially across 1988/89? 2) Do GOA properties maintain stationary relationships with other indices, at both the GOA and basin-scale, across 1988/89? 3) How often do shifts occur in spatial patterns of variability the oceanographic properties of GOA? I test the covariance between the PDO, NPGO, and GOA climate variability to illustrate the relationships that GOA variability has with large-scale climate indices. To address the first two questions, the late 1900s were broken into three time periods: 1969-1988, 1989-2008, and 1969-2008 (first period, second period, and full period, respectively). The first time period represents the climate variability leading up to the late 1980s climate shift, while the second period represents climate variability following the late 1980s shift (Yeh et al. 2011). The period encompassing both the first and second periods represents the

variability of the continuous period from 1969 through 2008. To address the third question, a period of 1940-2008 was used in conjunction with EOF analyses applied to 15-year single and adjacent rolling windows. 15-year rolling windows help to identify shifts of different durations that shorter and longer windows are not able to distinguish.

Empirical orthogonal function (EOF) analyses are used to summarize GOA property variability into principal component (PC) time series and EOF spatial loadings (hereafter "spatial patterns"). The first and second period dominant PCs (PC1) and dominant spatial patterns (EOF1) are compared with PCs and spatial patterns calculated from the full period to test the stationarity of individual property indices. PCs and spatial patterns were compared among indices in all periods to test the stationarity of relationships among indices. To test the frequency of climate shifts in the GOA, rolling EOF analyses are used to compare the spatial patterns of adjacent periods of individual properties. Single rolling EOF analyses are used to compare the amount of variance explained by the two leading EOFs (EOF1 and EOF2). Also, the spatial pattern and PCs of each window were compared to the full period PC and spatial pattern for each property to observe possible changes throughout the 1900s and early 2000s.

3.2 Methods

3.2.1 Data

The PDO index is approximately defined as the PC1 of SST anomalies, with the anthropogenic climate trend removed, poleward of 20º N in the North Pacific from 1900-1993 (Zhang et al. 1997; Mantua and Hare 2002; http://research.jisao.washington.edu/pdo/PDO.latest.txt). The PDO index is a monthly

resolved time series from 1900-2017. The NPGO index is defined as the PC2 of SSHa poleward of 20º N in the North Pacific (http://www.o3d.org/npgo/npgo.php).

This study focused solely on the GOA region in the North Pacific bounded by 54-62º N and 152-120º W (Figure 3.1). Properties from the SODA model version 2.2.4 were used in the analysis. SODA 2.2.4 provides monthly averages for a suite of properties on a 0.5º x 0.5º spatial grid (Carton and Giese 2008). Six variables are used in the analysis: SST, SSHa, SSS, wind stress, MLD, and vertical velocity. Anomalies were calculated by averaging monthly values of each grid cell and subtracting the averages from each month during the time period. The anomaly was calculated for each property to remove the seasonal cycle from the data over the period or window. An EOF analysis was used to describe the variability of the anomalies for each property with PC time series and EOF spatial patterns for each period or window. PC time series were correlated using a Pearson correlation coefficient and were noted at a level of significance of 0.05 and 0.01. Spatial patterns were correlated using the methods from Smith et al. (2012).

3.2.2 Comparing Different Indices Across 1988/89

To test if GOA indices maintain stationary relationships with other indices across 1988/89, each index was correlated to the PC1 from each property and the PDO and NPGO indices using Pearson correlation coefficients. The PC1 time for each property in either the first, second, or full period was correlated to the PC1 of each property and the NPGO and PDO indices in the same period. The first and second period PC1 of each property were also correlated to the full period PC1 for each property.

Similarly, the EOF1 spatial pattern for each property index in the first, second, or full period was correlated to the other property EOF1 spatial patterns from the same

period. To compare inter-period relationships, the first and second period spatial patterns were correlated to the full period spatial patterns of other indices. First period spatial patterns were correlated with second period spatial patterns among the properties. A rolling 15-year-window EOF analysis was used to compare the spatial patterns of both EOF1 and EOF2 of SST and SSHa since they are often considered to be interchangeable, especially in the definitions of the PDO or NPGO (Mantua et al. 1997; Di Lorenzo et al. 2008).

Indices did not maintain a stationary relationship if the first period, second period, and full period PC correlations did not maintain a similar correlation coefficient with the same level of significance. Similarly, a stationary relationship was not maintained if the correlation between spatial patterns in each time period did not remain consistent over time.

3.2.3 Comparing the Variability of Individual Indices Across 1988/89

To test the stationarity of individual indices both temporally and spatially across 1988/89, the correlation between PC1 from each variable in the first and second periods was calculated with respect to the full period PC1. First and second period EOF1 spatial patterns for each property were correlated with respect to the full period spatial pattern. First and full period spatial patterns from the same property were also correlated. A shift was documented in an individual property if the first and second period PCs and spatial patterns did not maintain consistent correlations or a consistent level of significance across 1988/89.

3.2.4 Frequency of Shifts in the Variability of Climate Properties in the GOA

To observe PC and spatial pattern variability throughout the mid to late 1900s and early 2000s, adjacent rolling 15-year-EOF analyses were used to compare EOF1 and EOF2 spatial patterns across windows. Dates were selected around a minimum correlation in the time series (if present) to observe the spatial patterns that are associated with the time series. Spatial patterns were compared from 1940-2008 to determine the frequency of changes in climate variability and to explore the frequency of such shifts in the GOA. The anomaly was removed for each 15-year window to focus on comparing the variability between the two time periods. A single rolling 15-year-window EOF analysis was used to compare the percent variance explained by EOF1 and EOF2 by subtracting the variance explained by the EOF2 from the variance explained by EOF1. A minimum in the resulting correlation time series for the spatial correlations may represent a shift in variability.

A rolling 15-year-window EOF analysis was used to compare individual property spatial patterns to their full period spatial pattern from 1940-2008. A rolling 15-year-window EOF analysis was also used to compare individual property PCs with the corresponding 15-year period within the respective full period PC. The seasonal mean was removed from each 15-year period to form seasonal anomalies to be incorporated into each EOF analysis.

3.3 Results

3.3.1 Stationarity of Relationships Between Different Indices Across 1988/89

When correlated during the same period, property PC1s (Figure 3.2) and EOF1s (Figure 3.3) had varying correlations. The PC1 of SST was not significantly correlated

with the PC1 of SSHa in the full period ($p > 0.05$) but was significantly correlated ($p < 0.01$) to the PC1 of SSHa in the first and second periods ($r = 0.52$ and $r = 0.40$, respectively) (Figure 3.2). The EOF1 of SST was correlated with the EOF1 of SSHa in the full period at $K = 0.51$, in the first period at $K = 0.36$, and in the first period at $K = 0.73$ (Figure 3.3). The PC1 of SST was not significantly correlated to SSS PC1 in the full period ($p > 0.05$) but was significantly correlated at a significance level of $p < 0.01$ in both the first and second periods ($r = 0.46$ and $r = 0.32$, respectively) (Figure 3.2). The EOF1 of both SST and SSS were correlated in the full period at $K = 0.54$, and similar correlations in both the first and second periods ($K = 0.37$ and $K = 0.38$, respectively) (Figure 3.3). The EOF1 of SST was correlated with the EOF1 of vertical velocity in the full period at $K = 0.28$, in the first period at $K = 0.13$, and in the second period at $K = 0.18$ (Figure 3.3). SST PC1 was significantly correlated to MLD PC1 ($p < 0.01$) during the full, first, and second periods ($r = 0.60$, $r = 0.34$, and $r = 0.52$, respectively) (Figure 3.2). The EOF1 of SST was correlated with the EOF1 of MLD in the full period at $K = 0.91$, in the first period at $K = 0.61$, and in the second period at $K = 0.88$ (Figure 3.3). The PC1 of SST was not significantly correlated with the PC1 of wind stress in the full period ($p > 0.05$) but was significantly correlated at a significance level of $p < 0.01$ in both the first and second periods ($r = 0.21$ and $r = 0.18$, respectively) (Figure 3.2). The EOF1 of SST was correlated with the EOF1 of wind stress in the full period at $K = 0.90$, in the first period at $K = 0.32$, and in the second period at $K = 0.87$ (Figure 3.3). The PC1 of SST was significantly correlated with the PDO index at a significance level of $p < 0.01$ in the full, first, and second periods ($r = 0.56$, $r = 0.77$, and 0.64, respectively) (Figure 3.2). The PC1 of SST was significantly correlated with the NPGO index at a significance

level of $p < 0.01$ in the full and second periods ($r = 0.38$ and $r = 0.47$, respectively) but not significantly correlated in the first period ($p > 0.05$) (Figure 3.2).

The PC1 of SSHa was not significantly correlated to the PC1 of SSS in the full period ($p > 0.05$) but was significantly correlated in the first period ($r = 0.16$, $p = 0.02$) and the second period ($p > 0.01$, $r = 0.44$) (Figure 3.2). The EOF1 of SSHa was correlated with the EOF1 of SSS in the full period at $K = 0.82$, in the first period at $K = 0.52$, and in the second period at $K = 0.53$ (Figure 3.3). The PC1 of SSHa was not significantly correlated with the PC1 of vertical velocity during any of the three periods ($p > 0.05$; Figure 3.2). The EOF1 of SSHa was correlated with the EOF1 of vertical velocity in the full period at $K = 0.85$, in the first period at $K = 0.86$, and in the second period at $K = 0.37$ (Figure 3.3).The PC1 of SSHa was significantly correlated with the PC1 of MLD at a significance level of $p < 0.01$ during the full and second periods ($r = 0.12$ and $r = 0.17$, respectively) but was not significantly correlated during the first period ($p > 0.05$) (Figure 3.2). The EOF1 of SSHa was correlated with the EOF1 of MLD in the full period at $K = 0.51$, in the first period at $K = 0.25$, and in the second period at $K = 0.61$ (Figure 3.3). The PC1 of SSHa was significantly correlated with the PC1 of wind stress at a significance level of $p < 0.01$ during the first period ($r = 0.25$) but was not significantly correlated during the full or second periods ($p > 0.05$) (Figure 3.2). The EOF1 of SSHa was correlated with the EOF1 of wind stress in the full period at $K = 0.97$, in the first period at $K = 0.73$, and in the second period at $K = 0.74$ (Figure 3.3). The PC1 of SSHa was significantly correlated with the PDO index at a significance level of $p < 0.01$ during the full, first, and second periods ($r = 0.23$, $r = 0.64$, and $r = 0.120$, respectively; Figure 3.2). The PC1 of SSHa was significantly correlated with the NPGO

index at a significance level of $p < 0.01$ during the full, first, and second periods ($r = 0.57$, $r = 0.29$ and $r = 0.78$, respectively; Figure 3.2).

The EOF1 of SSS was correlated with the EOF1 of vertical velocity in the full period at $K = 0.81$, in the first period at $K = 0.70$, and in the second period at $K = 0.68$ (Figure 3.3). The PC1 of SSS was significantly correlated with the PC1 of MLD at a significance level of $p < 0.01$ during the full, first, and second periods ($r = 0.20$, $r = 0.19$, and $r = 0.20$, respectively; Figure 3.2). The EOF1 of SSS was correlated with the EOF1 of MLD in the full period at $K = 0.65$, in the first period at $K = 0.79$, and in the second period at $K = 0.43$ (Figure 3.3). The PC1 of SSS was significantly correlated with the PC1 of wind stress at a significance level of $p < 0.01$ during the full and second periods ($r = 0.18$ and $r = 0.24$, respectively) but not significantly correlated in the first period ($p > 0.05$) (Figure 3.2). The PC1 of SSS was significantly correlated with the PDO index at a significance level of $p < 0.01$ during the first and second periods ($r = 0.46$ and $r = 0.46$, respectively) but not significantly correlated in the full period ($p > 0.05$) (Figure 3.2). The PC1 of SSS was significantly correlated with the NPGO index at a significance level of $p < 0.01$ during the full, first, and second periods ($r = 0.26$, $r = 0.28$, and $r = 0.78$, respectively; Figure 3.2).

The PC1 of vertical velocity was not significantly correlated with any PC1 of any property in any period ($p > 0.05$; Figure 3.2). The EOF1 of vertical velocity was correlated with the EOF1 of MLD in the full period at $K = 0.35$, in the first period at $K = 0.50$, and in the second period at $K = 0.19$ (Figure 3.3). The EOF1 of vertical velocity was correlated with the EOF1 of wind stress in the full period at $K = 0.73$, in the first period at $K = 0.96$, and in the second period at $K = 0.77$ (Figure 3.3).

When correlated between different periods, indices also had varying consistency in their correlations (Figure 3.4-3.5). First and second period EOF1 correlations were highlighted if the difference between the full and first period EOF1 correlation of a property and the full and second period EOF1 correlation was greater or equal than 0. or a shift in significance level.

The PC1 of full period SST was not significantly correlated with the PC1 of wind stress in the first period ($p > 0.05$) but was significantly correlated with the PC1 in the second period ($r = 0.16$, $p = 0.01$) (Figure 3.4). Spatially, the first EOF of full period SST had a weaker correlation with the EOF1 of several first period properties than the EOF1 of second period properties including SSHa ($K = 0.03$ and $K = 0.55$, respectively), SSS ($K = 0.07$ and $K = 0.54$, respectively), MLD ($K = 0.72$ and $K = 0.88$, respectively), and wind stress ($K = 0.41$ and $K = 0.87$, respectively) (Figure 3.5 a-b). The EOF1 of first period SST was correlated with the EOF1 of the second period of SSHa ($K = 0.11$), SSS ($K = 0.67$), MLD ($K = .78$), and wind stress ($K = 0.81$) (Figure 3.5 c).

The PC1 of full period SSHa was significantly correlated with the PC1 of SST in the first period ($r = 0.25$, $p < 0.01$) but the significance and correlation were reduced when correlated with the PC1 in the second period ($r = 0.14$, $p = 0.02$) (Figure 3.4). The PC1 of full period SSHa was not significantly correlated with the PC1 of SSS in the first period ($p > 0.05$) but was significantly correlated with the PC1 in the second period ($r = 0.25$, $p < 0.01$). Similarly, the PC1 of full period SSHa was not significantly correlated with the PC1 of MLD in the first period ($p >0.05$) but was significantly correlated with the PC1 in the second period ($r = 0.23$, $p < 0.01$). The PC1 of full period SSHa was significantly correlated with the PC1 of wind stress in the first period ($r = 0.19$, $p < 0.01$)

but was not significantly correlated in the second period ($p > 0.05$). Similarly, the PC1 of full period SSHa was significantly correlated with the PDO index in the first period ($r = 0.41$, $p < 0.01$) but was not significantly correlated in the second period ($r = 0.23$, $p > 0.01$). The PC1 of full period SSHa was significantly correlated with the NPGO index in both the first and second periods at a significance level of $p < 0.01$, but the correlation strengthened in the second period compared to the first period correlation ($r = 0.64$ and $r = 0.48$, respectively). Spatially, the EOF1 of full period SSHa had weaker correlations with the EOF1 of two first period properties than the EOF1 of second period properties: SST ($K = 0.09$ and $K = 0.67$, respectively) and MLD ($K = 0.14$ and $K = 0.62$, respectively) (Figure 3.5). The EOF1 of full period SSHa had a stronger correlation with the EOF1 of first period vertical velocity than the EOF1 of second period vertical velocity ($K = 0.88$ and $K = 0.48$, respectively; Figure 3.5 a-b). The EOF1 of first period SSHa was correlated with the EOF1 of the second period of SST ($K = 0.31$), vertical velocity ($K = 0.57$), and MLD ($K = 0.55$) (Figure 3.5 c).

The PC1 of full period SSS was not significantly correlated with the PC1 of SSHa in the first period ($p > 0.05$) but was significantly correlated with the PC1 of the second period ($r = 0.35$, $p < 0.01$) (Figure 3.4). Similarly, the PC1 of full period SSS was not significantly correlated with the PC1 of wind stress in the first period ($p > 0.05$) but was significantly correlated with the PC1 of the second period ($r = 0.26$, $p < 0.01$) (Figure 3.4). The PC1 of full period SSS was significantly correlated with the PC1 of MLD in the first period ($r = 0.15$, $p = 0.02$) and significantly correlated with the PC1 of the second period ($r = 0.18$, $p < 0.01$) (Figure 3.4). Spatially, the EOF1 of full period SSS had stronger correlations with the EOF1 of two first period properties than the EOF1 of

second period properties: SST (K = 0.69 and K = 0.35, respectively) and MLD (K = 0.75 and K = 0.46, respectively) (Figure 3.5 a-b). The EOF1 of first period SSS was correlated with the EOF1 of the second period of SST (K = 0.14) and MLD (K = .49) (Figure 3.5 c).

The EOF1 of full period vertical velocity had stronger correlations with the EOF1 of three first period properties than the EOF1 of second period properties: SST (K = 0.36 and K = 0.17, respectively), MLD (K = 0.43 and K = 0.24, respectively), and wind stress (K = 0.99 and K = 0.80, respectively) (Figure 3.5 a-b).

The PC1 of full period MLD was significantly correlated with the PC1 of SST in both the first and second periods at a significance level of $p < 0.01$, but the correlation stronger in the second period ($r = 0.49$) than the first period ($r = 0.33$) (Figure 3.4). The PC1 of full period MLD was not significantly correlated with the PC1 of SSHa in the first period ($p > 0.05$) but was significantly correlated with the PC1 of the second period ($r = 0.18$, $p < 0.01$). Similarly, the PC1 of full period MLD was not significantly correlated with the PC1 of wind stress in the first period ($p > 0.05$) but was significantly correlated with the PC1 of the second period ($r = 0.21$, $p < 0.01$). Spatially, the EOF1 of full period MLD had similar correlations with the EOF1 of both first and second period SSHa (K = 0.54 and K = 0.48, respectively; Figure 3.5 a-b), but the correlations between the EOF1 of first period MLD had a much lower correlation with the EOF1 of second period SSHa (K =0.09; Figure 3.5 c) than the full period correlations.

The PC1 of full period wind stress was not significantly correlated with the PC1 of SST in the first period ($p > 0.05$) but was significantly correlated with the PC1 of the second period ($r = 0.18$, $p = 0.02$) (Figure 3.4). Similarly, the PC1 of full period wind

stress was not significantly correlated with the PC1 of SSS in the first period ($p > 0.05$) but was significantly correlated with the PC1 of the second period ($r = 0.23$, $p < 0.01$).

When the spatial patterns of SSHa and SST were compared, multiple minima occurred throughout the time-period (Figure 3.6). Three minima occurred in the late 1950s, one in the mid- and late-1970s, and one in the early 2000s. The peak correlation occurred in January 1993. The high variability throughout the time period shows that the spatial loadings for SSHa and SST do not vary together.

3.3.2 Stationarity of an Index Across 1988/89

The PC1 of each full period property maintained a relatively consistent correlation with the respective PC1 of each of the first and second periods (Figure 3.2). Similarly, the EOF1 of each full period property maintained a relatively consistent correlation with the respective EOF1 of each of the first and second periods (Figure 3.3). Correlations were reported if there was a shift in correlation greater or equal to 0.15. The correlation between the EOF1 of the first period and the EOF1 of the second period for both SSHa ($K = 0.36$) and SSS ($K = 0.61$) (Figure 3.5 a) were weaker than the correlations between the EOF1 of the full period and the EOF1 of each of the first and second periods for SSHa ($K = 0.82$ and $K = 0.81$, respectively) and SSS ($K = 0.85$ and $K = 0.93$, respectively) (Figure 3.5 a-b). The PC1s and EOF1s that were correlated within each property are presented in Figures 3.7-3.12.

3.3.3 Climate Variability Shifts

In the rolling adjacent-15-year-windows EOF analysis, EOF1 spatial patterns for both SST and SSHa each displayed a minimum correlation during the mid-late 1980s (Figure 3.13 a-b). SSHa had the lower of the two correlations in June 1986 at $K = 0.10$

while the correlation minimum for SST was K = 0.3919 in September 1983. SSS EOF correlations were the most variable with three minima spread throughout the time period. MLD, vertical velocity, and wind stress all maintained relatively consistent correlations throughout the entire period (Figure 3.13 d-f).

When compared spatially at multiple points around a minimum correlation throughout the adjacent window correlations, SST experienced a mild change that returned to the pre-1980s spatial pattern (Figure 3.13 a, 3.14). SSHa spatial pattern experienced a slow change over time that was maintained past the late 1980s (Figure 3.13 b, 3.15). The difference in variance explained also shows minimums in the mid-late 1980s for both SST and SSHa (Figure 3.16 a-b).

Correlations between the EOF1 of the 15-year-window and the EOF1 of the respective full period property resulted in a single minimum correlation for SST (K = 0.60, March 1984), MLD (K = 0.78, August 1992), and wind stress (K = 0.79, March 1976) (Figure 3.17). SSHa correlations were variable, with the minimum correlation occurring in August 1979 (K = 0.58; Figure 3.17 b). The 15-year-window EOF1 of SSS was least correlated with the EOF1 of full period SSS in January 1986 (K = 0.32; Figure 3.17 c) and generally had a lower correlation throughout the entire time period for both EOF1 and EOF2 correlations. Overall, most properties had generally high correlations throughout the time period.

Correlations between the PC1 of the property 15-year window and the corresponding 15-year window from the full period property PC1, resulted in generally high correlations throughout the analysis period (Figure 3.18). The correlation between the PC1 of full period SST and the PC1 of 15-year SST and the correlation between the

PC2 of full period SST and the PC2 of 15-year SST had the lowest values (r = 0.69 and r = 0.52, respectively) in March of 1984. The correlation between the PC2 of full period SST and the PC1 of 15-year SST also has a maximum correlation (r = 0.84) in March of 1984.

The correlation between the PC1 of full period SSHa and the PC1 of 15-year SSHa had the lowest value (r = 0.65; Figure 3.18 b) in September of 1978. The correlation between the PC2 of full period SST and the PC1 of 15-year SST also had a maximum correlation (r = 0.85; Figure 3.18 a) in September of 1978. The correlation between the PC2 of full period SSHa and the PC2 of 15-year SSHa had the lowest correlation in August 1990 where a local minimum (r = 0.71) was also calculated for the correlation between the PC1 of full period SSHa and the PC1 of 15-year SSHa and a local maximum (r = 0.69) was calculated for the correlation between the PC2 of full period SSHa and the PC1 of 15-year SSHa.

The correlation between the PC1 of full period SSS and the PC1 of 15-year SSS had a minimum correlation (r = 0.38) and the PC2 of 15-year SSS had a local minimum correlation (r = 0.45) in January of 1986 (Figure 3.18 c). The correlation between the PC2 of full period SSS and the PC1 of 15-year SSS also had a maximum correlation (r = 0.86) in January of 1986.

The correlation between the PC1 of full period MLD and the PC1 of 15-year MLD and the correlation between the PC2 of full period MLD and the PC2 of 15-year MLD had the lowest values (r = 0.83 and r = 0.66, respectively; Figure 3.18 e) in November 1981. The correlation between the PC2 of full period MLD and the PC1 of 15-year MLD also has a maximum correlation (r = 0.84) in October 1981.

The difference of the variance explained by the EOF1 and EOF2 in each 15-year period was extremely variable among properties (Figure 3.16). For SST, EOF1 explained a much higher proportion of GOA variability around 1969 and in the late 1990s (Figure 3.16 a). For SSHa, EOF1 explained a higher proportion of the variance than EOF2 in the late 1940s, but EOF1 and EOF2 explained very similar amounts of variance in the 1980s and 1990s (Figure 3.16 b). The EOF1 of wind stress explained similar amounts of variance as EOF2 from 1960-1980 but was the two diverged after 1980 (Figure 3.16 f). The amount of variance explained by EOF1 compared to EOF2 for SSS generally stayed low throughout the time series with a minimum in the late 1980s and a maximum in the mid 1990s (Figure 3.16 c). EOF1 for MLD generally explained at least 5% more variance than EOF2 with a maximum of over 15% difference in the late 1990s and a minimum in the mid 1970s. Vertical velocity maintained a stable difference in variance explained by EOF1 compared to EOF2 (Figure 3.16 d).

3.4 Discussion

Climate shifts in the North Pacific have been characterized by physical shifts, like the change in phase of the PDO in the 1970s (Hare and Mantua 2000; Litzow 2006; Overland et al. 2008; Yeh et al. 2011), or biological shifts, such as in the 1980s (Hare and Mantua 2000; Litzow 2006; Overland et al. 2008). Both shifts represent a change in the North Pacific climate, but the focus of this study was to observe shifts in the patterns of oceanographic variability that are present in a shift between modes of variability such as in the late 1980s, instead of a shift in the phase of the dominant mode of variability such as in the late 1970s. While both shifts are characterized by changing ecological processes and relationships, the shift in the late 1980s has been difficult to specifically characterize

in both physical and biological processes. The 1980s shift is characterized by a wide range of species shifts (Mantua and Hare 2002; Litzow 2006), but not all species in the GOA experienced synchronous shifts specific to the late 1980s (Puerta et al. 2018), let alone 1988/89. A lack of specificity in the timing of shifting population dynamics and a lack of support in physical processes in the GOA makes pinpointing the late 1980s and specifically 1988/89 as the boundary of two climate patterns, difficult.

Using 1988/89 as an a priori split, testing the stationarity of individual properties across the late 1980s with 20-year length periods revealed a possible shift in the relationship between SST and SSHa. Most of the other property correlations between EOFs or PCs produced results that were similar to Hare and Mantua's (2000) and Litzow's (2006) depicting a lack of physical support for a shift in a single property or index. Certain properties, such as SSS, exhibited shifts in relationships only in either the PC correlations or the EOF correlations but not both.

Of the properties addressed in the a priori analysis of property relationships, the relationship between SST and SSHa across 1988/89 exhibited a shift in both the EOF1 and PC1 correlations (Figure 3.2-3.3). The first period correlation between PC1s for SST and SSHa was stronger than the second period correlation. The full period correlation was not significant and near zero, possibly describing a change in the sign of the correlation across the late 1980s. A change in the sign of the relationship across the 1980s would cause the correlations to cancel each other out and give a near zero correlation coefficient, therefore providing evidence for a shift in the relationship between the PCs across the late 1980s. The correlations between the EOF1s in each of the three periods for SST and SSHa were not consistent. The correlations between the EOF1 of full period

SST and the EOF1 of first or second period SSHa and the correlations between the EOF1 of full period SSHa and the EOF1 of first or second period SST were also not consistent. Correlations between EOF1 of the first and second periods of both SST and SSHa were not consistent either. The inconsistency of the spatial correlations between SST and SSHa also possibly describes a shifting spatial pattern.

Both SST and SSHa were less correlated with the PDO index and better correlated with the NPGO index in the second period than in the first period (Figure 3.2). Full period SSHa was significantly correlated with the first period PDO index but was not significantly correlated with the second period PDO index. Also, the correlation between the EOF1s of first and second period SSHa was much lower than the correlations between the EOF1 of full period SSHa and the first and second period EOF1s (Figure 3.2).

Shifting relationships between SST and SSHa variability has not really been observed in the North Pacific. Casey and Ademeck (2002) found distinct modes of SST-SSHa variability in the North Pacific in the 1990s which correlated significantly with the PDO pattern. Mantua et al. (2002) described the PDO as being defined by the first mode of SST variability or SSHa variability in the North Pacific. Similarly, Di Lorenzo et al. (2008) described the NPGO as being defined by the second mode of SSHa variability or SST variability. When compared specifically, the EOFs and PCs of SST and SSHa do not maintain stationary relationships over time. Since the EOFs and PCs are not consistent over time between the two properties, using both SST and SSHa as defining variables could express different definitions for the PDO and NPGO if the shifting patterns extend into the entire North Pacific from the GOA. So, assuming that SST and SSHa covary in a

stationary manner over time becomes problematic. The rolling 15-year-window spatial correlations between SST and SSHa (Figure 3.6) were consistent in the late 1980s through the early 2000s supporting Casey and Ademeck's (2002) findings, but before the 1980s, the correlations were extremely variable making SST and SSHa unreliable predictors of one another.

It should be noted that the a priori analyses were sensitive to the length of the periods. The periods were chosen to have even lengths of 20 years due to the limits of available data in the second period. Equal length windows were used to reduce the likelihood of the full period EOF analyses describing the main mode of variability as the more prevalent pattern in the time series (due to a longer time series) instead of the dominant pattern throughout both periods. When the first period was extended to include more of the mid 1900s, when the PDO phase was more prominently negative, the a priori results changed to express a significant change in the EOF1 and EOF2 spatial patterns and PC1 and PC2 time series for SSHa.

There was support for a single shift in the 1980s by both SSHa and SST adjacent rolling-15-year-window analyses. In adjacent 15-year windows, EOF1 correlations for both SST and SSHa had minimum correlations around the mid 1980s (Figure 3.13 a-b). A minimum in the difference in variance explained by EOF1 and EOF2 for SSHa was present throughout the 1980s (Figure 3.16 b) when the difference was small enough to observe a switch in the dominant mode of variability was possible throughout the 1980s. If the difference between the variance explained by the first and second modes of variability is small enough, the second mode of variability may be able to explain more of the variability of a property, and therefore become the dominant mode of variability.

Also, a strong correlation between the 15-year PC2 of SST and the PC1 of full period SST was at a maximum in the mid 1980s coinciding with minima in both the SST PC1 and SST PC2 correlations (Figure 3.18).

Of the indices that exhibited a shift in the 1980s, SSHa maintained a consistent 15-year EOF spatial pattern for more than a few years as present in SST, following the late 1980s (Figure 3.17 b). The pattern change coincides well the findings from Kilduff et al. (2015), where salmon became better correlated with the NPGO after the late 1980s. The region used by Killduff et al. (2015) was farther south along the North American coast than the GOA, but a shift in the region just south of the GOA supports a possible shift in the GOA during the same period. The NPGO index was also significantly correlated with more indices in the second period than the first period.

The EOF and PC changes shown by Yeh et al. (2011) in the late 1980s were not expressed in this study. Similar periods of study were used with the same technique, but when focused on only the GOA region, the shift was not as clear in many properties, but evidence is present in both SST and SSHa that a shift occurred. The EOFs for SST diverge for a short period in the 1980s to a new pattern but return after less than a decade to pre-1980 patterns (Figure 3.17). The spatial pattern shift was not sustained like that of SSHa in the adjacent 15-year-window correlations. Neither SST nor SSHa show spatial pattern shifts similar to that of Yeh et al. (2011) across 1988/89.

Overall, there is a lack of a coherent shift in any property in the late 1980s to a new sustained EOF and PC in the GOA. While SSHa shows a sustained spatial pattern shift in a single analysis, the evidence from the other analyses continue to support the lack of a shift in physical processes as seen in the literature (Litzow 2006).

The climate shift in 1988/89 has mainly been documented in biological indices (Hare and Mantua 2000; Litzow 2006) but not all species support the shift (Puerta et al. 2018). Similarly, there is some documented support for the shift in physical processes (Yeh at al. 2011; Kilduff et al. 2015), but the GOA region still lacks strong physical support from multiple properties. SSHa may exhibit a shift in variability in the GOA, but the study was unable to pinpoint the timing of the shift. If large-scale processes and shifts are not recorded in the GOA regional physical processes, then the use of large-scale summaries as corollaries for ecological processes in the GOA region may not be the best approach.

Overall, there is weak support for a physical shift in the GOA. Both the PDO and NPGO do not have the strongest or most consistent correlations with all of the GOA indices in this study. With the vast number of climate and ocean models available, the PDO and NPGO should be limited in their use in regional biological and ecological studies. Models can be used to summarize and understand regional dynamics that actually impact ecosystems and species dynamics. While studies have shown that species can be more related to large-scale climate trends (Forchhammer et al. 2001), the likelihood that oceanic species with short lifespans react to long term climate trends over their respective environments is quite low. Models can provide specific, reliable data that can offer some insight to the underlying processes that influence ecological conditions and fish production

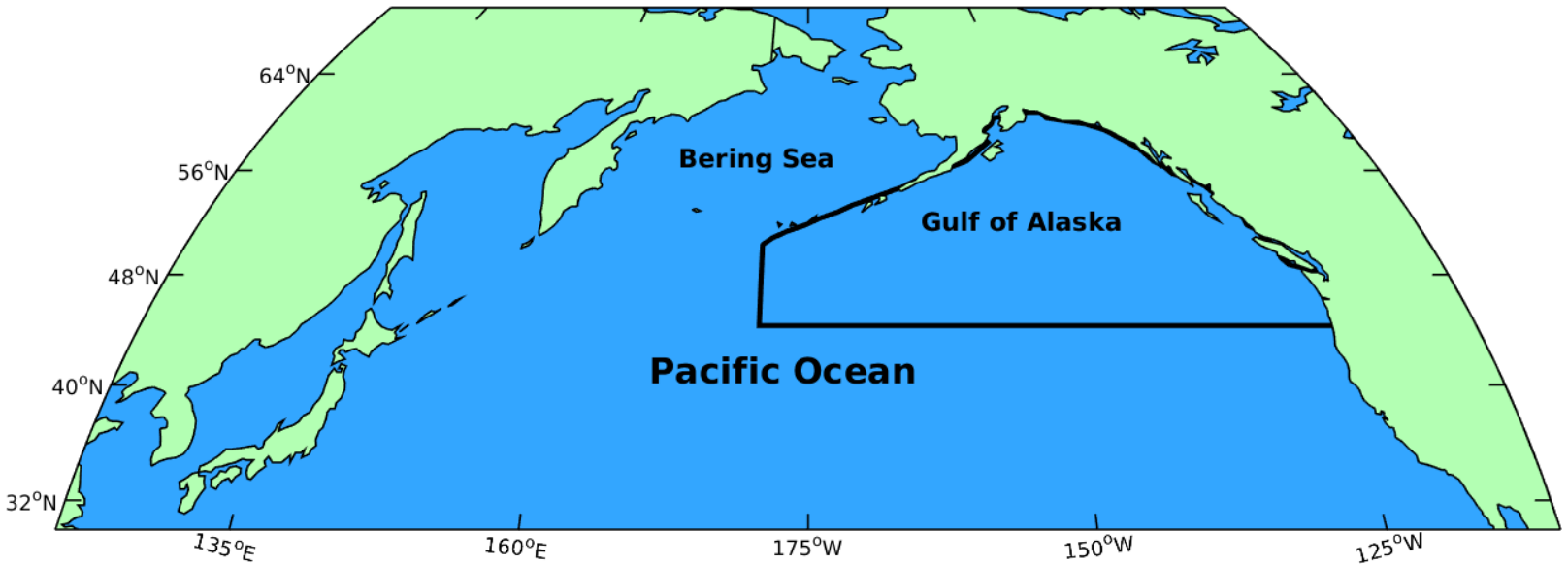

Figure 3.1. Pacific Ocean with the Bearing Sea and Gulf of Alaska. Study area is outlined in black.

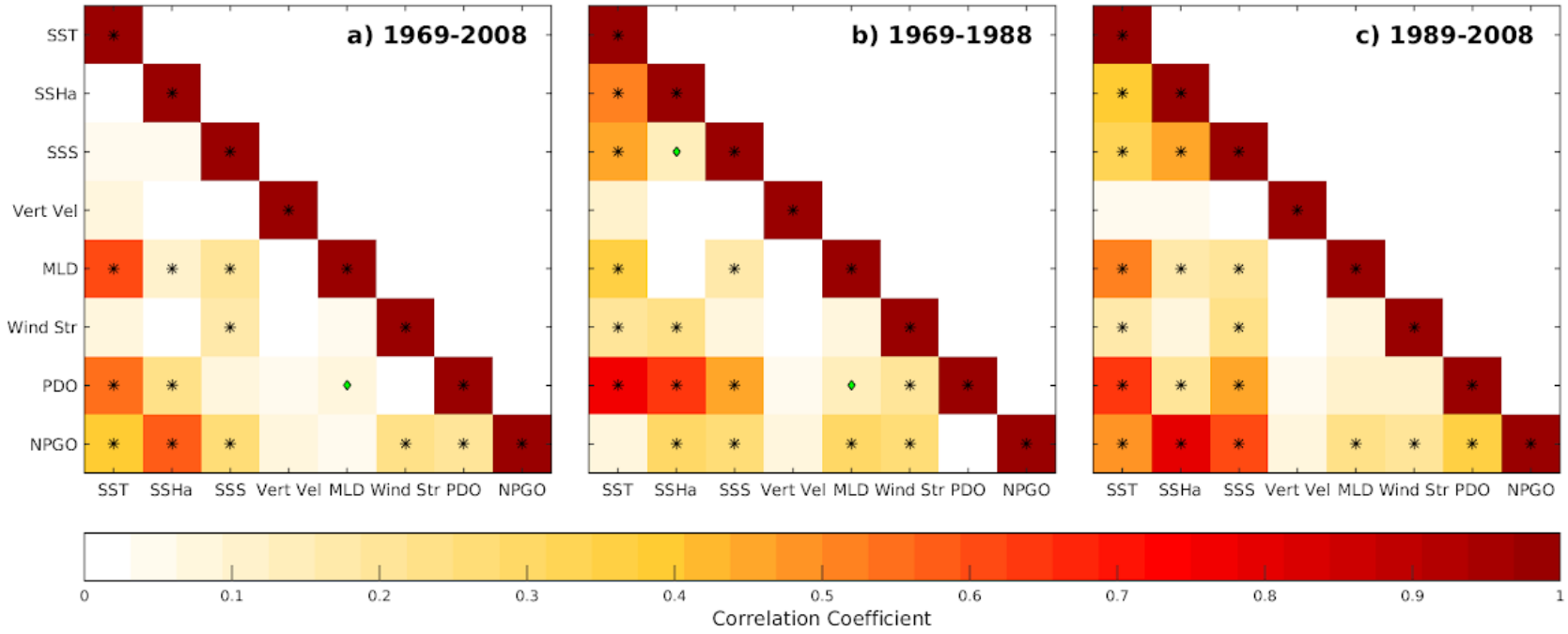

Figure 3.2. Principal component correlations among properties and climate indices in the same time period plotted as absolute values of correlations for a) the full period, b) the first period, and c) the second period. A black asterisk represents significance level of 0.01 and a green diamond represents significance level of 0.05.

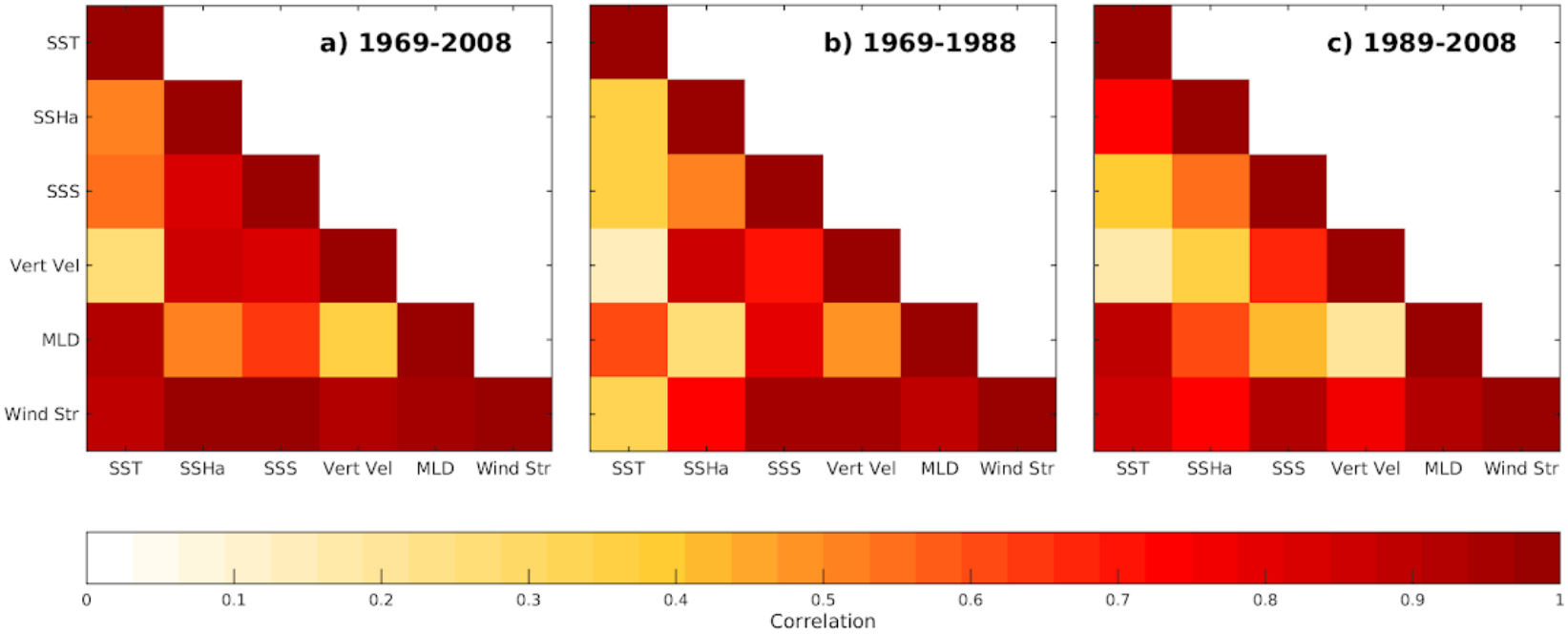

Figure 3.3. Spatial pattern correlations among properties and climate indices in the same time period plotted as absolute values of correlations for a) the full period, b) the first period, and c) the second period.

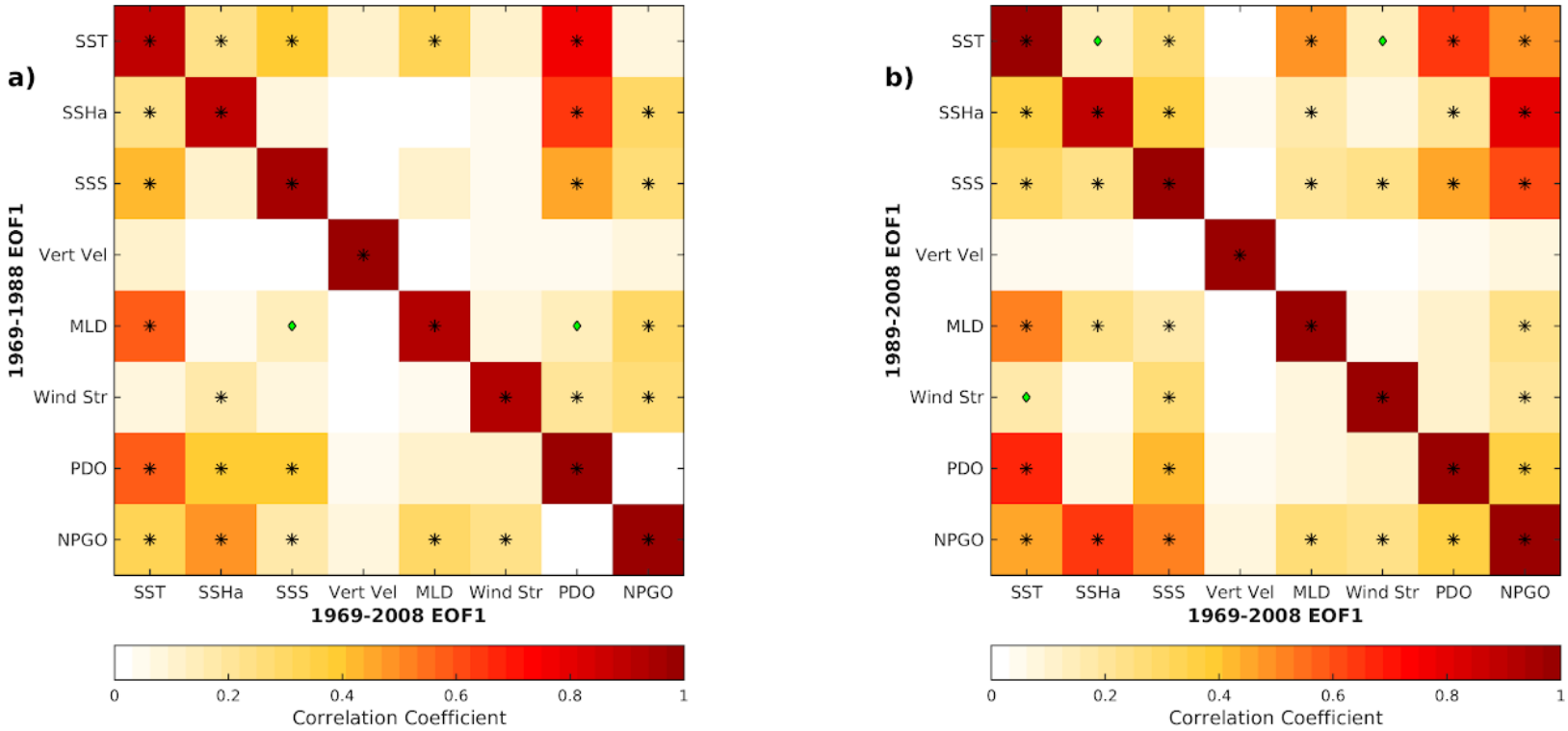

Figure 3.4. Principal component correlations among properties in either the first or second period compared to the full period plotted as absolute values of correlations for a) the first period and the full period, and b) the second period and the full period. A black asterisk represents significance level of 0.01 and a green diamond represents significance level of 0.05.

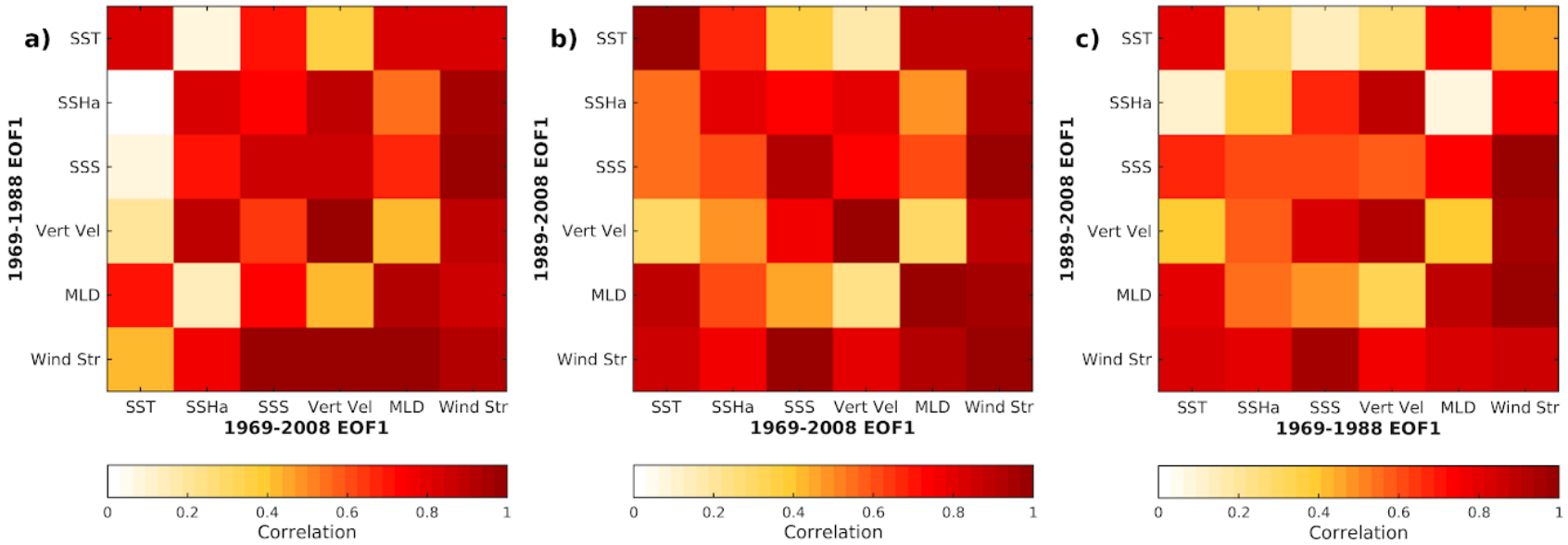

Figure 3.5. Spatial pattern correlations among properties in different time periods for a) the first period and the full period, and b) the second period and the full period, and c) the first period and second period.

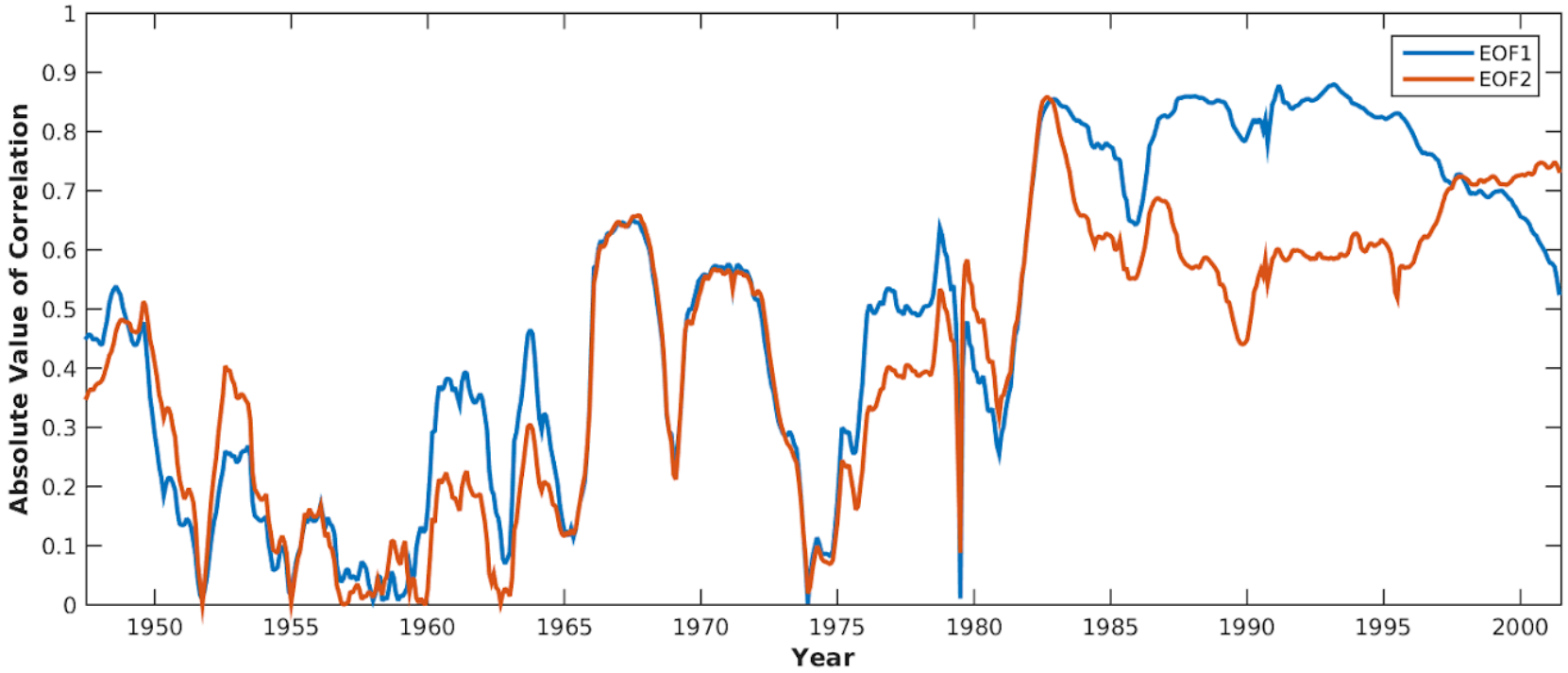

Figure 3.6. Correlation between sea surface height anomaly 15-year spatial loadings and sea surface temperature 15-year spatial loadings plotted as absolute values for a) EOF1 (blue line) and b) EOF2. Correlation is plotted on the center month of the 15-year window.

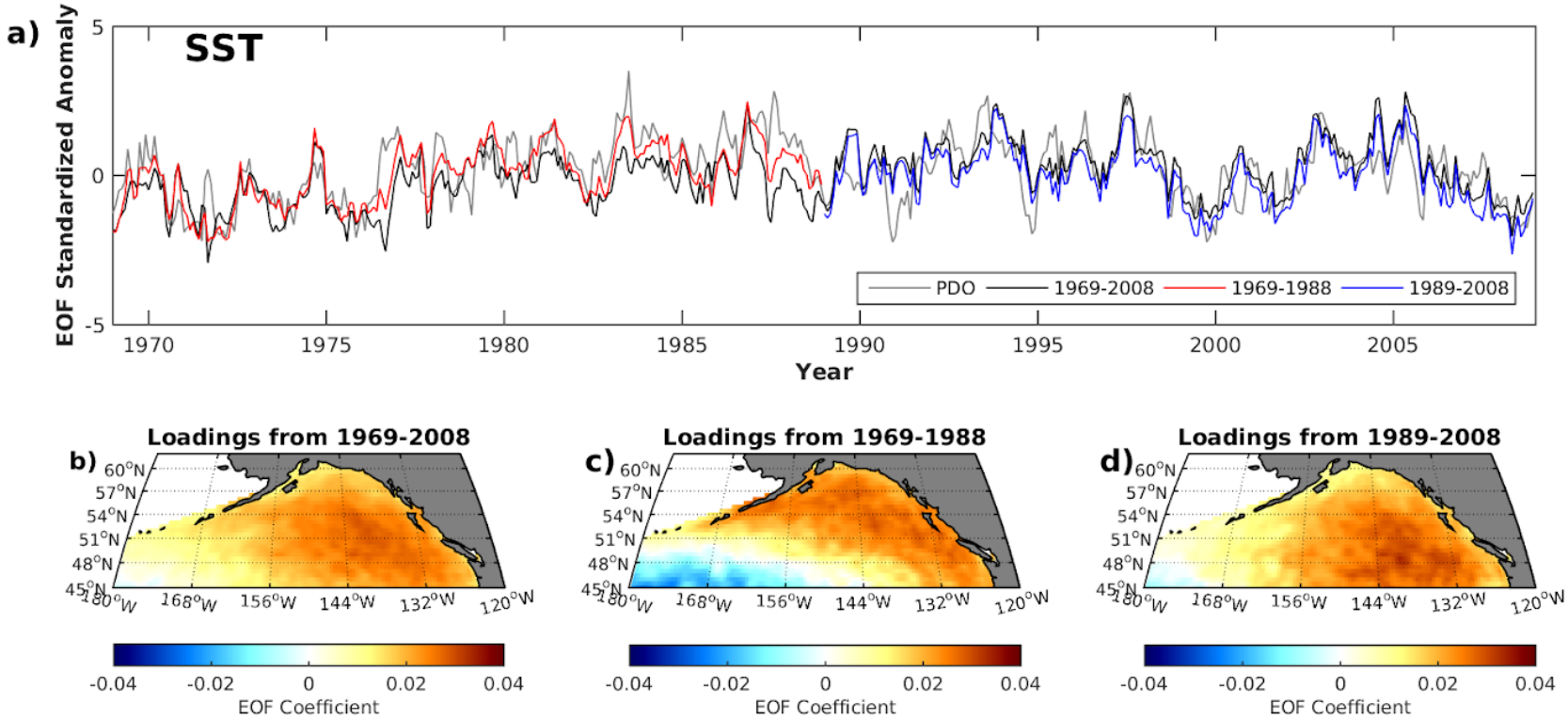

Figure 3.7. a) Sea surface temperature PC1 time series for the first period (blue line), second period (red line), and full period (black line) overlaid on the PDO index (gray line). The spatial loadings for each period b) full period, c) first period, and d) second period.

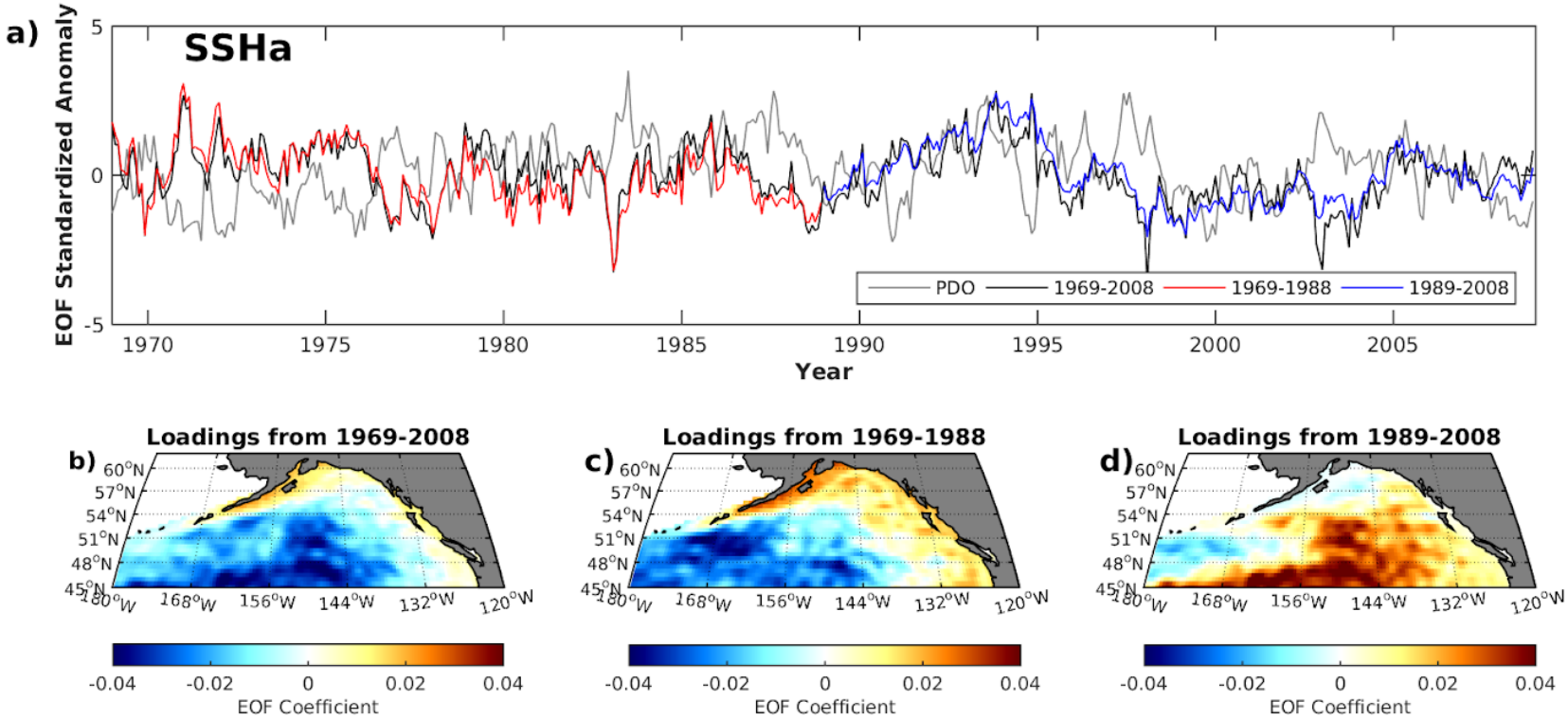

Figure 3.8. a) Sea surface height anomaly PC1 time series for the first period (blue line), second period (red line), and full period (black line) overlaid on the PDO index (gray line). The spatial loadings for each period b) full period, c) first period, and d) second period.

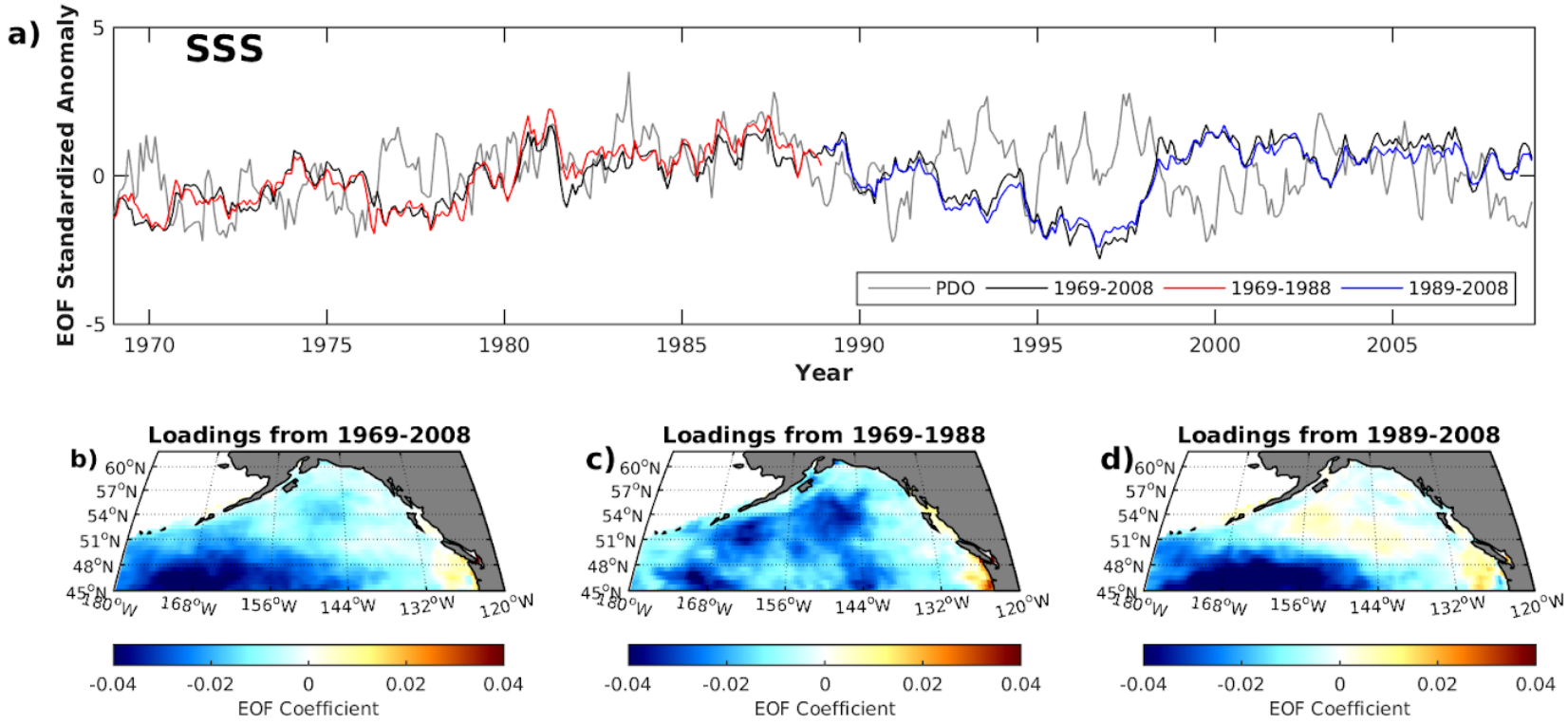

Figure 3.9. a) Sea surface salinity PC1 time series for the first period (blue line), second period (red line), and full period (black line) overlaid on the PDO index (gray line). The spatial loadings for each period b) full period, c) first period, and d) second period.

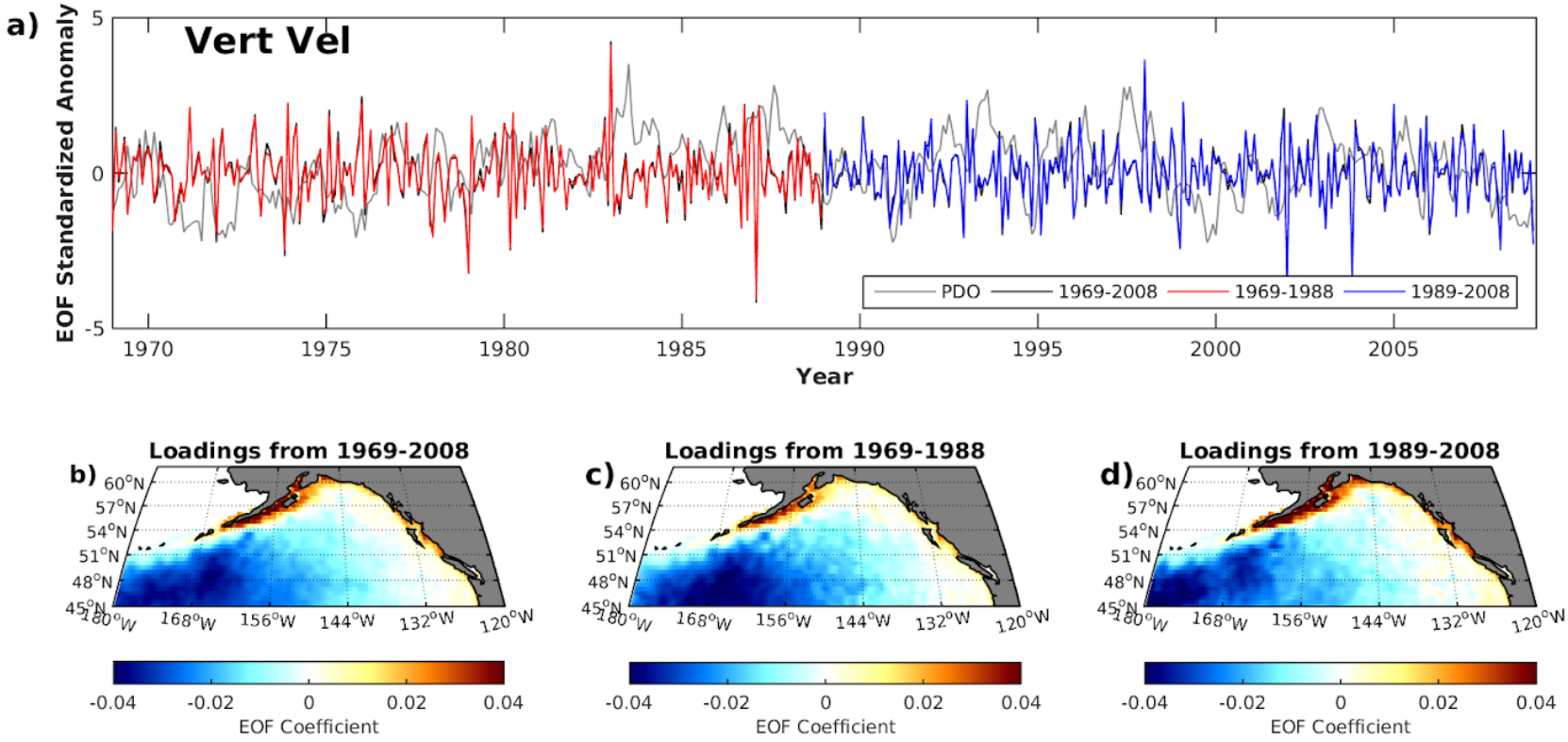

Figure 3.10. a) Vertical velocity PC1 time series for the first period (blue line), second period (red line), and full period (black line) overlaid on the PDO index (gray line). The spatial loadings for each period b) full period, c) first period, and d) second period.

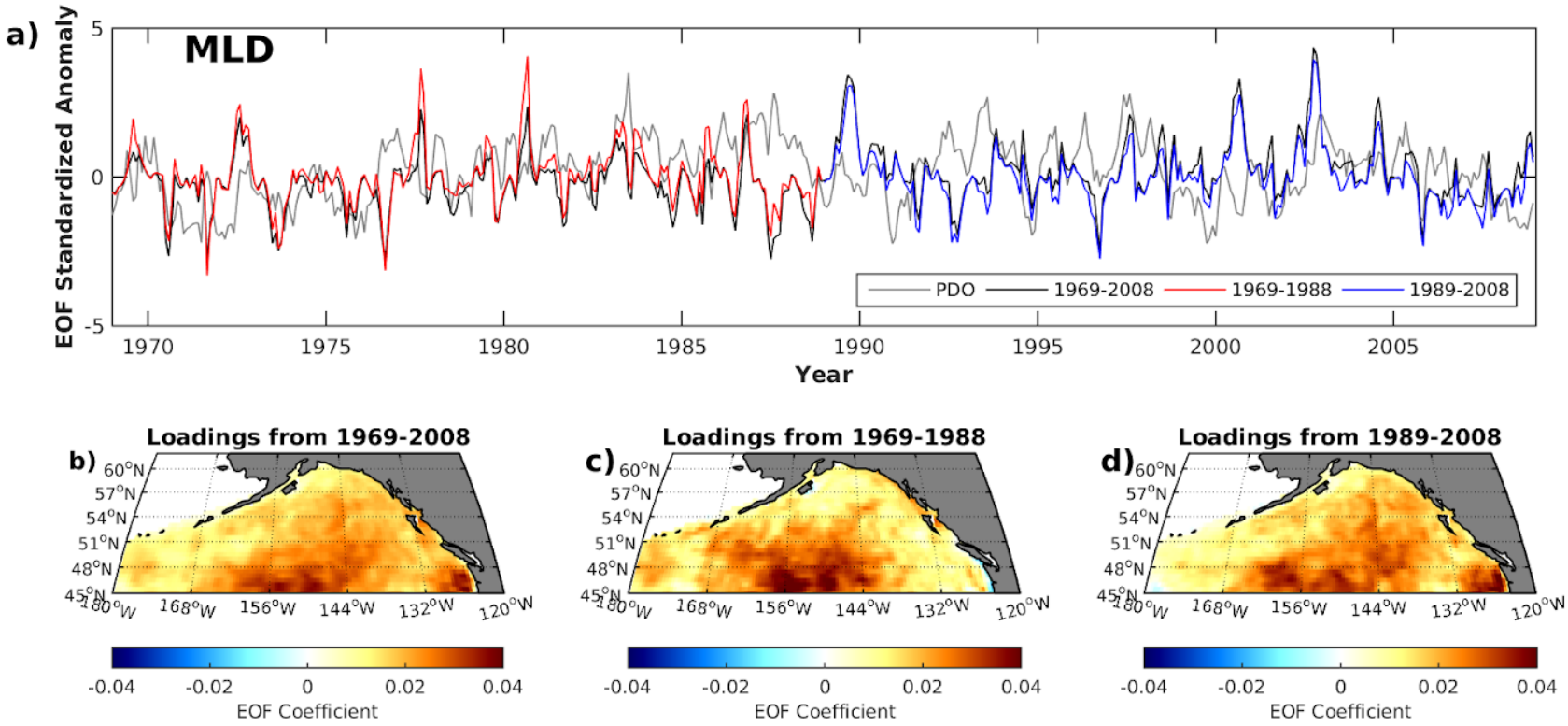

Figure 3.11. a) Mixed layer depth PC1 time series for the first period (blue line), second period (red line), and full period (black line) overlaid on the PDO index (gray line). The spatial loadings for each period b) full period, c) first period, and d) second period.

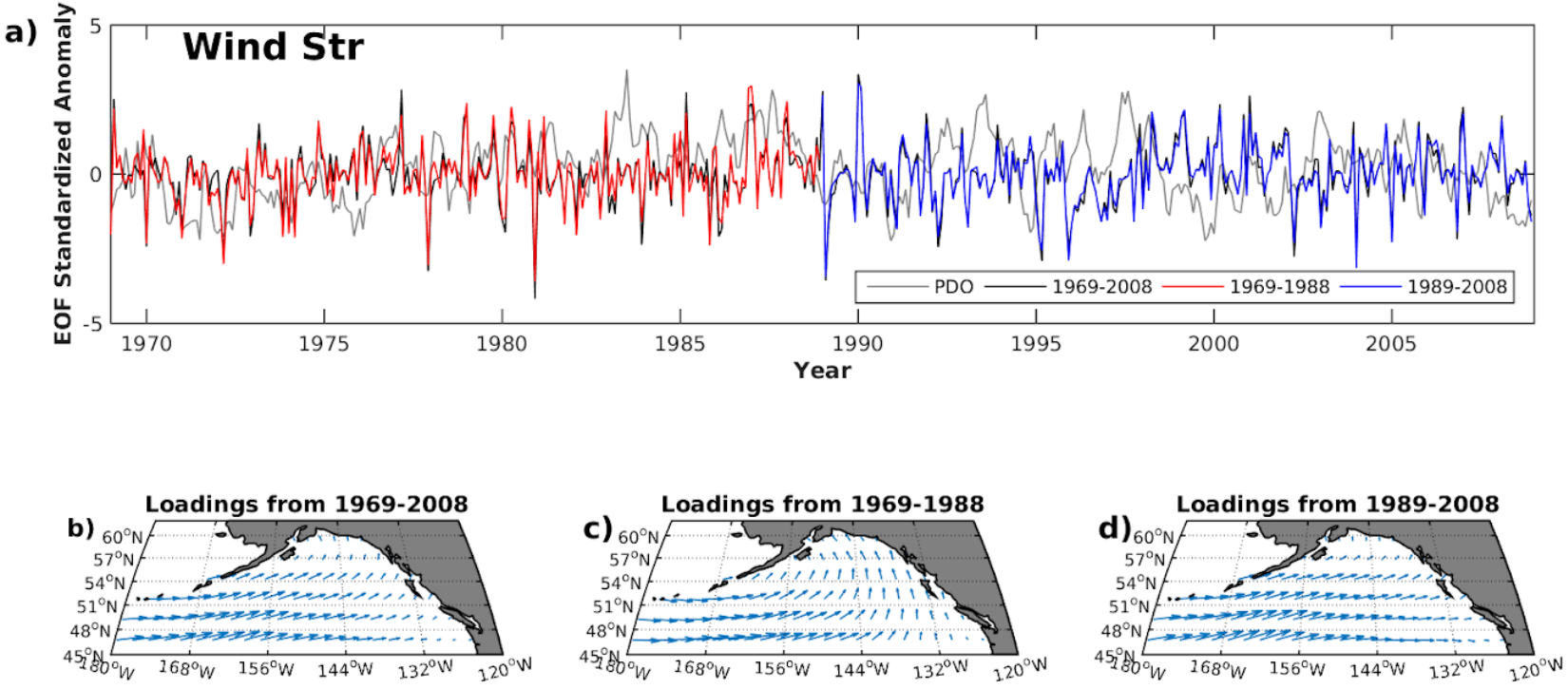

Figure 3.12. a) Wind stress PC1 time series for the first period (blue line), second period (red line), and full period (black line) overlaid on the PDO index (gray line). The spatial loadings for each period b) full period, c) first period, and d) second period.

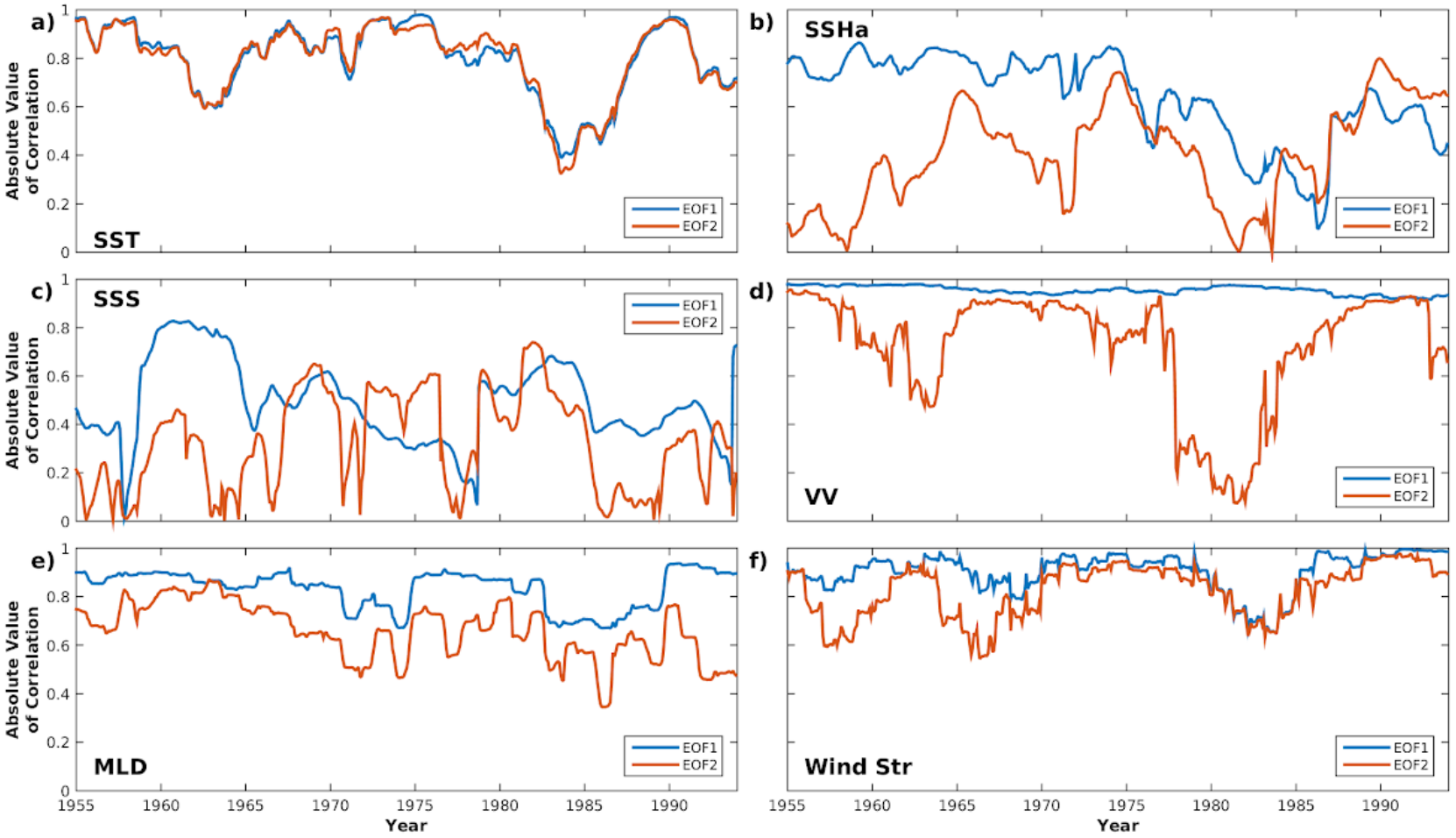

Figure 3.13. Absolute value of correlations between spatial patterns for the same EOF in adjacent 15-year windows a) sea surface temperature, b) sea surface height anomalies, c) sea surface salinity, d) vertical velocity, e) mixed layer depth, and f) wind stress. EOF1 (blue line) and EOF2 (orange line) plotted at the middle month between windows.

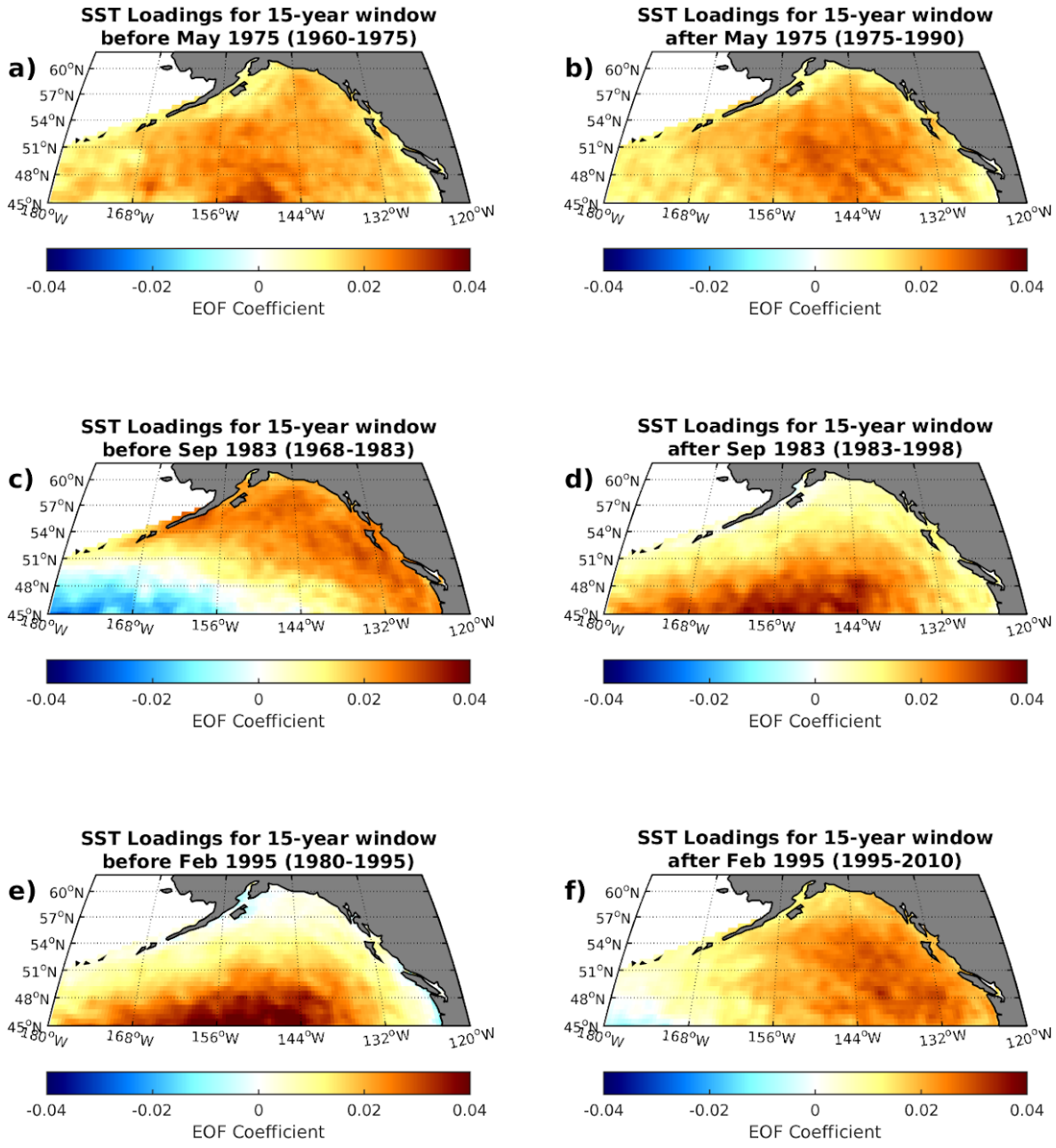

Figure 3.14. Sea surface temperature EOF1 spatial loadings for selected months for a) 15 years prior to May 1975 (1960-1975), b) 15 years after May 1975 (1975-1990), c) 15 years prior to September 1983 (1968-1983), d) 15 years after September 1983 (1983-1998), e) 15 years prior to February 1995 (1980-1995), f) 15 years after February 1995 (1995-2010).

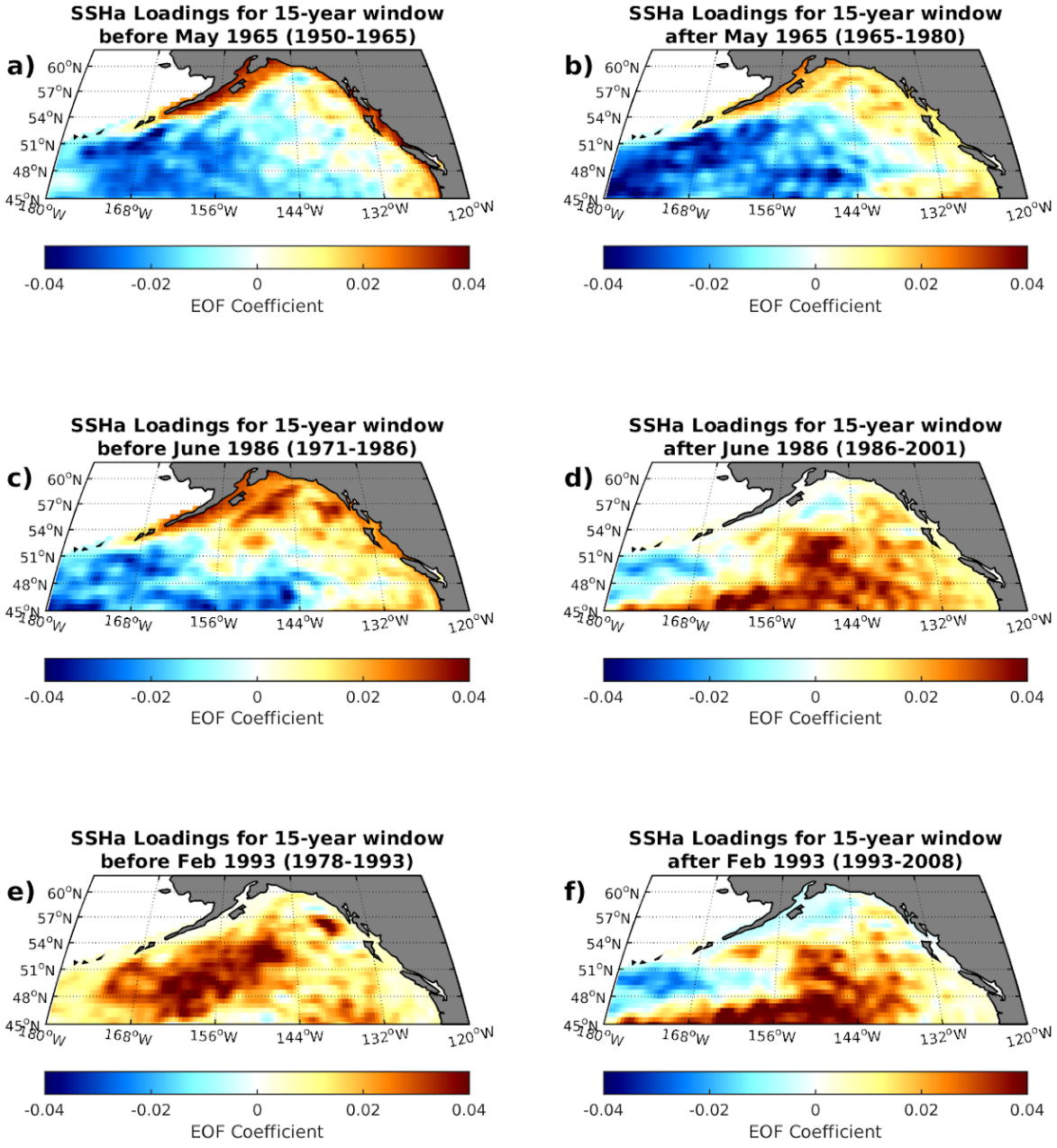

Figure 3.15. Sea surface height anomaly EOF1 spatial loadings for selected years a) 15 years prior to May 1965 (1950-1965), b) 15 years after May 1965 (1965-1980), c) 15 years prior to June 1987 (1971-1986), d) 15 years after June 1986 (1986-2001), e) 15 years prior to February 1994 (1979-1994), f) 15 years after February 1994 (1994-2009).

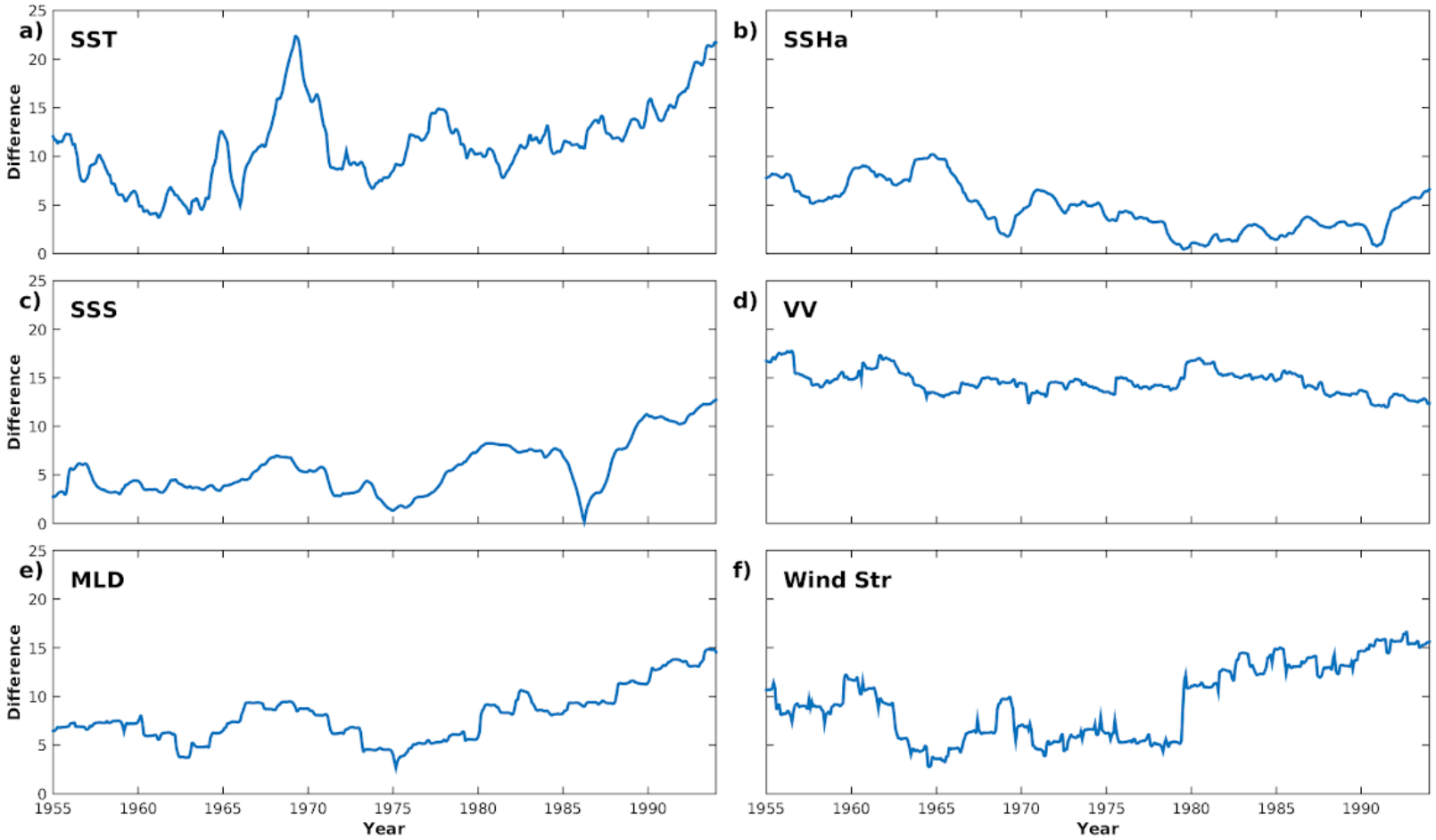

Figure 3.16. Difference between variance explained by EOF1 and EOF2 for a rolling 15-year-window plotted in the middle month of the window for a) sea surface temperature, b) sea surface height anomalies, c) sea surface salinity, d) vertical velocity, e) mixed layer depth, and f) wind stress.

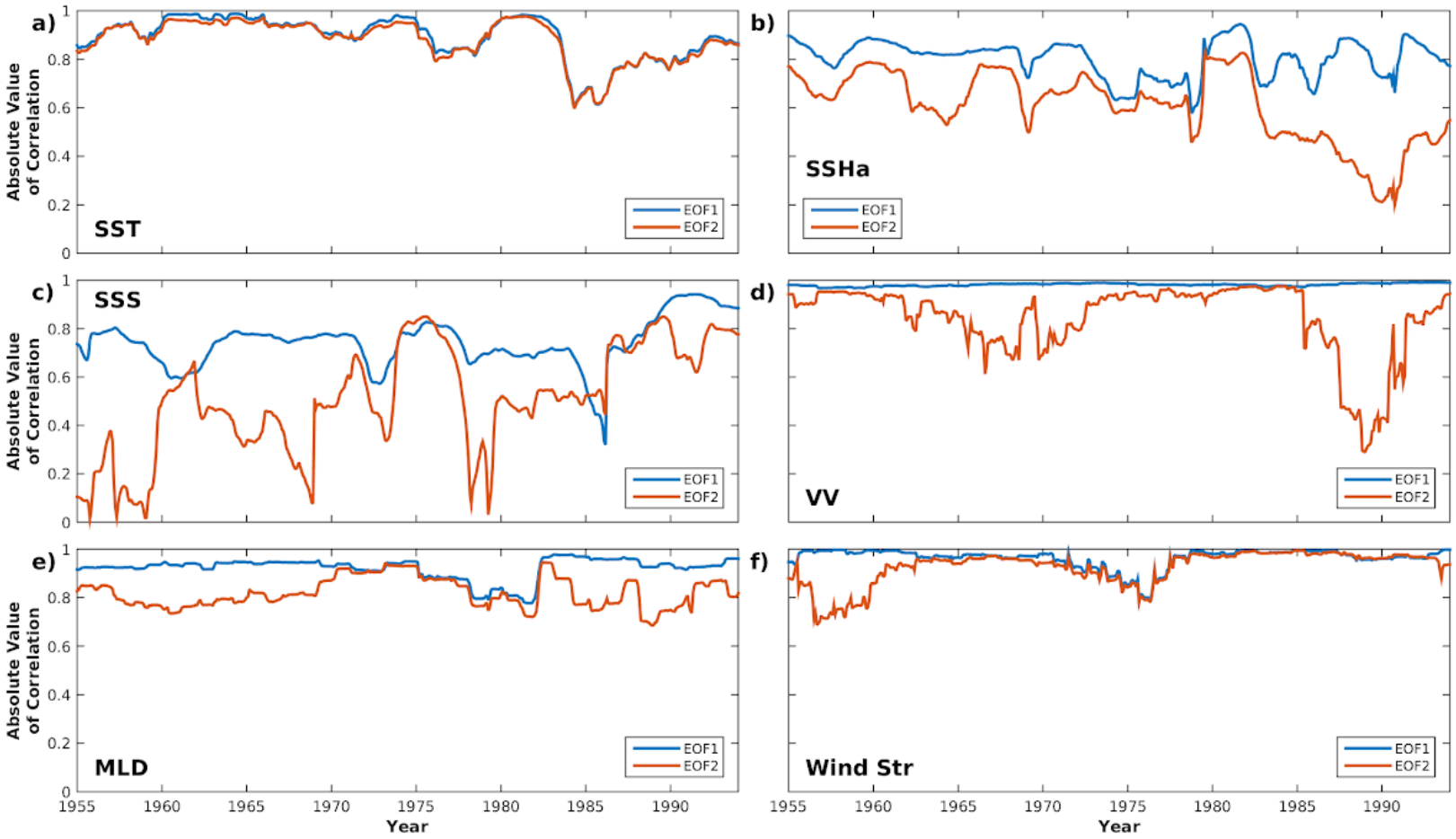

Figure 3.17. Absolute value of correlation between 15-year rolling window EOF spatial pattern and the full period spatial pattern for a) sea surface temperature, b) sea surface height anomalies, c) sea surface salinity, d) vertical velocity, e) mixed layer depth, and f) wind stress. EOF1 (blue line) and EOF2 (orange line) plotted at the middle month of the 15-year window.

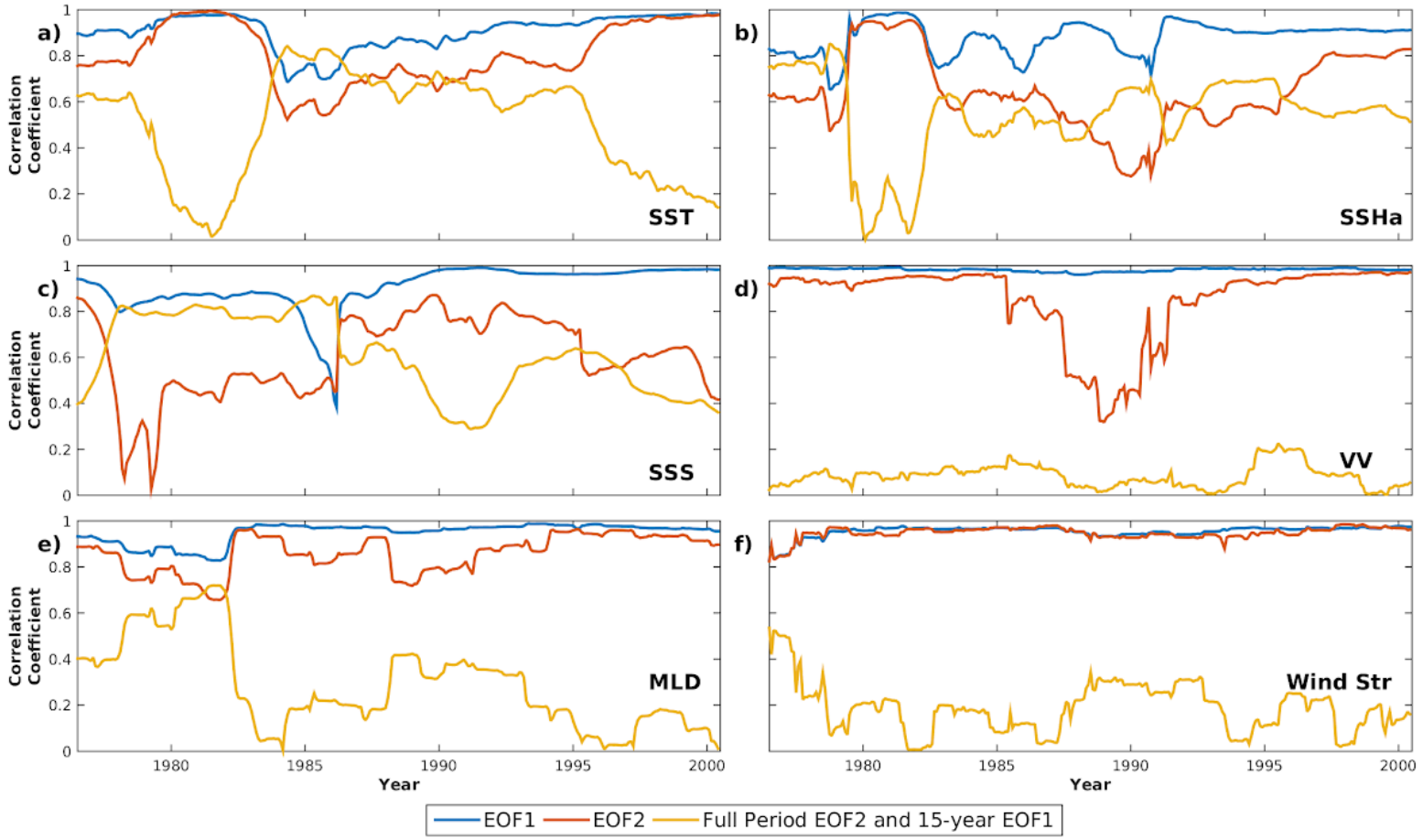

Figure 3.18. Absolute value of correlations between 15-year window PCs and full period PCs for a) sea surface temperature, b) sea surface height anomalies, c) sea surface salinity, d) vertical velocity, e) mixed layer depth, and f) wind stress. Each plot compares PC1 correlations (blue line), PC2 correlations (orange line), and PC1 of the full period to PC2 of the 15-year window (yellow line). Correlations are plotted on the middle month of the 15-year window

3.5 References

Alexander AM, Scott DJ, Deser C (2000) Processes that influence sea surface temperature and ocean mixed layer depth variability in a coupled model. J Geophys Res 5(16):823–842. doi: 10.1029/2000JC900074

Barnier B, Siefridt L, Marchesiello P (1995) Thermal forcing for a global ocean circulation model using a three-year climatology of ECMWF analyses. J Mar Syst 6:363–380. doi: 10.1016/0924-7963(94)00034-9

Buchheister A, Miller TJ, Houde ED, Secor DH, Latour RJ (2016) Spatial and temporal dynamics of Atlantic menhaden (*Brevoortia tyrannus*) recruitment in the Northwest Atlantic Ocean. ICES J Mar Sci 73(4):1147–1159. doi: 10.1093/icesjms/fvs260

Calman J (1987) Introduction to sea-surface topography from satellite altimetry. Johns Hopkins APL Technical Digest 8(2):206–211.

Casey KS and Ademeck D (2002) Sea surface temperature and sea surface height variability in the North Pacific Ocean from 1993 to 1999. J Geophys Res 107:3099–3110. doi: 10.1029/2001JC001060

Carton JA, Giese BS (2008) A Reanalysis of ocean climate using simple ocean data assimilation (SODA). Monthly Weather Review 136:2999–3017.

Clark WG, Hare SR (2011) Effects of climate and stock size on recruitment and growth of Pacific halibut. Fisheries Management 22:852–862.

Cloern JE, Jassby AD, Schrage TS, Nejad E, Martin C (2015) Ecosystem variability along the estuarine salinity gradient: examples from long-term study if San Francisco Bay. Limnol Oceanogr 62(S1):S272–S291. doi: 10.1002/lno.10537

Di Lorenzo E, Schneider N, Cobb KM, Chhak K, Franks PJS, Miller AJ, McWilliams JC, Bograd SJ, Arango H, Curchister E, Powell TM, Rivere P (2008) North Pacific Gyre Oscillation links ocean climate and ecosystem change. Geophys Res Lett 35:1–6. doi: 10.1029/2007GL032838

Donguy JR, Henin C (1976) Anomalous navifacial salinities in the tropical Pacific Ocean. J Mar Res 27(9):693–714.

Downton MW, Miller KA (1998) Relationships between Alaskan salmon catch and North Pacific climate on interannual and interdecadal time scales. Can J Fish Aquat Sci 55(10):2255–2265.

Ferland J, Gosselin M, Starr M (2011) Environmental control of summer primary production in the Hudson Bay system: The role of stratification. J Mar Syst 88:385–400.

Freeland HJ (2006) What proportion of the North Pacific Current finds its way into the Gulf of Alaska? Atmos - Ocean 44:321–330. doi: 10.3137/ao.440401

Forchhammer MC, Clutton-Brock TH, Lindstrom J, Albon SD (2001) Climate and population density induce long-term cohort variation in a northern ungulate. J Anim Ecol 70:721–729. doi: 10.1046/j.0021-8790.2001.00532.x

Hare SR, Mantua NJ (2000) Empirical evidence for North Pacific regime shifts in 1977 and 1989. Prog Oceanogr 47:103–145.

Hare SR, Mantua NJ, Francis RC (2011) Inverse production regimes: Alaska and west coast pacific salmon. Fisheries 24(1):6–14.

Hurrell JW (1995) Decadal trends in the North Atlantic Oscillation: regional temperatures and precipitation. Science 269:676–679.

Kerr RA (2000) A North Atlantic climate pacemaker for the centuries. Science 288(5473):1984–1986.

Kilduff DP, Di Lorenzo E, Botsford LW, Teo SLH (2015) Changing central Pacific El Ninos reduce stability of North American salmon survival rates. Proc Nat Acad Sci 112(35):10962–10966. doi: 10.1073/pnas.1503190112

Litzow MA (2006) Climate regime shifts and community reorganization in the Gulf of Alaska: how do recent shifts compare with 1976/1977? ICES J Mar Sci 63:1386–1396. doi: 10.1016/j.icesjms.2006.06.003

Lukas R, Lindstrom E (1991) The mixed layer of the western equatorial Pacific Ocean. J Geophys Res, 96:3343–3358.

Mantua NJ, Hare SR, Zhang Y, Wallace JM, Francis RC (1997) A Pacific interdecadal climate oscillation with impacts on salmon production. Bull Amer Meteor Soc 78:1069–1079.

Mantua NJ, Hare SR (2002) The Pacific Decadal Oscillation. J Ocean 58:35–44.

Martin JH, Gordon M, Fitzwater SE (1991) The case for iron. Limnol Oceanogr 36:1793–1802.

Moore MM, Arango HG, Di Lorenzo E, Cornuelle BD, Miller AJ, Neilson DJ (2004) A comprehensive ocean prediction and analysis system based on the tangent linear and adjoint of a regional ocean model. Ocean Model 7:227–258.

Overland JE, Rodionov S, Minobe S, Bond N (2008) North Pacific regime shifts: Definitions, issues and recent transitions. Prog Oceanogr 77:92–102. doi: 10.1016/j.pocean.2008.03.016

Post E, Forchhammer MC, Stenseth NC (1999) Population ecology and the North Atlantic Oscillation (NAO). Ecol Bull 47:117–125.

Puerta P, Ciannelli L, Rykaczewski RR, Opiekun M, Litzow, MA (2018) Do Gulf of Alaska fish and crustacean populations show synchronous non-stationary responses to climate? Manuscript submitted for publication.

Valcu M, Kempenaers B (2010) Spatial autocorrelation: an overlooked concept in behavioral ecology. Behav Ecol 21(5):902–905.

Wendler G, Gordon T, Stuefer M (2017) On the precipitation and precipitation change in Alaska. Atmos 8:253–262.

Wilson C, Ademeck D (2001) Correlations between surface chlorophyll and sea surface height in the tropical Pacific during the 1997–1999 El Niño-Southern Oscillation event. J Geophys Res 106:31175–31188.

Yeh SW, Kang YJ, Noh Y, Miller AJ (2011) The North Pacific climate transitions of the winters of 1976/77 and 1988/89. J Clim 24:1170–1183. doi: 10.1175/2010JCLI3325.1

Zhang Y, Wallace JM, Battisti DS (1997) ENSO-like interdecadal variability: 1900-93. J Clim 10:1004–1020. doi: 10.1175/1520-0442

Chapter 4

Conclusions

4.1 Summary and Conclusions

The 1988/89 climate shift in the North Pacific (Hare and Mantua 2000; Litzow 2006; Overland et al. 2008; Yeh et al. 2011) was well documented in biological time series (Hare and Mantua 2000; Litzow 2006). Yeh et al. (2011) observed a reorganization of sea surface temperature (SST) and sea level pressure empirical orthogonal function (EOF) spatial patterns throughout the North Pacific after the 1980s. A long-term warming trend associated with the climate shifts in the late 1980s (Yeh et al. 2011; Jo et al. 2013) and the late 1990s (Jo et al. 2013) led to a dipole-like structure for SST anomalies in the North Pacific. These changes have been associated with changes in the Artic Oscillation leading to a North Pacific Gyre Oscillation (NPGO)-like pattern in SST (Yeh et al. 2011; Jo et al. 2013).

Regionally, Kilduff et al. (2015) observed a shift in the relationship between Pacific salmon survival rates association near the bifurcation of the North Pacific Current and North Pacific climate indices after the 1980s. The historic association between the Pacific Decadal Oscillation (PDO) and salmon indices, described by Mantua et al. (1997), was no longer a good predictor of salmon survival as the NPGO index became much more strongly correlated with salmon survival (Kilduff et al. 2015).

In the Gulf of Alaska (GOA), the 1988/89 shift was less clear in physical processes. In Chapter 3, I tested the stationarity of relationships between GOA-wide

indices across 1988/89, resulting in limited support for a shift in individual property indices. Testing among properties revealed a decoupling of the variability in SST and sea surface height anomalies (SSHa) across 1988/89. Both the principal component (PC) time series and the EOF spatial patterns relationships showed changes. The PC time series correlations became weaker while the EOF spatial pattern correlations became stronger across 1988/89. Both SST and SSHa showed shifts in the mid 1980s when spatial patterns were compared between adjacent 15-year windows. The shift in SST was short-lived and returned to the pre-1980s spatial pattern by the early 1990s. The SSHa shift remained through the early 1990s at the limit of the analysis. The correlation between 15-year SST and SSHa EOF spatial patterns were extremely variable until the mid 1980s, where the correlation remained steady for over a decade.

While no individual property maintained a shift in both PCs and EOF spatial patterns across 1988/89, the variable relationship between SST and SSHa is important for GOA-wide dynamics. The PDO index, defined by variability in SST anomalies and SSHa in the North Pacific (Zhang et al. 1997), was associated with Pacific salmon survival in the GOA (Mantua et al. 1997). The relationship between the PDO index and salmon survival in the northern California Current declined after the late 1980s (Kilduff et al. 2015), while salmon-survival became better correlated to the NPGO index. In Chapter 2, Pacific salmon indices showed a reduced correlation with pre-1989 SST PC1 from the GOA shelf. SST PC1 along the GOA shelf was highly correlated with the PDO index, therefore salmon indices in the GOA showed a similar decline in relationship strength with the PDO index as the study by Kilduff et al. (2015).

GOA shelf SSHa PC1also showed a strong correlation with salmon indices in the GOA before 1989, but the correlation also declined after 1988. Kilduff et al. (2015) showed an increase in the correlation between the NPGO index, defined by the second PC of SSHa in the North Pacific, and salmon survival. The shift in the EOF1 spatial pattern of SSHa from Chapter 3, shifts from a PDO-like pattern to an NPGO-like pattern. The change in spatial pattern in SSHa and the loss of correlation between GOA salmon indices and PC1 of SSHa, coinciding with an increase in correlation of California Current salmon survival with the second PC2 of North Pacific SSHa, supports a shift between the dominant and secondary EOF spatial patterns and PC time series in SSHa in the late 1980s.

Overall, the reorganization of the North Pacific SST EOF1 pattern in the late 1990s (Yeh et al. 2011; Jo et al. 2013) and the GOA SSHa EOF1 spatial pattern both occur in the late 1980s, both coinciding with a loss of correlation with salmon indices. A shift from the EOF1 pattern of SSHa to the EOF2 pattern, while not strongly supported in this thesis, may have occurred in the GOA leading to shifting physical processes and changing correlations with biological indices. Future exploration of the relationships between local leading and secondary PCs may help decipher local climate, physical, and biological shifts in the GOA.

4.2 References

Hare SR, Mantua NJ (2000) Empirical evidence for North Pacific regime shifts in 1977 and 1989. Prog Oceanogr 47:103–145. doi: 10.1016/S0079-6611(00)00033-1

Jo HS, Yeh SW, Kim CH (2013) A possible mechanism for the North Pacific regime shift in winter of 1998/1999. Geophys Res Lett 40:4380–4385. doi: 10.1002/grl.50798

Kilduff DP, Di Lorenzo E, Botsford LW, Teo SLH (2015) Changing central Pacific El Ninos reduce stability of North American salmon survival rates. Proc Nat Acad Sci 112(35):10962–10966. doi: 10.1073/pnas.1503190112

Litzow MA (2006) Climate regime shifts and community reorganization in the Gulf of Alaska: how do recent shifts compare with 1976/1977? ICES J Mar Sci 63:1386–1396. doi: 10.1016/j.icesjms.2006.06.003

Mantua NJ, Hare SR, Zhang Y, Wallace JM, Francis RC (1997). A Pacific interdecadal climate oscillation with impacts on salmon production. Bull Amer Meteor Soc, 78, 1069–1079.

Overland JE, Rodionov S, Minobe S, Bond N (2008) North Pacific regime shifts: Definitions, issues and recent transitions. Prog Oceanogr 77:92–102. doi: 10.1016/j.pocean.2008.03.016

Yeh SW, Kang YJ, Noh Y, Miller AJ (2011) The North Pacific climate transitions of the winters of 1976/77 and 1988/89. J Clim 24:1170–1183. doi: 10.1175/2010JCLI3325.1

Zhang Y, Wallace JM, Battisti DS (1997) ENSO-like interdecadal variability: 1900-93. J Clim 10:1004–1020. doi: 10.1175/1520-0442